Intraspecific polyploidization and its ecological significance in perennial plants: variations in morphological traits and life-history traits, distribution patterns, and the evolution of vegetative reproduction

（多年生植物における種内倍数化とその生態的重要性：
形態形質と生活史形質の変異、分布パターン、ならびに無性生殖の進化）

Yuki Shiotani

Graduate School of Environmental Science, Hokkaido University

2024

Contents

Summary

Polyploidization, a duplication of complete chromosome sets, is a common phenomenon in plants and regarded as drivers of speciation and diversification within species. Polyploidization often causes the changes in morphological traits, life-history traits, mating systems, and distribution patterns of plants. However, little is known about the mechanisms of the establishment of newly formed polyploid populations, geographic segregation between diploid and polyploid populations, and the significance of vegetative reproduction in polyploids. In this study, I compared various morphological and ecological characteristics between the diploid and autotetraploid populations of *Parasenecio kamtschaticus* under natural conditions and by the reciprocal transplant experiments to reveal the ecological significance of polyploidization on the diversification and distribution pattern within a single species.

Parasenecio kamtschaticus is composed of three taxonomic groups (combinations of taxon and cytotype): diploid *P. kamtschaticus* var. *kamtschaticus* (hereafter 2x-*kam*), tetraploid *P. kamtschaticus* var. *kamtschaticus* (hereafter 4x-*kam*), and tetraploid *P. kamtschaticus* var. *bulbifer* (hereafter 4x-*bulb*). Although 2x-*kam* and 4x-*kam* populations are maintained by sexual seed production, 4x-*bulb* can reproduce vegetatively by forming bulbils. These taxonomic and cytotype groups are mainly distributed differently at the geographic scale, i.e., 2x-*kam* is common in deciduous cool-temperate forests, 4x-*kam* is common in evergreen boreal forests, and 4x-*bulb* mainly grows at higher elevations around treeline. Throughout the study, I aimed to answer the following questions; how do the morphological and ecological traits differ among three groups in the natural and common garden environments, and how do these differences explain the habitat differentiation among the groups (Chapter I)? How high is the

plasticity of the traits specific to diploid and tetraploid, and are these traits advantageous at its own habitat condition (Chapter II)? How does the ability of vegetative reproduction relate to polyploidization, and how is vegetative reproduction associated with the expansion to higher elevations (Chapter III)?

In Chapter I, I conducted morphological measurements (plant height, maximum leaf area, leaf number, and floral bud number) and a hand-pollination experiment (simple bagging, self-pollination, and outcross-pollination) in the natural populations, and surveyed the phenological traits (leaf emergence date, flowering onset date, and flowering cessation date) in a common garden among three groups of *P. kamtschaticus*. In the morphological measurements, 4x-*kam* showed larger plant height and leaf size than 2x-*kam* and 4x-*bulb*, and 4x-*bulb* produced smaller number of floral buds than 2x-*kam* and 4x-*kam*. Size-dependency of leaf production was apparent in 4x-*kam*, while size-dependency of flower production was apparent in 2x-*kam*. All intraspecific groups indicated low self-compatibility and depended on outcrossing for seed production. In the common garden experiment, 4x-*bulb* showed slower growth initiation but earlier and shorter flowering period than 2x-*kam* and the 4x-*kam*, whereas leafing and flowering periods of 2x-*kam* and 4x-*kam* were largely overlapped. The comparative results between 2x-*kam* and 4x-*kam* indicated that polyploidization caused morphological increment and higher resource allocation to vegetative growth, resulting in the niche separation of 4x-*kam* toward boreal forests, where higher light-harvesting ability is required due to shaded conditions. On the other hand, 4x-*bulb* showed different morphological and life-history traits from the same ploidy 4x-*kam*, indicating that 4x-*bulb* may evolve independently from 4x-*kam* to adapt to high elevation habitat, where a rapid phenological progress and vegetative reproduction are advantageous due to a cool and short growing season.

In Chapter II, I conducted a reciprocal transplant experiment at a resident site of 2x-*kam* (deciduous forest at TOEF) and a resident site of 4x-*kam* (evergreen forest at NRO) to clarify the mechanisms driving a geographic separation between diploid (2x-*kam*) and tetraploid (4x-*kam*) populations. For the experiment, two source populations in each of the diploids and tetraploids populations were chosen, and transplanted in each experimental site. Furthermore, reciprocal seed sowing experiment was conducted. I tested the degree of local adaptation in each ploidy level by the measurements at three life-history stages across two years, i.e., (1) germination and seedling stage, (2) flowering stage, and (3) growth stage. Any significant advantage at its own habitat was not detected at the germination and seedling stage (germination and seedling survival rates) and at the flowering stage (flower production) in both cytotypes. At the growth stage, however, the 4x-*kam* populations showed larger stature and leaf size than the 2x-*kam* populations at NRO. At TOEF, the 4x-*kam* populations produced larger leaves than the 2x-*kam* populations as well as NRO, but plant height did not differ between 4x-*kam* and 2x-*kam*. A lack of reproductive superiority of 2x-*kam* at TOEF might be due to the poor-nutrient soil conditions, and this possibility was supported by the re-transplant experiment in the common garden. Thus, 4x-*kam* may be more advantageous on the floor of evergreen forests owing to the higher light-harvesting ability compared to 2x-*kam*. On the other hand, 2x-*kam* may outcompete 4x-*kam* in deciduous forests due to the vigorous reproductive ability at smaller size, resulting in a rapid population growth even if nutrient is limited.

In Chapter III, ecological significance of vegetative reproduction associated with polyploidization was evaluated. I compared bulbil and flower production among 2x-*kam*, 4x-*kam*, and 4x-*bulb* along the elevational gradient. Although bulbil production was

observed in all plants of the 4x-*bulb* populations, it was rare and occasional for the 2x-*kam* and 4x-*kam* populations. Nevertheless, the 4x-*kam* populations showed higher bulbil formation ability than the 2x-*kam* populations. Regarding 4x-*bulb* populations, flower production ability clearly decreased at high elevation, whereas bulbil production ability was independent on the elevation. These results suggest that bulbil production was a crucial trait to compensate the decreasing activity of sexual reproduction at higher elevation, and polyploidization might promote the potential ability of bulbil formation, leading to the evolution of a bulbiferous phenotype, *P. kamtschaticus* var. *bulbifer*. In addition, I conducted a phylogenetic analysis using the chloroplast DNA (cpDNA) across three taxonomic groups to clarify the evolutionary process of 4x-*bulb*. Unfortunately, the DNA analysis was insufficient to reveal the detail evolutionary process due to low genetic variation.

The present study revealed that polyploidization causes a morphological increment and a potential of bulbil formation in *P. kamtschaticus*. These changes might promote the diversification of habitat use within the species, i.e., expansion to boreal forests and high elevation region. Because there were no significant differences in the phenological traits and low self-compatibility between 2x-*kam* and 4x-*kam*, reproductive interference may be inevitable when they cooccur. Thus, the niche separation of tetraploids should be crucial and the adaptation to boreal forests might be accelerated owing to a large stature. Vegetative reproduction by active bulbil production might enable 4x-*bulb* to grow at high elevation habitat, but 4x-*bulb* maintained the ability of seed production by outcrossing. This indicates the importance of sexual reproduction to maintain the genetic diversity even under the frequent vegetative reproduction. Because ecological significance of

polyploidization may vary among species, continuous studies are necessary to understand the diverse evolutionary processes in plants related to polyploidization.

General introduction

Polyploidization, a process acquiring additional complete sets of chromosomes, is an important evolutionary driver of speciation and diversification in plants (Soltis and Soltis 1999; Ramsey and Ramsey 2014, Otto and Whitton 2000; Rice et al. 2019). Almost all of the angiosperms are assumed to be originated from the ancestral polyploidization (Wood et al. 2009), and 24 % of present vascular species are speculated to be recently derived by polyploidization within the same genera (Barker et al. 2016). Many studies reported that polyploidization often affects various morphological, physiological, and ecological traits, such as the changes in cell and body size (Balao et al. 2011; Becker et al. 2022), hormone balance (Dai et al. 2015), life-history traits and mating system (i.e., flower number: Vleugels et al. 2016; anthesis: Diallo et al. 2023; selfing ability: Otto 2007), and the shift of distribution range (Stuessy et al. 2004). The diversification of growing habitat and rapid speciation are more likely to occur in polyploid lineages (Han et al. 2020). On the other hand, ecological consequences of polyploidization are various among species.

Despite many empirical studies on polyploidization, understanding of the impact of polyploidization on ecological traits is still limited. One possible reason is that previous studies have mainly focused on allopolyploids rather than autopolyploids (Šingliarová et al. 2023). Allopolyploids originate from the hybridization between different species, and their phenotypic traits are derived as a product of hybridization, i.e., the mixture of different genomes. In contrast, autopolyploids are formed by whole genome duplication of a single species without addition of new genetic information. To clarify the direct effects of polyploidization, therefore, intraspecific comparisons of ecological properties between autopolyploids and the ancestral diploids are crucial.

The process of establishment of neo-polyploid populations has been controversial issue. Although the accidental formation of polyploids is common in plants, new polyploids are often excluded immediately at the early stage of establishment due to a frequent crossing with dominant diploid progenitors, resulting in the production of inviable offspring having odd chromosome numbers (Levin 1975). This obstacle to polyploid establishment is called the minority cytotype exclusion (MCE: Levin 1975). For the establishment of polyploid populations, acquisition of specific mechanism mitigating the negative effects of the MCE is crucial. Self-compatibility or asexual reproduction is often regarded as the effective mechanisms to overcome the MCE (Otto and Whitton 2000; Fowler and Levin 2016) because these reproductive systems enhance the chance of crossing between the same ploidy level. Furthermore, some ecological shifts, e.g., temporal isolation of anthesis and spatial segregation of growing habitat are effective to reduce the risk of crossing with the dominant diploid progenitors (Petit et al. 1999), resulting in a mitigation of the MCE. Because these processes are not mutually exclusive, comprehensive investigation is needed to understand how a certain polyploid group has been established.

It has been reported that polyploid populations often have different distribution pattern from the ancestral diploid populations (Karunarathne et al. 2018). Allopatric distributions of diploid and polyploid populations are common rather than sympatric mixed-ploidy populations, and the polyploid populations tend to be distributed in harsher environments than diploid populations (Otto et al. 2007; Godfree et al. 2017). Although different distribution patterns between diploids and polyploids may reflect the differentiation of niche preference, other non-adaptive process, such as historical background and occasional dispersal, may also reflect the present distributions. A

clarification of the mechanisms causing distribution shifts in polyploid populations is crucial, but there are few studies based on the experimental approaches, such as reciprocal transplant experiments in the field (McIntyre and Strauss 2017; Hülber et al. 2018).

Because polyploid populations often exist in harsh environments, such as high elevation habitat (Zozomová-Lihová et al. 2015; Knotek and Kolář 2018; Wang et al. 2021), some ecological characteristics promoting the expansion to higher elevations are expected (Brochmann et al. 2004; Pluess and Stöcklin 2005). Generally, sexual reproduction tends to be harder at higher elevations due to low temperature, frost damage, and short growing season (Kudo and Suzuki 2002; Kudo 2021). A shift to vegetative reproduction may be an effective strategy to maintain the populations at high elevation habitat. It is noteworthy that polyploids are often associated with the ability of vegetative reproduction compared to the ancestral diploids (Herben et al. 2017; Van Drunen and Husband 2019). Thus, the acquisition of vegetative reproduction ability by polyploidization may enable the polyploids to migrate upper elevations, resulting in a niche separation. However, little is known about underlying mechanisms of the linkage between vegetative reproduction and polyploids.

In this study, I studied the impacts of polyploidization on morphological traits, life-history traits, distribution pattern, and the ability of vegetative reproduction by the comparisons between diploid and polyploid populations across various environments. I selected *Parasenecio kamtschaticus* (Asteraceae) as a study species, that is a perennial herb inhabiting understory of forest zone in northern Japan. This species is classified into two varieties, *P. kamtschaticus* var. *kamtschaticus* and *P. kamtschaticus* var. *bulbifer*. The former variety includes diploid populations and tetraploid populations, while the latter variety is composed of only tetraploid populations (Nakagawa 2006). Furthermore,

P. kamtschaticus var. *bulbifer* can reproduce vegetatively by forming bulbils, and their growing habitat is in subalpine regions (Kudo and Hirao 2020). Therefore, this species is ideal plants to study the ecological importance of polyploidy.

The present study is composed of three chapters. In Chapter I, I compared the morphological traits and life-history traits among populations of three groups in *P. kamtschaticus* having different ploidy level (diploid vs. tetraploid) and reproductive mode (sexual reproduction vs. vegetative reproduction). Furthermore, I conducted a pollination experiment to clarify the differences in reproductive characteristics among the groups. In Chapter II, I conducted a reciprocal transplant experiment between multiple diploid and tetraploid populations to test the existence of niche differentiation between them. In Chapter III, I investigated the activity of vegetative reproduction along the elevation gradient and the effects of polyploidization on the extent of vegetative reproduction to test the advantages of polyploidization at high elevations. Throughout the studies, I discuss how polyploidization creates the diversification of ecological traits and distribution patterns, and how polyploids mitigate the MCE and expand to new habitats.

Study plants

Parasenecio kamtschaticus (Maxim.) Kadota (Asteraceae) is a perennial herb growing in forest floor of cool temperate forests. Two variety species are included in this species: *P. kamtschaticus* (Maxim.) Kadota var. *kamtschaticus* and *P. kamtschaticus* (Maxim.) Kadota var. *bulbifer* (Koidz.) Kadota (Kadota et al. 2017). The former (var. *kamtschaticus*) is widely distributed in northeastern Asia (Aleutians, Kamchatka, Sakhalin, Kurils, Ussuri, northeastern China, Korea, and northern Japan), while the latter (var. *bulbifer*) is endemic in Hokkaido of northern Japan (Kadota et al. 2017). Furthermore, *P. kamtschaticus* var. *kamtschaticus* include two cytotype populations: diploids (2n = 2x = 60) and tetraploids (2n = 4x = 120), while all *P. kamtschaticus* var. *bulbifer* populations are tetraploids (2n = 4x = 120) (Nakagawa 2006). The polyploid system of *P. kamtschaticus* is known to be autotetraploid (Kudo and Hirao 2020). Major distribution area of *P. kamtschaticus* var. *kamtschaticus* is in lowland and montane forests of Hokkaido and subalpine forests of Tohoku in Japan. In contrast, the distribution of *P. kamtschaticus* var. *bulbifer* is limited in subalpine to alpine regions of central Hokkaido, and this variety species has two reproductive modes; sexual reproduction via seeds and vegetative reproduction via axil bulbils (Nakagawa 2006; Kudo and Hirao 2020). Leaf emergence of *P. kamtschaticus* var. *kamtschaticus* usually initiates in April, flowering occurs during late July to August, and seeds mature from September to early October (Kudo and Hirao 2020). The distributions of these taxonomic and cytotype groups are separated geographically within Hokkaido, and the formation of mixed-ploidy populations is rare (Nakagawa 2006; Kudo and Hirao 2020).

Chapter I: The effects of polyploidization on morphological and life-history traits in *Parasenecio kamtschaticus*

Introduction

The mechanisms accelerating within-cytotype crossing are advantageous for the establishment of neo-polyploids because these mechanisms can mitigate the MCE. For example, self-compatibility, vegetative reproduction, the separation of spatiotemporal niche may be crucial in the early establishment process of polyploids (Petit et al. 1997; Ramsey and Schemske 1998; Baldwin and Husband 2013; Theodoridis et al. 2013). Clarification of the mechanisms overcoming the MCE is crucial to understand the widespread success of polyploids in plants.

Polyploidization often accompanies the changes in morphological and ecological traits, resulting in the advances of polyploids into various environments. Polyploids tend to have different plant size, organ size, resource allocation patterns, and phenological traits from the diploid progenitors (Thébault et al. 2011, Aversano et al. 2012, Pegoraro et al. 2019). Furthermore, polyploids may mitigate the negative effects of inbreeding depression and may promote selfing ability due to a lower possibility of full homozygote of deleterious allele than diploids (Soltis and Soltis 2000, Otto 2007). However, the effects of polyploidization on these ecological characteristics are inconsistent among species. For example, increasing cell size is regarded as a common phenomenon in polyploids (Zhang et al. 2019; Becker et al. 2022), but the enlargement of plant size may not be always supported (Comai 2005). These changes in the morphological and ecological traits may contribute to the niche differentiation from the diploid progenitors. Polyploids tend to be distributed in severe environmental conditions in comparison with

the diploid progenitors (Baack and Stanton 2005). Thus, the ecological significance of the morphological differentiation is necessary to understand the mechanisms of the niche separation between diploids and polyploids.

Regarding *Parasenecio kamtschaticus*, Nakagawa (2006) revealed that the tetraploid *P. kamtschaticus* var. *kamtschaticus* (hereafter 4x-*kam*) showed larger leaf and plant height than the diploid *P. kamtschaticus* var. *kamtschaticus* (hereafter 2x-*kam*) and the tetraploid *P. kamtschaticus* var. *bulbifer* (hereafter 4x-*bulb*). It is known that the 2x-*kam* is obligate outcrosser (Kudo et al. 2008), but little is known about the mechanisms promoting the establishment of polyploid populations against the MCE and other ecological traits specific to the polyploidization in this species. Although 4x-*bulb* has been regarded as a different variety from 4x-*kam* due to the property producing bulbils, furthermore, it is unclear how extent they are ecologically differentiated. This chapter aims to clarify how polyploidization affects the morphological and life-history traits in *P. kamtschaticus*. I focus on the following questions: (1) Does polyploidization cause the self-compatibility in 4x-*kam* and 4x-*bulb*? (2) Are there phenological isolations (i.e., the extent of flowering overlap) among taxonomic groups? (3) Does polyploidization alter the ecological traits, such as plant size and resource allocation pattern?

Methods

Research sites

The previous studies (Nakagawa 2006; Kudo and Hirao 2020) reported the geographic distributions of 2x-*kam*, 4x-*kam*, and 4x-*bulb* in Hokkaido. Generally, 2x-*kam* populations are distributed from southwestern to eastern Hokkaido of the Pacific side, 4x-

kam populations are from eastern to northern Hokkaido, while 4x-*bulb* populations are in the mountain regions of central Hokkaido. As representative sites of individual taxonomic groups for the pollination experiment, Nopporo, and Akkeshi for 2x-*kam* populations, Teshio and Utoro for 4x-*kam* populations, and Maruseppu for 4x-*bulb* populations were selected (Fig. 1-1 A). For the measurements of morphological characteristics, following 11 populations were selected: Nopporo, Tomakomai, and Akkeshi for 2x-*kam* populations, Teshio, Utoro, Hamatonbetsu, Lake Mashu, and Mt. Moriyoshi for 4x-*kam* populations, Maruseppu, Mt. Aka, and Mt. Teshio for 4x-*bulb* populations (Fig. 1-1 B).

Pollination experiment in natural populations

In order to clarify the self-compatibility of *P. kamtschaticus*, I conducted a pollination experiment in natural populations in 2020. Three pollination treatments were conducted in the natural populations of the three groups, including both variety *kamtschaticus* and the variety *bulbifer* (2x-*kam*: Nopporo and Akkeshi populations, 4x-*kam*: Teshio and Utoro populations, 4x-*bulb*: Maruseppu population), i.e., simple bagging, self-pollination, and outcross pollination. Fifteen individuals per treatment were arbitrarily selected at 5-m intervals to avoid selecting samples from the same genets. All inflorescences in each plant were covered with fine-meshed bags before flowering. I performed self-pollination and outcross pollination for 2–5 flower heads per plant (each flower head usually includes five florets) during the flowering season by deposition of pollen grains on stigmas of each floret using cotton swabs, whereas any pollen depositions were not conducted in simple bagging treatment. I marked manipulated florets using a color paint to distinguish them from non-treated florets on the inflorescences. Then, I bagged the whole inflorescences again. Before seed dispersal in mid-September, I harvested all seeds from the manipulated inflorescences and the non-treated inflorescences as control. Collected seeds were dried

in silica gel at room temperature, then developed seeds and undeveloped seeds were counted in each plant.

A generalized linear model (GLM) was conducted to compare the seed-set rates (developed seeds to treated florets ratio) among the treatments in each population, postulating a negative binomial error distribution. In the GLM, the response variable was the number of developed seeds, the explanatory variable was pollination treatment, and the number of treated florets was set as an offset term. All statistical analysis were performed in R v3.6.1 (R Core Team 2019).

Reciprocal pollination experiment between taxonomic groups in a common garden

In order to clarify the extent of reproductive isolation among three taxonomic groups of *P. kamtschaticus*, I conducted a reciprocal pollination experiment between taxa or cytotypes using transplanted individuals in a common garden in 2022. I transplanted 2x-*kam* plants (17 individuals) from Tomakomai population, 4x-*kam* plants (20 individuals) from Teshio population, and 4x-*bulb* plants (21 individuals) from Maruseppu population to the common garden of Genome Dynamics Research Center of Hokkaido University in Sapporo (GDRC; N 43.072°, E 141.341°, 15 m elevation) in early summer (May to June) of 2020. I selected large sized individuals forming floral buds for the transplant. After two years of the transplant, I conducted the inter-cytotype and inter-variety pollination experiment. For the inter-cytotype pollination, pollen grains of 2x-*kam* (or 4x-*kam*) were deposited on the stigmas of 4x-*kam* (or 2x-*kam*). For the inter-variety pollination, pollen grains of 4x-*bulb* were deposited on the stigmas of 4x-*kam* (pollination of the opposite direction was not conducted due to small number of flowering individuals). Furthermore, a within-cytotype outcrossing pollination was conducted as control. Ten individuals were

used for each treatment, and the protocols of hand pollination, harvesting, and counting seeds were the same as those of the pollination experiment in the natural populations. Steel-Dwass test was conducted to assess which combination of the pollination treatments showed a significant difference.

Comparisons of morphological traits and reproductive performance among natural populations

To compare the morphological and reproductive traits among *P. kamtschaticus* taxonomic groups, I conducted a field survey in 11 natural populations (three 2x-*kam* populations, five 4x-*kam* populations, and three 4x-*bulb* populations) across four years (2020–2023). In each population, 10–20 individuals forming floral buds were randomly selected, and plant height, leaf number, maximum leaf area (MLA), and floral bud number were measured.

In the statistical analysis, each measured trait was compared among populations by Steel-Dwass test. Next, size-dependency of leaf production and flower reproduction was evaluated by generalized linear mixed effect models (GLMMs) in which maximum leaf area or floral bud number was the response variable, taxonomic group, height, and their interaction were set as the explanatory variables, and populations was set as a random factor. The GLMMs were performed using the package of lme4 (Bates 2011), postulating gamma error distribution (maximum leaf area) or Poisson error distribution (floral bud number). A principal components analysis (PCA) was also conducted based on all measured traits (maximum leaf area, plant height, floral bud number, and leaf number).

Phenological observation in a common garden

Phenological traits were compared among taxonomic groups at the GDRC common

garden using the transplanted plants for the pollination experiment. Phenological observation was conducted for three taxonomic groups (2x-*kam* plants from Tomakomai, 4x-*kam* plants from Teshio, and 4x-*bulb* plants from Maruseppu) at approximately 10-day intervals from April to September during three seasons (2021–2023), and the dates of leaf emergence, flowering initiation, and cessation of flowering were recorded. Furthermore, plant height, maximum leaf area, and floral bud number were measured at flowering time. Phenological events and performance traits were compared among taxonomic groups by GLMMs, postulating a Poisson error distribution (for floral bud number) or gamma error distribution (for phenological events, plant height, and maximum leaf area) with log-link function. In the GLMMs, the response variable was each of the phenological and performance traits, the explanatory variable was taxonomic group, and observation year was set as a random factor. Size-dependency of flower production was also tested by a GLMM in which floral bud number was the response variable, population, height, and their interaction were the explanatory variables, and observation year was set as a random factor. All statistical analyses were performed in the package of lme4 in R. In addition, PCA was also conducted based on all measured phenological characters (date of leaf emergence, flowering initiation, and cessation of flowering).

Results

Pollination experiment

The pollination experiment in the natural populations commonly showed low seed-set rates in the bagging and self-pollination treatments. The seed-set rates under natural conditions were significantly higher than those of the bagging and self-pollination

treatments, and bagged and self-pollinated plants produced very few seeds in all populations, suggesting self-incompatibility in every population (Table 1-1; Fig. 1-2 A–E). In addition, there was no significant difference in seed-set rates between the outcross treatment and natural pollination in all populations, suggesting no pollen limitation under natural conditions (Table 1-1; Fig. 1-2 A–E).

The pollination experiment conducted in the common garden showed that the seed-set rates of inter-cytotype pollination (2x-*kam* and the 4x-*kam*) were lower than that of outcross within a cytotype both in the 2x-*kam* and the 4x-*kam* (Fig. 1-3). In the 4x-*kam* individuals, the seed-set rates of the crossing with the 4x-*bulb* (within the same ploidy but between varieties) were relatively higher than the crossing with the 2x-*kam*, but lower than that of outcross within the 4x-*kam* (Fig. 1-3).

Comparisons of plant performance across natural populations

Morphological measurements revealed that plant height and maximum leaf area in the 4x-*kam* populations were larger than those in the 2x-*kam* and 4x-*bulb* populations (Fig. 1-4 A, C). In addition, the 4x-*bulb* populations showed smaller number of floral buds than the 4x-*kam* and 2x-*kam* populations (Fig. 1-4 D). There was no clear difference in leaf number among populations (Fig. 1-4 B). Regarding the size-dependency of leaf production, a significant interaction was detected between plant height and taxonomic group by the GLM. Size-dependency of leaf production was apparent in the 4x-*kam* populations compared to the 2x-*kam* and 4x-*bulb* populations (Table 1-2 a; Fig. 1-5 A). Regarding the size-dependency of floral bud production, a significant interaction was detected between plant height and taxonomic group by the GLM, indicating that flower production of the 2x-*kam* populations was larger than that of the 4x-*kam* and 4x-*bulb*

populations (Table 1-2 b; Fig. 1-5 B). The PCA result showed that the morphological traits were largely overlapped among the taxonomic groups, but the 4x-*kam* and the 4x-*bulb* showed clear differences in the morphological traits (Fig. 1-6 A).

Comparisons of plant performance and phenological traits in the common garden

In the common garden experiment, 4x-*bulb* plants showed smaller plant height, leaf area, and flower production than 2x-*kam* and 4x-*kam* plants (Table 1-3; Fig. 1-7). Flower production increased with plant size in every taxonomic group, but the extent of size-dependency was the smallest in 4x-*kam* plants (Table 1-3; Fig. 1-7 D). Regarding the phenological traits, leaf emergence time of 4x-*bulb* plants was later than that of 2x-*kam* and 4x-*kam* plants across years, whereas 4x-*bulb* plants initiated and finished flowering earlier than 2x-*kam* and 4x-*kam* plants (Table 1-4; Fig. 1-8). The PCA result showed that the phenological traits of 4x-*bulb* plants were clearly different from those of 2x-*kam* and 4x-*kam* plants, whereas there was large overlaps in the phenological traits between 2x-*kam* and 4x-*kam* plants (Fig. 1-6 B).

Discussion

Mechanisms mitigating the minority cytotype exclusion (MCE)

Very low seed-set rates of the reciprocal crossing between 2x-*kam* and 4x-*kam* plants indicate that the inter-cytotype crossing does not contribute to the fitness of both cytotypes. Although the physiological mechanism of the inter-cytotype incompatibility is unclear in the present study, 4x-*kam* individuals may experience the MCE at the early establishment stage due to a low seed formation by the frequency-dependent receipt of invalid pollen from the diploids. On the other hand, risk of the production of inviable

triploid offspring may be small between the cytotypes.

The pollination experiment in the natural populations showed no evidence for the acquisition of self-compatibility by the polyploidization in *P. kamtschaticus*. Furthermore, the common garden experiment showed no evidence for the phenological isolation between 2x-*kam* and 4x-*kam* due to a large flowering overlap between cytotypes. Therefore, neither self-compatible system nor phenological shift contributed to the mitigation of the MCE in *P. kamtschaticus*. Although several studies indicated that the polyploidization promoted self-compatibility (Siopa et al. 2020; Wakui and Kudo 2021), this tendency may be not always common in polyploid species (Mable 2004). In addition, phenological shifts by the polyploidization might be insufficient to avoid inter-cytotype crossing completely (Laport et al. 2016). When both of seed production by selfing and phenological isolation are not effective, only spatial separation is possible to mitigate the MCE for nep-polyploids. Allopatric distribution between 2x-*kam* and 4x-*kam* may be caused by the difference in niche preference (see next section). If so, immediate niche differentiation might lead to the establishment of tetraploid populations.

The effects of polyploidization on morphological traits and life-history traits

From the morphological comparisons in the natural populations, 4x-*kam* plants showed larger stature and leaf area than 2x-*kam* plants as reported in a previous study (Nakagawa 2006). Enlargement of plant size is often observed in polyploid plants (Stebbins 1971; Balao et al. 2011) due to an increase in cell size or number (Zhang et al. 2019). However, floral bud number of 4x-*kam* plants was not clearly different from 2x-*kam* plants, resulting in a lower size-dependency of flower production in 4x-*kam* plants. These results indicate that 2x-*kam* is superior to 4x-*kam* regarding the efficiency of population growth

because 2x-*kam* plants can produce more flowers and seeds at smaller size. In contrast, 4x-*kam* plants are likely advantageous in the competition for light capture due to the large stature. Furthermore, these ecological traits specific to cytotype were maintained in the common garden. Thus, 2x-*kam* and 4x-*kam* populations are ecologically differentiated, and each cytotype may have advantage in different life-stages, i.e., more flower/seed production in 2x-*kam* and more vegetative growth in 4x-*kam*. Thus, the polyploidization in *P. kamtschaticus* might cause a niche differentiation between the cytotypes via the changes in the morphological and ecological traits.

Post-polyploidization evolution in subalpine areas

Comparisons of the morphological and life-history traits in the natural populations and the common garden showed significant ecological differences between 4x-*kam* and 4x-*bulb* despite the same ploidy level. Generally, 4x-*bulb* individuals showed smaller height and leaf size than 4x-*kam* individuals. In addition, 4x-*bulb* showed later leaf emergence, earlier flowering time, and shorter flowering period than 4x-*kam*, resulting in a phenological isolation between them. Because 4x-*bulb* grows at higher elevations than 2x-*kam* and 4x-*kam* (Kudo and Hirao 2020), these traits may be adaptive in high elevation environment. Small sized leaf and short stature are adaptive response to high elevation environments to mitigate the damage by strong wind and irradiation (Körner 1999; Shimono et al. 2009). Because the risk of frost damage in early season increases with higher elevation (Kudo 2021), furthermore, later leaf emergence in 4x-*bulb* is advantageous to avoid the frost damage. At high elevation, short growing period due to cool temperature and late snowmelt time is a strong limiting factor for the establishment of seedlings. The shifts of flowering period in 4x-*bulb*, i.e., acceleration of flowering

onset time and short flowering periods, may be an adaptive response to complete seed maturation rapidly.

Previous studies predicted that 4x-*bulb* might be derived from 4x-*kam* ancestor based on the allozyme analysis (Kudo and Hirao 2020), indicating a post-polyploidization evolution in 4x-*bulb*. To adapt to high elevation environment, 4x-*bulb* might be exposed to the selective forces for small plant size, phenological shift, and the evolution of vegetative reproduction. It is noteworthy that the polyploidization in this species might lead to two different evolutionary process: (1) plant size increment for 4x-*kam*, and (2) a decrease in plant size and phenological shifts to short growing season for 4x-*bulb*. The crossing between 4x-*kam* and 4x-*bulb* showed lower seed-set success compared to the crossing within 4x-*kam* plants, indicating the moderate level of the reproductive isolation. Thus, 4x-*bulb* may be under ongoing speciation process from 4x-*kam*.

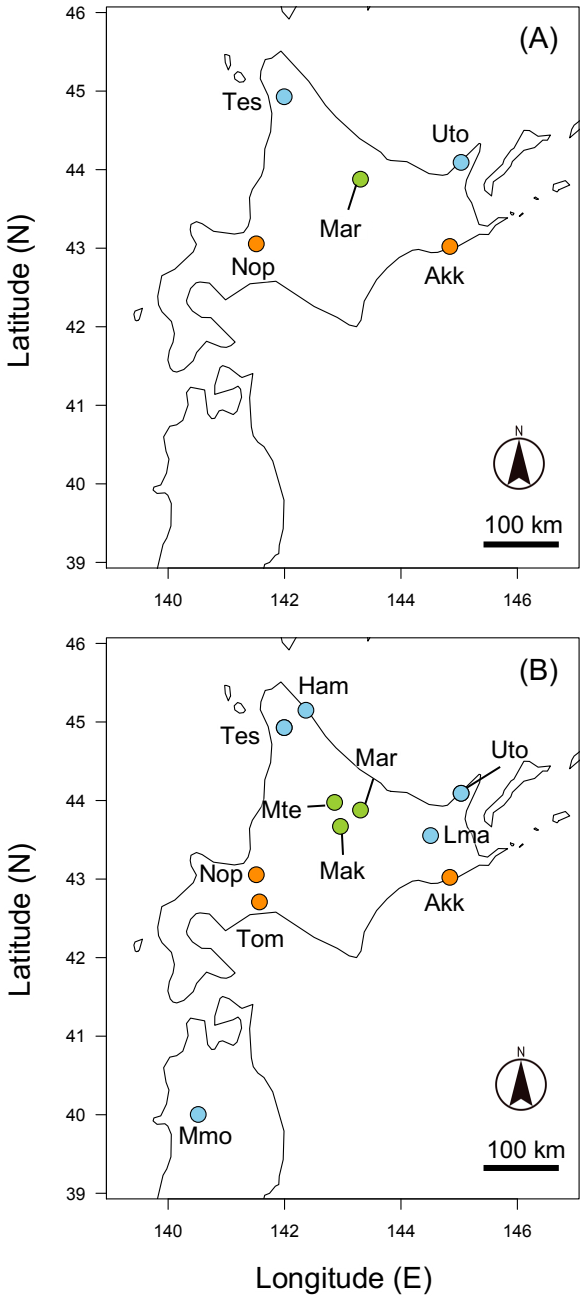

Figure 1-1. Geographical locations of study sites in Hokkaido and Honshu used for pollination experiment (A), and morphological measurement (B). Orange: 2x-*kam*, blue: 4x-*kam*, and green: 4x-*bulb* populations. Nop: Nopporo, Tom: Tomakomai, Akk: Akkeshi, Tes: Teshio, Uto: Utoro, Ham: Hamatonbetsu, Lma: Lake Mashu, Mmo: Mt. Moriyoshi, Mar: Maruseppu, Mak: Mt. Aka, Mte: Mt. Teshio.

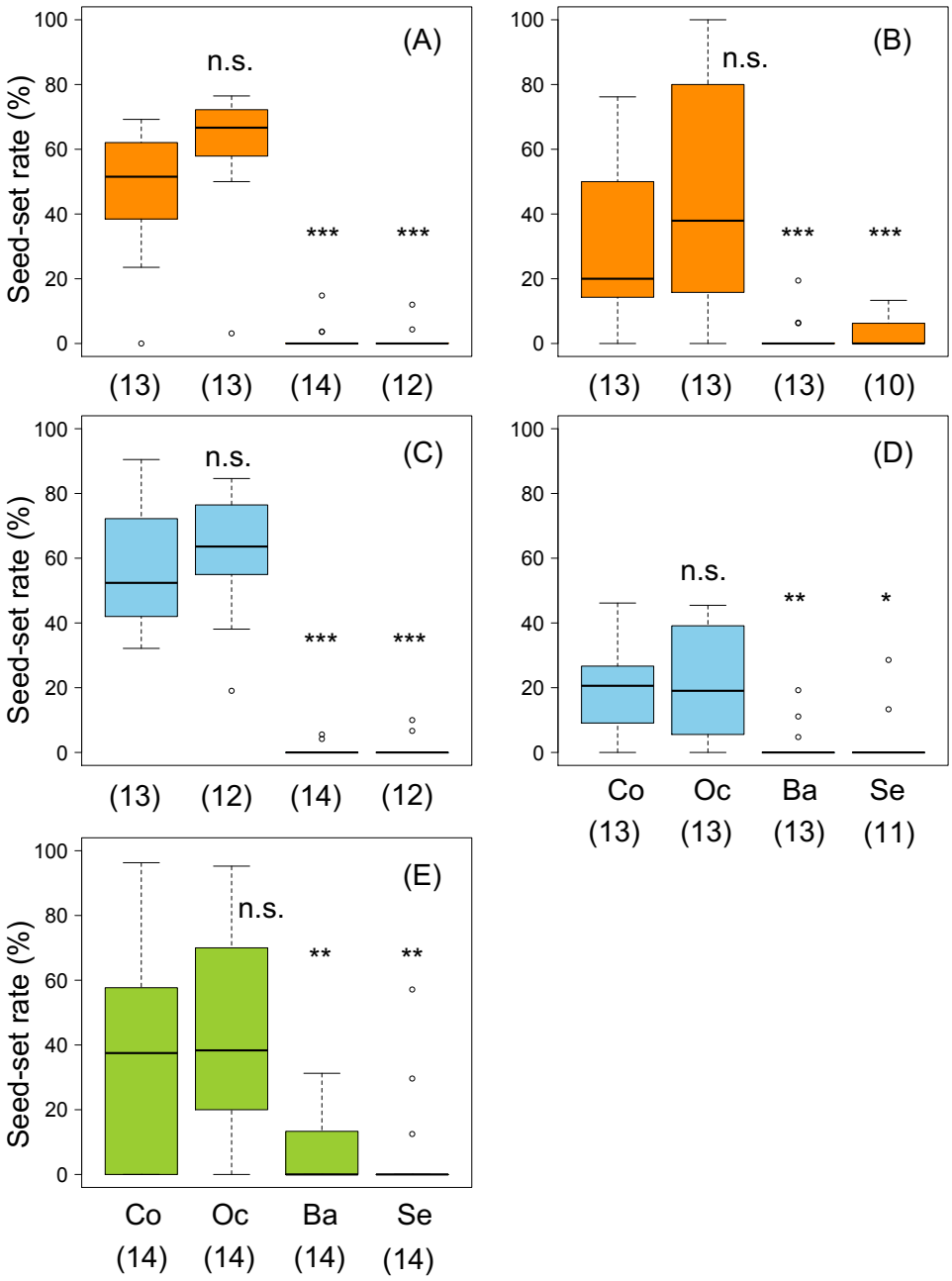

Figure 1-2. Results of the hand-pollination experiment conducted in the natural populations. (A) Akkeshi, (B) Nopporo, (C) Utoro, (D) Teshio, and (E) Maruseppu. Seed-set percentage in each treatment (Co: control, Oc: outcross pollination, Ba: simple bagging, Se: self-pollination) is shown. Orange: 2x-*kam*, blue: 4x-*kam*, and green: 4x-*bulb* populations. Sample size of each treatment is shown within parentheses. ***, **, * $P < 0.001$, 0.01, and 0.05, respectively.

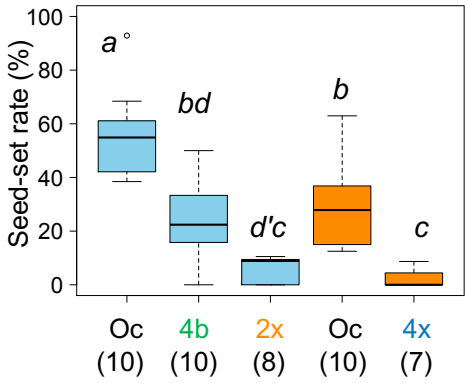

Figure 1-3. Results of the hand-pollination experiment conducted in the common garden in Sapporo. Seed-set percentage in each treatment (Oc: outcross pollination within same population, 4b: inter-variety crossing with 4x-*bulb*, 2x: inter-cytotype crossing with 2x-*kam*, 4x: inter-cytotype crossing with 4x-*kam*) is shown. Orange: recipient cytotype is 2x-*kam*; blue: recipient cytotype is 4x-*kam*. Sample size of each treatment is shown within parentheses. Different characters indicate significant difference in each species among treatments ($P < 0.05$, ': < 0.1, Steel-Dwass test).

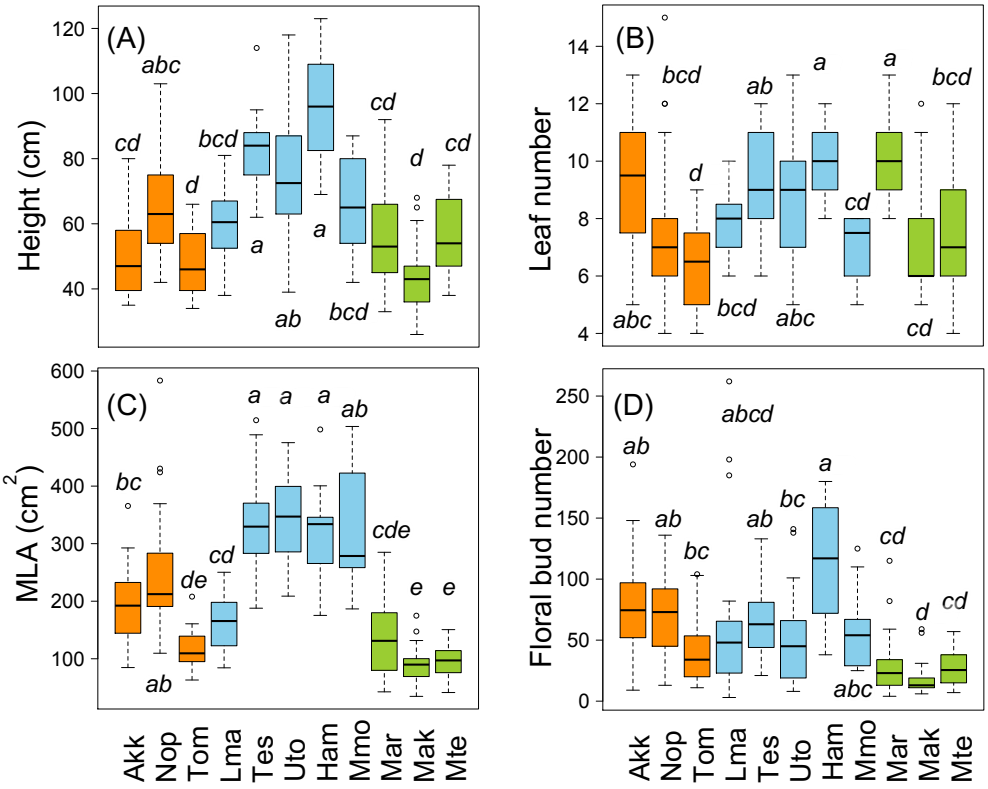

Figure 1-4. Comparisons of morphological traits among populations of *Parasenecio kamtschaticus* in the natural populations. (A) Plant height, (B) leaf number, (C) maximum leaf area, (D) floral bud number. blue: Orange: 2x-*kam*, blue: 4x-*kam*, and green: 4x-*bulb* populations. Different characters indicate significant difference in each species among treatments ($P < 0.05$, Steel-Dwass test).

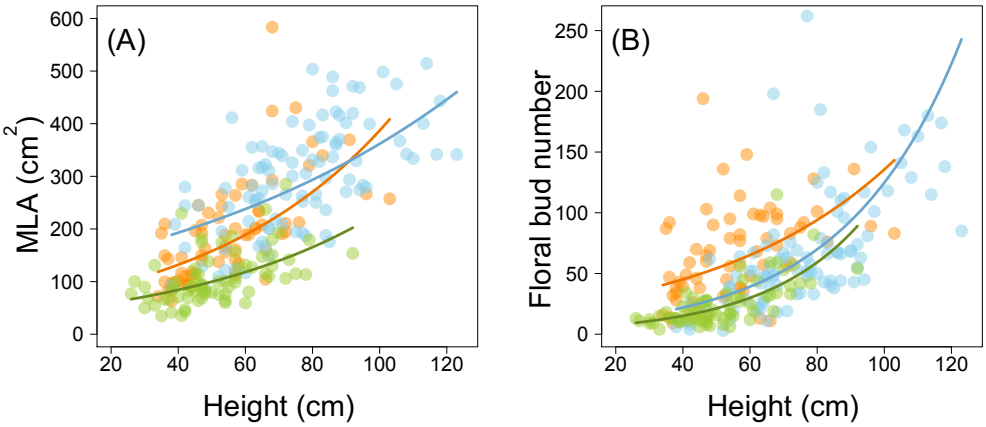

Figure 1-5. Relationship between plant height and maximum leaf area (A) and floral bud number (B) in the natural populations. Orange: 2x-*kam*, blue: 4x-*kam*, and green: 4x-*bulb* individuals.

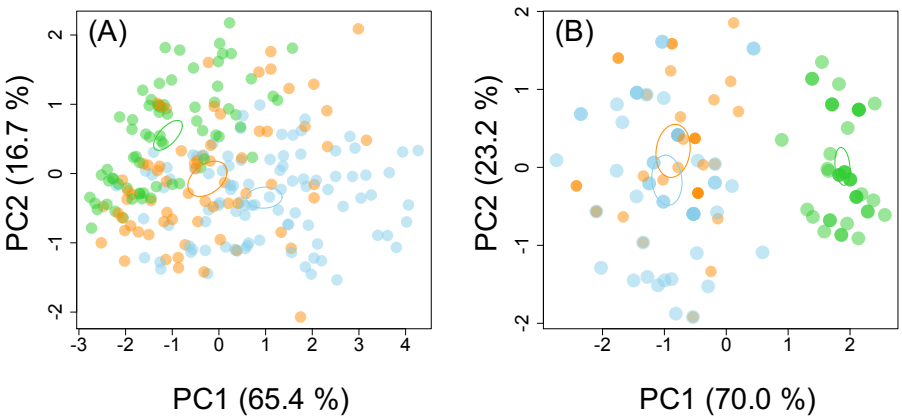

Figure 1-6. Results of the principal component analysis (PCA) based on the morphological traits in the natural populations (A), and the phenological traits in the common garden (B). Orange: 2x-*kam*, blue: 4x-*kam*, and green: 4x-*bulb* individuals. Circles indicate 95% inertia ellipses of standard error of taxonomic groups.

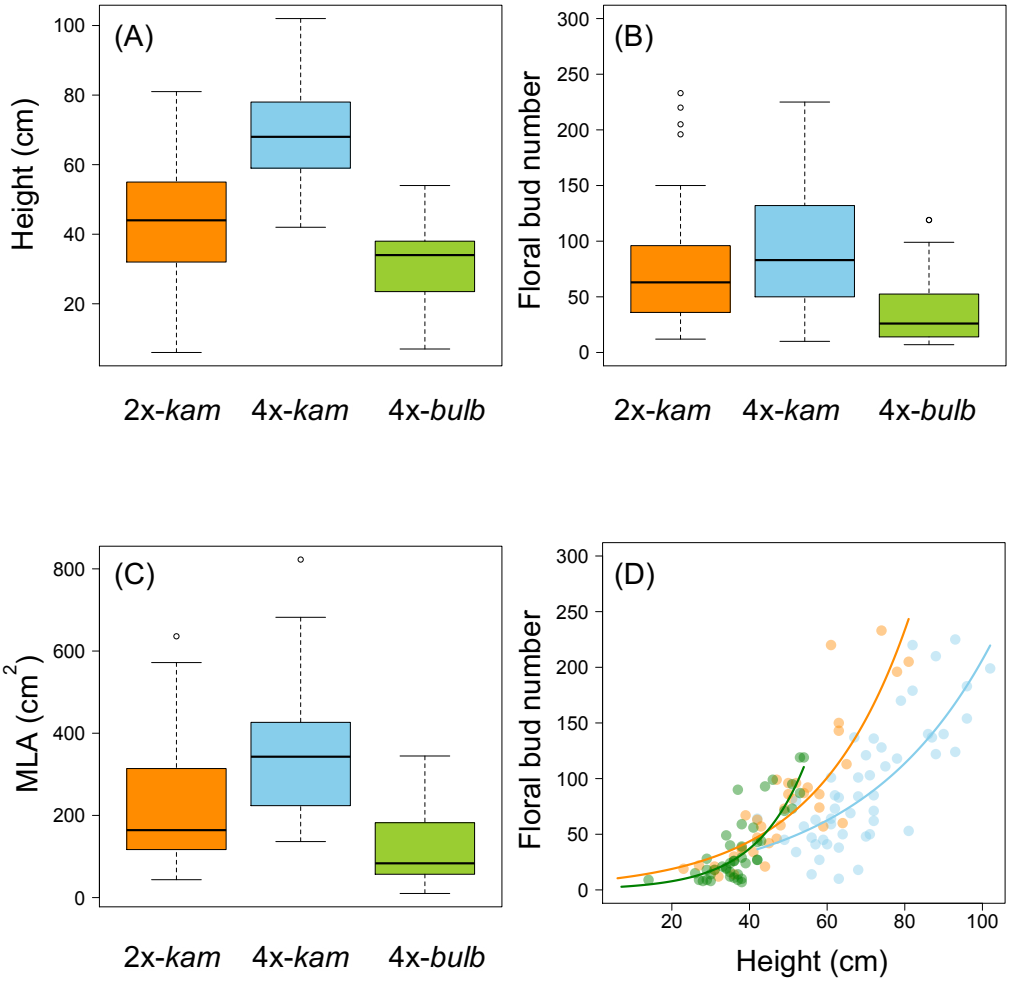

Figure 1-7. Comparisons of morphological traits among taxonomic groups of *Parasenecio kamtschaticus* in the common garden. (A) Plant height, (B) floral bud number, (C) maximum leaf area, and (D) the relationship between floral bud number and plant height. Each of A–D includes the three-year data (2021–2023).

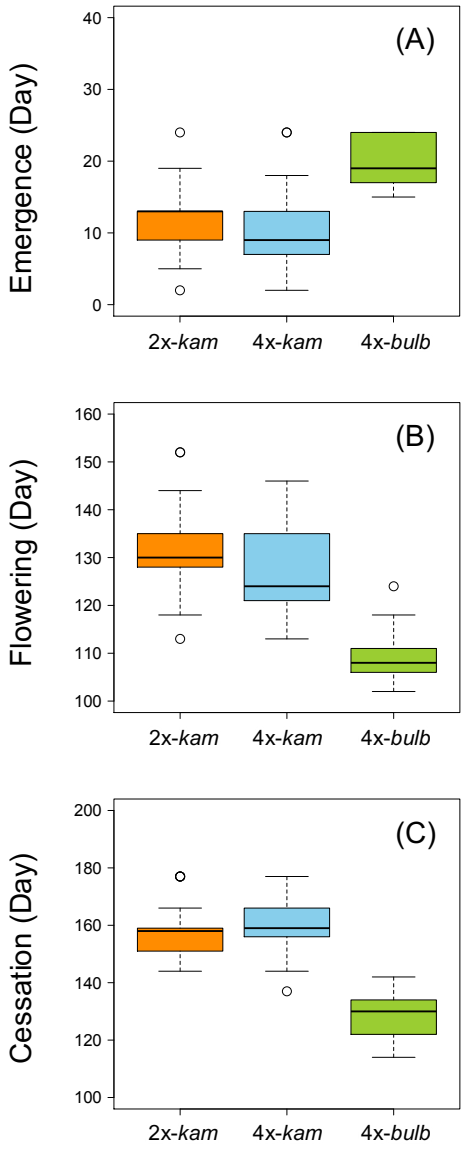

Figure 1-8. Comparisons of phenological traits among taxonomic groups of *Parasenecio kamtschaticus* in the common garden. (A) Leaf emergence date, (B) flowering onset date, and (C) flowering cessation date. Each day: day of the year from April 1. Three-years data (2021-2023) were pooled in each figure.

Table 1-1. GLM results of the pollination experiment in the natural populations. Estimated coefficient, standard error, *z* value, and *P* value are shown. Orange (Akkeshi and Nopporo populations): 2x-*kam*, blue (Teshio and Utoro populations): 4x-*kam*, green (Maruseppu population): 4x-*bulb*.

(a) Akkeshi

Variable	Coefficient	SE	z	*P*	
Intercept (Control)	-0.743	0.138	-5.396	< 0.001	***
Outcross pollination	0.239	0.193	1.242	0.214	
Bagging	-3.281	0.447	-7.338	< 0.001	***
Self-pollination	-3.499	0.533	-6.560	< 0.001	***

(b) Nopporo

Variable	Coefficient	SE	z	*P*	
Intercept (Control)	-1.188	0.289	-4.117	< 0.001	***
Outcross pollination	0.366	0.404	0.906	0.365	
Bagging	-2.235	0.531	-4.211	< 0.001	***
Self-pollination	-2.449	0.652	-3.754	< 0.001	***

(c) Teshio

Variable	Coefficient	SE	z	*P*	
Intercept (Control)	-1.668	0.321	-5.207	< 0.001	***
Outcross pollination	0.088	0.451	0.196	0.845	
Bagging	-1.830	0.567	-3.226	0.0013	**
Self-pollination	-1.479	0.582	-2.539	0.011	*

(d) Utoro

Variable	Coefficient	SE	z	*P*	
Intercept (Control)	-0.624	0.088	-7.085	< 0.001	***
Outcross pollination	0.132	0.125	1.060	0.289	
Bagging	-4.473	0.713	-6.271	< 0.001	***
Self-pollination	-4.124	0.713	-5.784	< 0.001	***

(e) Maruseppu

Variable	Coefficient	SE	z	*P*	
Intercept (Control)	-1.031	0.375	-2.750	0.006	**
Outcross pollination	0.222	0.525	0.424	0.672	
Bagging	-1.695	0.587	-2.887	0.004	**
Self-pollination	-1.576	0.574	-2.744	0.006	**

*** $P < 0.001$, ** $P < 0.01$, * $P < 0.05$. Intercept = Control

Table 1-2. GLM results of the size-dependency of leaf production (a) and flower production (b) in the natural populations. Estimated coefficient, standard error, *t* and *z* values, and *P* value are shown.

(a) Size-dependency of leaf production

Variable	Coefficient	SE	*t*	*P*	
Intercept	4.165	0.219	19.045	< 0.001	***
Plant height (PH)	0.018	0.003	6.608	< 0.001	***
4x-*kam*	0.678	0.287	2.360	0.018	*
4x-*bulb*	-0.406	0.305	-1.329	0.184	
PH × 4x-*kam*	-0.007	0.003	-2.251	0.024	*
PH × 4x-*bulb*	-0.001	0.004	-0.277	0.782	

*** $P < 0.001$, * $P < 0.05$. Intercept = 2x-*kam*, PH × 2x-*kam*.

(b) Size-dependency of flower production

Variable	Coefficient	SE	*z*	*P*	
Intercept	3.078	0.147	20.869	< 0.001	***
Plant height (PH)	0.018	0.001	17.285	< 0.001	***
4x-*kam*	-1.148	0.193	-5.936	< 0.001	***
4x-*bulb*	-1.722	0.223	-7.729	< 0.001	***
PH × 4x-*kam*	0.011	0.001	7.842	< 0.001	***
PH × 4x-*bulb*	0.016	0.002	7.850	< 0.001	***

*** $P < 0.001$, * $P < 0.05$. Intercept = 2x-*kam*, PH × 2x-*kam*.

Table 1-3. GLMM results of the morphological traits (plant height, maximum leaf area, and floral bud number) in each taxonomic group (2x-*kam*, 4x-*kam*, and 4x-*bulb*) in the common garden. Estimated coefficient, standard error, *t* and *z* values, and *P* value are shown.

(a) Plant height (PH) and maximum leaf area (MLA)

	PH				MLA			
Variable	Coefficient	SE	*t*	*P*	Coefficient	SE	*t*	*P*
Intercept	3.74	0.101	36.98	***	5.262	0.244	21.59	***
4x-*kam*	0.469	0.066	7.077	***	0.531	0.097	5.451	***
4x-*bulb*	-0.381	0.068	-5.622	***	-0.822	0.099	-8.302	***

*** $P < 0.001$. Intercept = 2x-*kam*.

(b) Floral bud number

Variable	Coefficient	SE	*z*	*P*
Intercept	4.211	0.200	21.011	***
4x-*kam*	0.255	0.023	10.810	***
4x-*bulb*	-0.900	0.032	-28.330	***

*** $P < 0.001$. Intercept = 2x-*kam*.

(c) Size-dependency of flower production

Variable	Coefficient	SE	*z*	*P*
Intercept	2.096	0.091	23.077	***
Plant height (PH)	0.042	0.001	29.049	***
4x-*kam*	0.245	0.111	2.187	*
4x-*bulb*	-1.602	0.156	-10.265	***
PH × 4x-*kam*	-0.012	0.002	-7.339	***
PH × 4x-*bulb*	0.036	0.003	10.823	***

*** $P < 0.001$, * $P < 0.05$. Intercept = 2x-*kam*, PH × 2x-*kam*.

Table 1-4. GLMM results of the phenological traits (leaf emergence date, flowering onset date, and flowering cessation date) in each taxonomic group (2x-*kam*, 4x-*kam*, and 4x-*bulb*) in the common garden. Estimated coefficient, standard error, *t* value, and *P* value are shown.

(a) Leaf emergence date

Variable	emergence	SE	*t*	*P*
Intercept	2.401	0.177	13.540	***
4x-*kam*	-0.205	0.082	-2.488	*
4x-*bulb*	0.573	0.085	6.741	***

*** $P < 0.001$, * $P < 0.05$. Intercept = 2x-*kam*.

(a) Flowering onset date

Variable	flowering	SE	*t*	*P*
Intercept	4.880	0.023	215.600	***
4x-*kam*	-0.030	0.012	-2.428	*
4x-*bulb*	-0.182	0.013	-14.210	***

*** $P < 0.001$, * $P < 0.05$. Intercept = 2x-*kam*.

(b) Flowering cessation date

Variable	flowering	SE	*t*	*P*
Intercept	5.045	0.023	215.700	***
4x-*kam*	0.028	0.011	2.448	*
4x-*bulb*	-0.189	0.012	-16.140	***

*** $P < 0.001$, * $P < 0.05$. Intercept = 2x-*kam*.

Chapter II: The mechanism driving a distinct distribution of the diploid and tetraploid populations in *Parasenecio kamtschaticus* var. *kamtschaticus*

Introduction

The distribution patterns of diploid and polyploid plants have received much attention in plant evolutionary ecology (Ramsey and Ramsey 2014). Polyploids are considered to be more tolerant to stressful conditions and likely to maintain the populations under harsh environments (Stebbins 1971; Godfree et al. 2017), resulting in wider or specific distributions different from the diploid progenitors (Levin 1983; Karunarathne et al. 2018). Regarding the polyploid distribution, niche differentiation reflecting the different ecological traits between diploids and tetraploids is often reported (Otto et al. 2007; Manzaneda et al. 2012). Inter-cytotype crossing, such as a crossing between diploid and tetraploid plants, often results in the production of sterile offspring. The niche differentiation of polyploids is an effective mechanism to mitigate the effects of minority cytotype exclusion (MCE: Levin 1975; Petit et al. 1999) and to establish polyploid populations.

Generally, polyploids tend to show different niche preference from diploids (López-Jurado et al. 2019; Wang et al. 2021), and they can exploit novel habitats to which they are pre-adaptive (Treier et al. 2009). Furthermore, niche differentiation often reflects local adaptation (Martin and Husband 2013) by which specific cytotype or phenotype inhabiting a habitat have greater fitness compared to newly migrated cytotype or phenotype to the habitat (Kawecki and Ebert 2004; Blanquart et al. 2013). There are some studies demonstrating the niche differentiation and local adaptation in polyploid taxa (McIntyre and Strauss 2017; Decanter et al. 2020). On the other hand, historical and

neutral process without adaptation (such as dispersal limitation and occasional invasion) may also affect the distribution patterns of polyploids (Godsoe et al. 2013; Casazza et al. 2017). To understand the diversification and evolution of widespread polyploid taxa, therefore, it is crucial to access what process causes the distribution pattern specific to polyploids.

Vigorous modification of morphological performance is an important characteristics in polyploids (McIntyre and Strauss 2017; Wei et al. 2019). Polyploids tend to grow faster (Sugiyama 2005) and reach at larger size than diploids (Segraves 2017; Corneillie et al. 2019), owing to the larger cell and organ sizes (Becker et al. 2022) and higher photosynthetic ability (Ulum et al. 2021). The vigorous performance brings about a competitive advantage in polyploids, as known as the widespread occurrence of polyploid invasive species (Cheng et al. 2020). On the other hand, little is known about the relationship between competitive ability and adaptability to various environmental conditions in polyploids, especially outside of their resident habitats.

As shown in Chapter I, there are large differences in the ecological traits between diploid and tetraploid phenotypes in *Parasenecio kamtschaticus* var. *kamtschaticus*. The 4x-*kam* plants (tetraploid) showed larger leaf area and plant height than the 2x-*kam* plants (diploid), whereas flower production did not differ between them, and size-dependency of flower production in the 2x-*kam* plants was superior to that in the 4x-*kam* plants. In addition, geographic distributions differed between the 2x-*kam* populations and the 4x-*kam* populations, indicating a possibility of niche differentiation. As Nakagawa (2006) reported, 4x-*kam* populations are distributed in the range of evergreen coniferous forests (boreal forests), while 2x-*kam* populations are distributed in the range of deciduous broad-leaved forests (cool-temperate forests) in Hokkaido. The environmental conditions

of forest floors were very different between the forest types, especially for the light conditions. Understory of deciduous forests was characterized by bright condition during the spring before canopy closure (Ida and Kudo 2010), whereas understory of evergreen forests was characterized by low light intensity throughout the year (Miyashita et al. 2012). This study inspected how the ecological traits of individual populations vary within and beyond the distribution range of each cytotype, and whether the cytotype-specific traits can explain the distribution patterns of 2x-*kam* and 4x-*kam* populations.

To test the niche differentiation between the diploid 2x-*kam* and the tetraploid 4x-*kam*, and the extent of their local adaptation, I conducted a reciprocal transplant experiment. Because local adaptation is expected to occur at various life stages (Hülber et al. 2018), I compared the performance between each ploidy phenotype at three stages; seed and seedling stage, flowering stage, and vegetative growth stage. I focused on the following question. (1) Do the tetraploids have ecological advantages across the environments compared to the diploids? (2) Do local cytotypes indicate higher performance than the foreign cytotypes in each original habitat condition? If so, which life stage contribute to the local adaptation?

Methods

A design of the reciprocal transplant experiment

To test the mechanisms of geographic segregation between 2x-*kam* populations and 4x-*kam* populations in Hokkaido, I conducted a reciprocal transplant experiment. Two sites were chosen for the reciprocal transplant experiment. One plot in the resident site of 2x-*kam* was established at Tomakomai Experimental Forest of Hokkaido University (TOEF; N 42.688°, E 141.573°, 25 m elevation) in a deciduous broad-leaved forest (natural forest

dominated by *Quercus crispula*). Another plot in the resident site of 4x-*kam* was established at Nayoro Research Office of Hokkaido University (NRO; N 44.327°, E 142.453°, 90 m elevation) in an evergreen coniferous forest (artificial forest of *Abies sachalinensis*). TOEF and NRO sites were located within the range of 2x-*kam* and 4x-*kam* distributions, respectively. I transplanted 2x-*kam* plants from two populations (Tomakomai and Akkeshi) and 4x-*kam* plants from two populations (Teshio and Utoro) to the experimental sites at TOEF and NRO. For the reciprocal transplant, I selected mature sized 20 plants forming floral scape in each population. The transplant was conducted in October 2020, when aboveground growth had been completed and started to wither to minimize the damage of transplant. Selected plants were planted in 8 columns and 10 rows at intervals of 60 cm, and the original populations of the plants were arranged alternately in each site (Fig. S2-1). In addition, I conducted a seed germination experiment in each experimental site. I collected mature seeds from the populations used for the transplant experiment, and 50 seeds per population were sowed on the 50 cell container (2.5 cm × 2.5 cm × 4.5 cm depth) in each site in November 2020. Thus, the overall design was 80 plants and 200 seeds from four source populations and two ploidy levels per experimental site. Furthermore, the plants grown in the GDRC common garden (See Chapter I) were also used as a reference of plant performance under good environmental conditions. Because the GDRC common garden is characterized by bright and nutrient-rich soil conditions, transplanted individuals may show the potential growth and reproduction activities without environmental stress. The landscape of the experimental sites and the common garden are shown in Figure 2-1.

In order to investigate the seasonal changes in environmental conditions, I measured air temperature at the height of 50 cm, illuminance (lux), and volumetric water content

(VWC %) of soil at the depth of 12 cm in each site and the common garden. By data loggers incorporating luxmeter and thermometer (HOBO logger CO-UA-002-08; Onset Computer, MA, USA), illuminance and air temperature were measured at 1-hour intervals from April 13 to October 2 in 2022. The illuminance was converted into the photosynthetic photon flux density (PPFD) by combined data with illuminance and PPFD using a HOBO logger and a quantum sensor (S-LIA-M003; Onset Computer, MA) in Nopporo Forest Park (N 43.033°, E 141.517°, 75 m elevation), in a deciduous broad-leaved forests in 2022. VWC was measured at approximately 1-month intervals from April 13 to September 4 in 2023 using a soil moisture sensor (HydroSense II; Campbell Scientific, USA). I compared VWC values among three sites (TOEF, NRO, and GDRC) using GLM postulating a gamma error distribution in which day of the year from April 1st, site, and their interaction were set as the explanatory variables. After that, the best-fit model was selected by the model selection by Akaike's information criterion (AIC) using "MuMIn" package in R.

Comparisons of cell size and photosynthetic traits

In order to check the anatomical difference between cytotypes, I measured the cell size of leaves in each source population. Three types of cells (epidermal cell, spongy tissue cell, and guard cell) were observed under an optical microscope (BX43, Olympus, 200X magnification). I collected the second-positioned leaves of six individuals originated from each source population that were grown at TOEF and NRO experimental sites in flowering season. I cut the leaves into small pieces (approximately 1 cm^2), placed the leaf piece on a glass slide, and added a few drops of water. Then, five cells per leaf piece and the cell type were randomly observed, and those of section area (epidermal cells) or

surface area (spongy tissue cells and guard cells) were measured using the free software ImageJ (ver. 1.53k; Schneider et al. 2012).

I measured photosynthetic properties of plants originated from the source populations that were grown in the experimental sites and the common gardens in 2021. The measurements were conducted in early summer before flowering (May 24 for TOEF and May 31 for GDRC) and late summer during the flowering season (July 28 for GDRC, August 17 for TOEF, and August 27 for NRO) for a second-positioned leaf for 3–5 individuals per population. The measurements were conducted under three light conditions (1500, 1000, and 0 $\mu mol \cdot m^{-2} \cdot s^{-1}$) of photosynthetically active radiation provided using the LI-6400 system (Li-Cor, Lincoln, NE, USA) at constant leaf temperature (25°C). From these measurements, I obtained maximum photosynthetic rate (A_{max}: maximum values under 1000 or 1500 $\mu mol \cdot m^{-2} \cdot s^{-1}$) and dark respiration rate (R_d: values under 0 $\mu mol \cdot m^{-2} \cdot s^{-1}$).

The size of each cell type was analyzed by GLMM, in which the explanatory variable was original population and experimental site, including their interaction, and individual plant was set as the random factor. In the GLMs for the comparison of photosynthetic traits, the response variable was A_{max} or R_d, and the explanatory variables were season (May and July), original population, and their interaction. All statistical analyses were performed postulating a gamma error distribution. The best-fit model was selected as mentioned before.

Comparisons of morphological traits and reproductive performance among populations

To inspect the differences in performance traits among population groups across the experimental sites, I measured morphological traits and reproductive performance at three

stages; (1) germination and seedling stage, (2) flowering stage, and (3) vegetative growth stage. Comparisons of these traits among population groups were conducted in each experimental site.

Seed germination rate was measured in each experimental site after snowmelt in May 2021, and the survival rate of seedlings were recorded in May 2022. GLMs postulating a binomial error distribution were performed to compare the germination rate and the survival rate, setting original population as the explanatory variable. To compare the reproductive performance at flowering stage, I recorded flowering rate (flowering individual / planted individual ratio) and floral bud number in each experimental site and the common garden during three seasons (2021–2023). In addition, I measured plant height and maximum leaf area (as parameters of vegetative growth) of all transplanted individuals at approximately 10-day intervals during three seasons (2021–2023). GLMs were performed for flowering rate (binomial error distribution), floral bud number (Poisson error distribution), maximum leaf area, and plant height (gamma error distribution), in which original population, research year, and their interaction were set as the explanatory variables. In addition, size-dependency of flower production was compared by GLMM postulating a Poisson error distribution, in which floral bud number was the response variable, plant height, population, and their interaction were the explanatory variables, and research year was the random effect. The data of the first year (2021) were excluded from the analyses to remove the effect of transplant. The best-fit model was selected as mentioned before.

Many plants grown at TOEF did not produce flowers in the second year (2022), probably due to low nutrient stress (see results). In order to clarify the reason of the low reproductive performance at TOEF, I newly transplanted a half number of plants grown

at TOEF to GDRC in 2023. This re-transplant treatment was conducted to adjust the same size structure between TOEF and GDRC. The comparisons of flowering rate, floral bud number, maximum leaf area, and plant height were performed using GLMs between the plants left at TOEF and moved to GDRC in 2023. In the GLM, site, original population, and their interaction term were set as the explanatory variables and error distribution was the same as mentioned above.

Results

Environmental conditions of the experimental sites and the common garden

TOEF site showed high PPFD during the early season (April to May), but low PPFD during the summer (June to August) due to canopy closure (Fig. 2-2 A). GDRC common garden showed relatively high PPFD throughout the season due to a slight cover of canopy trees (Fig. 2-2 C). In contrast, NRO site showed low PPFD throughout the growing season due to continuous shading by evergreen trees (Fig. 2-2 B). Seasonal pattern of air temperature was similar among sites (Fig. 2-2 D–F). In the best-fit model for VWC (soil moisture), the interaction term was removed, and the VWC values were significantly high at TOEF, and clearly decreased as season progressed in all sites (Table 2-1, Fig. 2-2 G).

Cell size and photosynthetic ability of each population

There were no significant differences in epidermal cell size and spongy tissue cell size among original populations, while 4x-*kam* plants (Teshio and Utoro) showed larger guard cell than the 2x-*kam* plants (Tomakomai and Akkeshi) (Table 2-2, Fig. 2-3).

For the photosynthetic properties, plants showed higher photosynthetic rate (A_{max})

and dark respiration rate (R_d) in early summer (May) than those in the mid-summer (July) in every population group grown at TOEF and GDRC (Tables 2-3, 2-4, Fig. 2-4; note that there was no measurement in May for NRO). There were no significant differences in A_{max} among population groups at NRO and GDRC and in R_d at all sites. Although there were significant differences in A_{max} among population groups at TOEF, no consistent tendency was detected between the ploidy levels.

Comparisons of seed germination rate and seedling survival rate among population groups

In the reciprocal transplant experiment, the 4x-*kam* seeds from Teshio population showed significantly lower germination rate than other populations at TOEF, a resident site of 2x-*kam*, whereas there was no significant difference in germination rate among population groups at NRO, a resident site of 4x-*kam* (Table 2-5; Table S2-1). Generally, seeds from all populations showed higher germination rate at TOEF (42–78 %) compared to NRO (20–38 %).

For seedling survival rate, 'population factor' was removed in the best-fit GLMs at both TOEF and NRO (Table 2-5). In contrast to germination rate, seedling survival rate was higher at NRO (50–79 %) compared to TOEF (5–24 %; Table S2-1).

Comparisons of flower production among population groups

The 4x-*kam* plants originated from Utoro population showed significantly higher flowering rate than the plants from other populations at TOEF, a non-resident site of 4x-*kam* (Table 2-6, Table S2-2, Fig. 2-5). On the other hand, significant difference in flower production was not detected among original populations at NRO and GDRC (Table 2-6). Thus, there was no population group that showed higher flower production at their

resident site. Regarding TOEF, all population groups showed low flowering rate compared to NRO (Fig. 2-5 A, C) and GDRC (Fig. 2-6 A).

Although there was a significant difference in floral bud number among population groups at TOEF, plants from the 2x-*kam* populations (Akkeshi and Tomakomai) were not superior to plants from the 4x-*kam* populations even at the resident site (Table 2-7 a, Table S2-2, Fig. 2-5 D). At NRO, plants from the 4x-*kam* population groups were not superior to plants from the 2x-*kam* populations (Table 2-7 b, Table S2-2; Fig. 2-5 B). However, plants from Akkeshi and Tomakomai populations, non-resident at NRO, greatly decreased flower production in 2023 compared to the plants from the resident 4x-*kam* populations (Table 2-7 B, Fig. 2-5 B). At GDRC, plants from Teshio showed larger flower production than plants from Tomakomai across years (Table 2-7 c, Table S2-2).

Comparisons of growth traits among population groups

The 4x-*kam* plants originated from Teshio and Utoro populations showed larger maximum leaf area than the 2x-*kam* plants originated from Akkeshi and Tomakomai populations at both experimental sites (Table 2-8, Table S2-3, Fig. 2-7 A, C). The 4x-*kam* plants were taller than the 2x-*kam* plants at NRO, but there was no significant difference among the population groups at TOEF (Table 2-9, Table S2-3; Fig. 2-7 B, D). This was because the 2x-*kam* plants showed taller stature at TOEF than at NRO, whereas the 4x-*kam* plants showed opposite pattern (Table S2-3).

In GDRC, the 4x-*kam* plants originated from Teshio population showed larger maximum leaf area and plant height than the 2x-*kam* plants originated from Tomakomai population (Tables 2-8 c and 2-9 c). In addition, maximum leaf area and plant height of the 2x-*kam* and 4x-*kam* plants reached at the peak almost the same period in each year

(Figs. 2-8 and 2-9). The significant interaction between plant height and population groups in the GLMM indicated that the extent of size-dependency of flower production was higher in 2x-*kam* than in 4x-*kam* at NRO and GDRC, whereas there was no size-dependency at TOEF, probably because small number of flowering individuals might mask the tendency (See "PH" in Table 2-10 a, Figs. 2-6 E, 2-10 A, B).

Inspection for the low flowering activity at TOEF by a re-transplant to GDRC

In the re-transplant experiment, the plants moved to GDRC showed larger maximum leaf area than those left at TOEF, whereas plant height decreased in GDRC at marginal level (Table 2-11, Table S2-4; Fig. 2-11). Furthermore, the plants moved to GDRC showed higher flowering rate and produced more floral buds than those left at TOEF. Thus, the low ability of flower production at TOEF might be related to the environmental conditions.

Discussion

Niche differentiation between polyploids and diploids

As described in Chapter I, 4x-*kam* plants had larger leaf size and plant height, but less size-dependency of flower production than 2x-*kam* plants in natural populations. These trends were maintained in the transplant experiment at NRO and in the common garden (GDRC), indicating that 2x-*kam* and 4x-*kam* were genetically differentiated. On the other hand, leaf size and plant height of 4x-*kam* plants decreased close to those of 2x-*kam* at TOEF, indicating the loss of the general superiority of polyploids under specific conditions. The decrease in the general superiority of polyploids is reported also in the previous studies conducting reciprocal transplant experiments (Flegrová and Krahulec

1999; Hülber et al. 2018). The results of present study suggest that the superiority of polyploids in *P. kamtschaticus* var. *kamtschaticus* reflects the niche separation to different habitat conditions between diploids and tetraploids. On the other hand, consistent polyploid superiority is found in some invasive species, for example, Yang et al. (2021) indicated that *Solidago canadensis* increased the extent of allelopathy by polyploidization, leading to general success without niche differentiation. Thus, the ecological trends in the superiority of polyploids may vary among species.

Variation in the ecological advantages of polyploids among the life-history stages

The relative superiority of resident cytotype has been observed in multiple life-history stages in polyploid species (Hülber et al. 2018). Also in the present study, the possibility of local adaptation in 4x-*kam* plants varied among the life-history stages. In the gemination experiment, the 4x-*kam* seeds from Teshio population showed higher geremination rate at NRO (resident site) but lower geremination rate at TOEF (alien site). However, seeds from other populations showed no superiority for germinability in the resident site, and there was no consistent tendency in each ploidy level. At the subsequent seedling stage, there was no evidence of the local adaptation for survival rate in all populations in the resident site.

Although there was no difference in flowering rate among populations at NRO, the number of floral buds in 2x-*kam* plants decreased in the second year, while 4x-*kam* plants produced floral buds vigorously also in the second year at NRO. Although observation of longer period is necessary, it may suggest the adaptability of 4x-*kam* plants to shaded conditions. At TOEF, however, flowering rates and floral bud number of all populations were lower than those at NRO even in 2x-*kam* plants, probably due to poor nutritional

soil conditions because of the volcanic products with little organic matter in Tomakomai region. Consequently, the reciprocal transplant experiment did not clearly support the possibility of local adaptation at the flowering stage at TOEF.

At the vegetative growth stage, finally, consistent patterns of performance traits were observed between diploids and tetraploids across years. Regarding leaf size, 4x-*kam* plants produced larger leaves than 2x-*kam* plants at both NRO (resident site of 4x-*kam*) and TOEF (resident site of 2x-*kam*), suggesting that 4x-*kam* plants were more competitive in terms of light harvesting. In addition, plants from all populations were larger at NRO than at TOEF, indicating the plasticity responding to shaded conditions under evergreen coniferous forests. Regarding plant height, 4x-*kam* plants was taller than 2x-*kam* plants at NRO, whereas there was no significant difference between 2x-*kam* plants and 4x-*kam* plants at TOEF. Consequently, local adaptation of 4x-*kam* plants may exist at the vegetative growth stage.

Establishment of 4x-*kam* at understory of evergreen coniferous forests owing to the pre-adaptive morphological traits

The present study indicated the evidence of niche differentiation and the advantage of 4x-*kam* plants at the vegetative growth stage under evergreen coniferous forests, which is consistent with the reported cytotype distribution in natural populations (Nakagawa 2006; Kudo and Hirao 2020). The possible explanation for this pattern is the pre-adaptation of 4x-*kam* to shaded environment of boreal forests. As mentioned in Chapter I, 4x-*kam* plants can reach at larger size more rapidly than 2x-*kam* plants in natural populations. Although I speculated that the larger stature of tetraploids might be caused by the increment of individual cell size and/or the improvement of photosynthetic ability by the polyploidization, the increment of cell size was found only in the guard cell, while the

photosynthetic ability was not improved in 4x-*kam* plants. Therefore, the patterns of cell size and photosynthetic ability by polyploidization may be inconsistent among species (Gao et al. 2017; Chen et al. 2021; Becker et al. 2022). Other factors, such as the increases in cell number and cell division rate might be attributed to larger leaf size and stature (Zhang et al. 2019) in 4x-*kam* plants. The morphological features of higher stem and larger leaf size are regarded as competitive traits (Grime 1977), and those features should be advantageous for the competition under shaded conditions. Thus, enlarged stature of 4x-*kam* plants may be a probably pre-adaptive to grow under boreal forests characterized by limited light conditions throughout the year, and they can grow well compared to 2x-*kam* plants there.

On the other hand, 4x-*kam* plants did not show larger stature than 2x-*kam* plants at TOEF. One possible reason is higher nutrient requirements in 4x-*kam* plants. Polyploidization may causes the increasing nutrient requirements (Anneberg and Segraves 2023), which may lead to less growth in nutrient-poor environments. From the results, reproductive performance of all populations was more limited at TOEF, although other environmental conditions, such as soil moisture and air temperature were almost the same as NRO. It was noteworthy that the re-transplanted plants from TOEF to GDRC improved the flowering rate and floral bud production compared to the plants left at TOEF. These results indicates that the soil conditions at TOEF negatively affect the reproductive performance. The soil of TOEF consists of coarse-grained immature soil formed by the eruption of Mt. Tarumae, whrere organic soil layer was very thin (Sakuma 1987). The possibility that nutrient-poor soil decreased reproductive performance at TOEF was also supported by the results of Chapter I, i.e., floral bud production in Tomakomai population was very small compared to other 2x-*kam* and 4x-*kam* populations. It seems that 4x-*kam*

plants requiring more nutrients than 2x-*kam* plants cannot grow well there.

Implication for the process driving different distribution between 2x-*kam* and 4x-*kam*

Results of the reciprocal transplant experiment suggest that current distribution patterns of 2x-*kam* and 4x-*kam* are likely caused by the niche differentiation between them. In the shaded floor of boreal forests, 4x-*kam* plants may be able to outcompete 2x-*kam* plants by the competitive ability for light capture, which are pre-adaptive to shaded environments. On the other hand, in the seasonally bright floor of cool-temperate forests, 2x-*kam* plants may be able to outcompete 4x-*kam* plants by the vigorous reproductive ability, resulting in a rapid population growth. On the other hand, 2x-*kam* populations are distributed as well as 4x-*kam* populations in the eastern part of Hokkaido, where evergreen coniferous forests are common (Nakagawa 2006). Morphological traits may vary among populations even in the same ploidy level as shown in the present study. Thus, the presence of 4x-*kam* populations with small stature may cause partial dominance of 2x-*kam* populations with large stature in boreal forests. Furthermore, the tolerance to nutrient-poor soil may affect the distribution patterns between diploid and tetraploid populations. As shown in the present study, the advantage of 4x-*kam* plants may be decreased on nutrient-poor soil. Thus, actual distribution patterns of 2x-*kam* and 4x-*kam* populations may reflect not only forest type but also soil conditions.

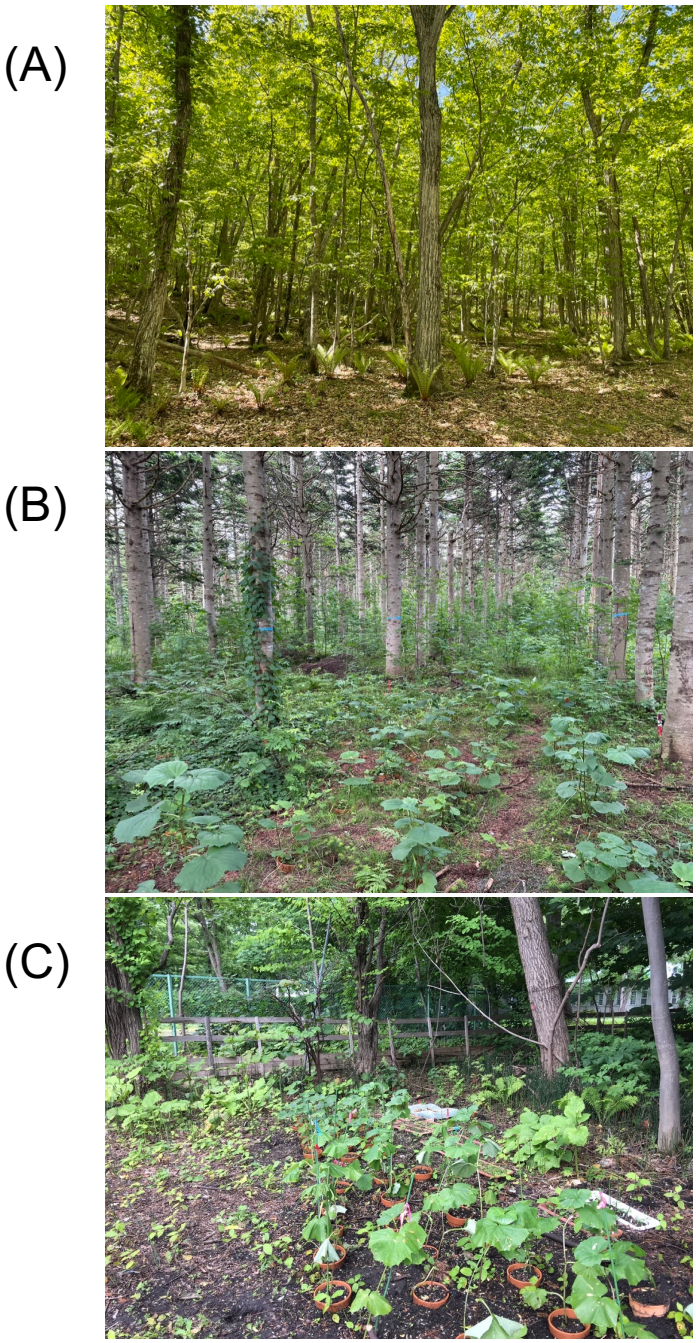

Figure 2-1. The landscapes of experimental sites and common garden. (A) Tomakomai Experimental Forest, Hokkaido University (TOEF), (B) Nayoro Research Office, Hokkaido University (NRO), and (C) experimental garden of Genome Dynamics Research Center, Hokkaido University (GDRC).

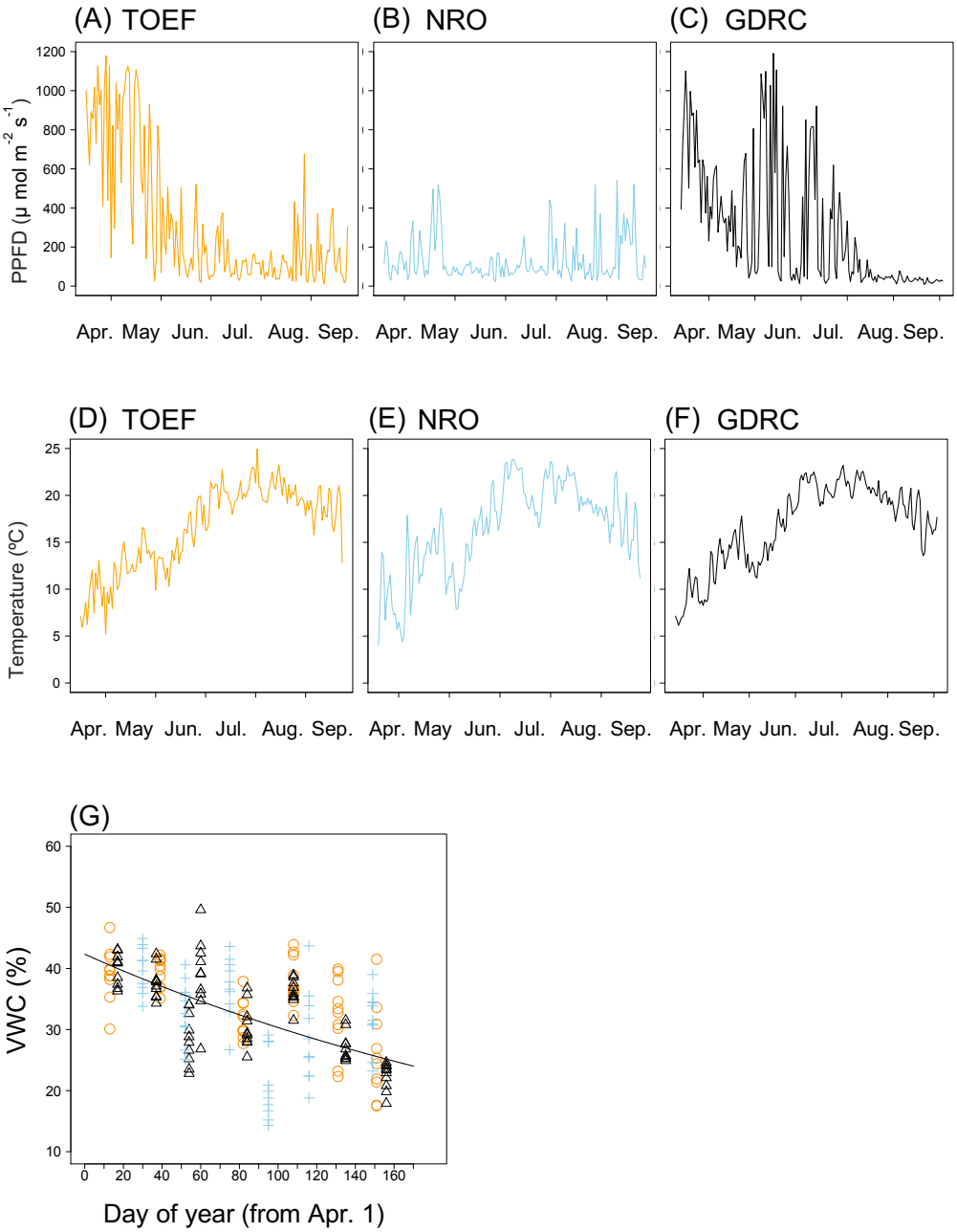

Figure 2-2. Environmental conditions of each experimental site. (A)–(C) seasonal pattern of daily maximum photosynthetic photon flux density (PPFD), (D)–(F) daily mean temperature, and (G) volumetric water content (VWC). Orange lines: TOEF, blue lines: NRO, and black lines: GDRC for (A)–(F). Circles: TOEF, crosses: NRO, and triangles: GDRC for (G).

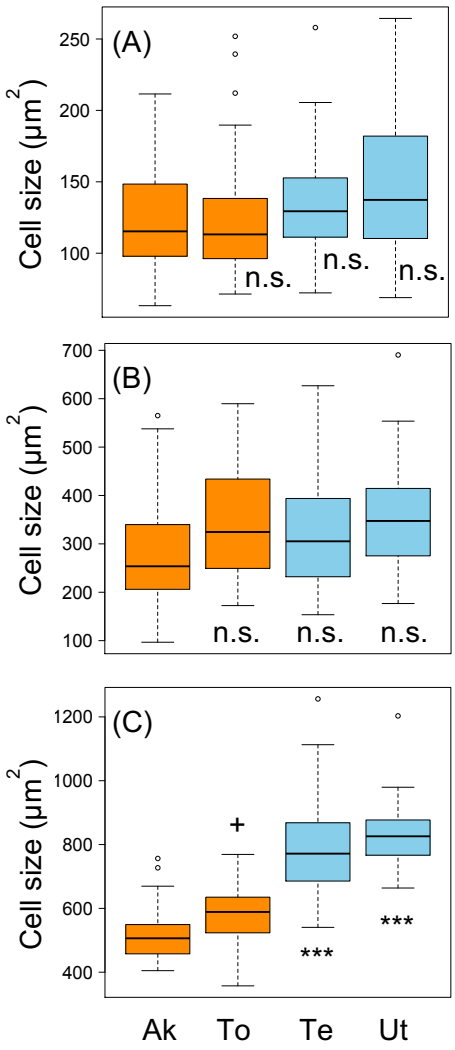

Figure 2-3. Comparisons of cell sizes among population groups. (A) epidermal cell, (B) spongy tissue cell, and (C) guard cell. Orange boxes: 2x-*kam*, blue boxes: 4x-*kam*. Ak: Akkeshi, To: Tomakomai, Te: Teshio, Ut: Utoro. *** $P < 0.001$, + $P < 0.1$.

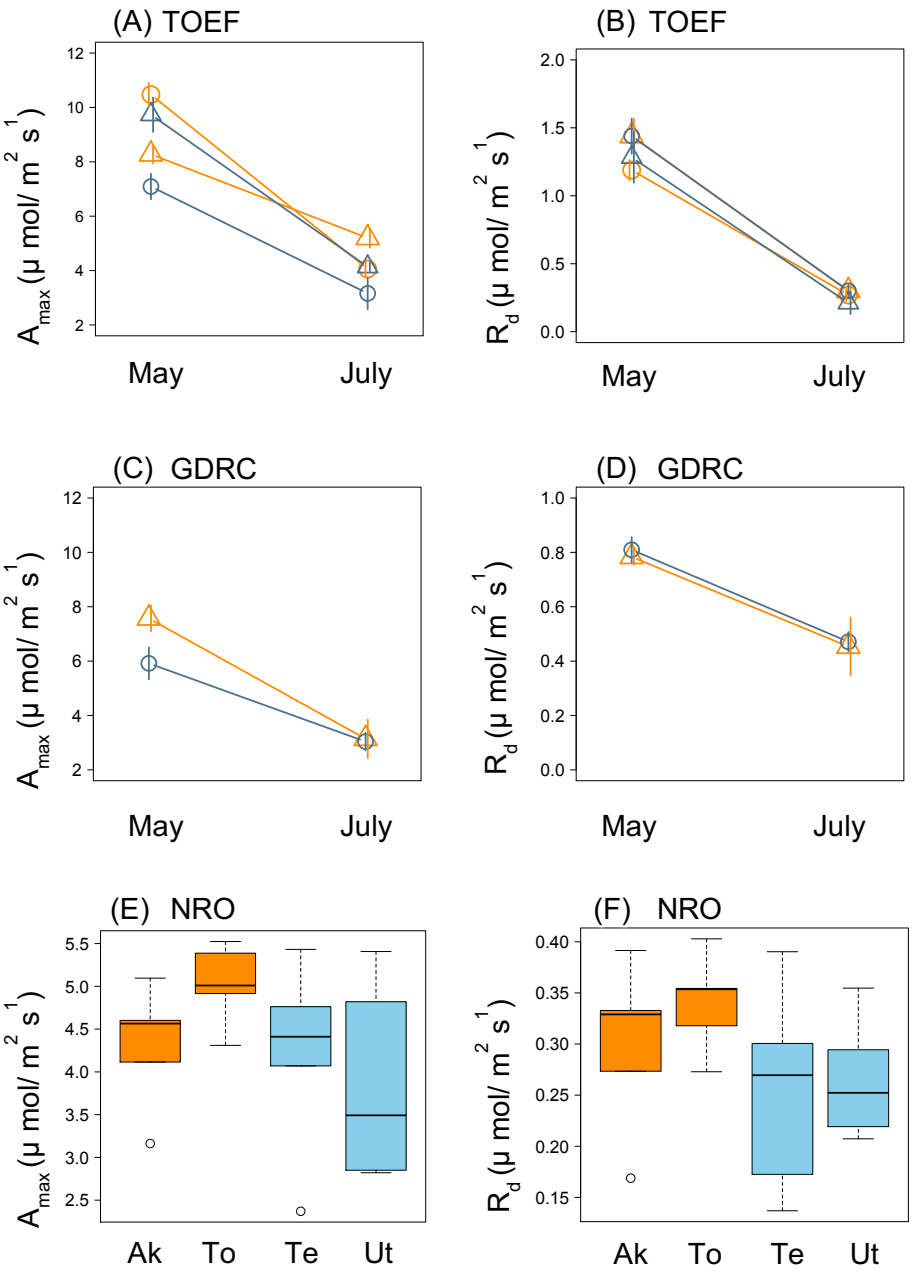

Figure 2-4. Comparisons of maximum photosynthetic rate (A_{max}) and dark respiration rate (R_d) among original populations grown at TOEF (A)–(B), GDRC (C)–(D), and NRO (E)–(F). Measurements at TOEF and GDRC were conducted in May and July, but measurement at NRO was conducted only in July. Orange circle: Akkeshi, orange triangle: Tomakomai, blue circle: Teshio, and blue triangle: Utoro for (A)–(D). Orange box: 2x-*kam*, blue box: 4x-*kam* for (E) and (F).

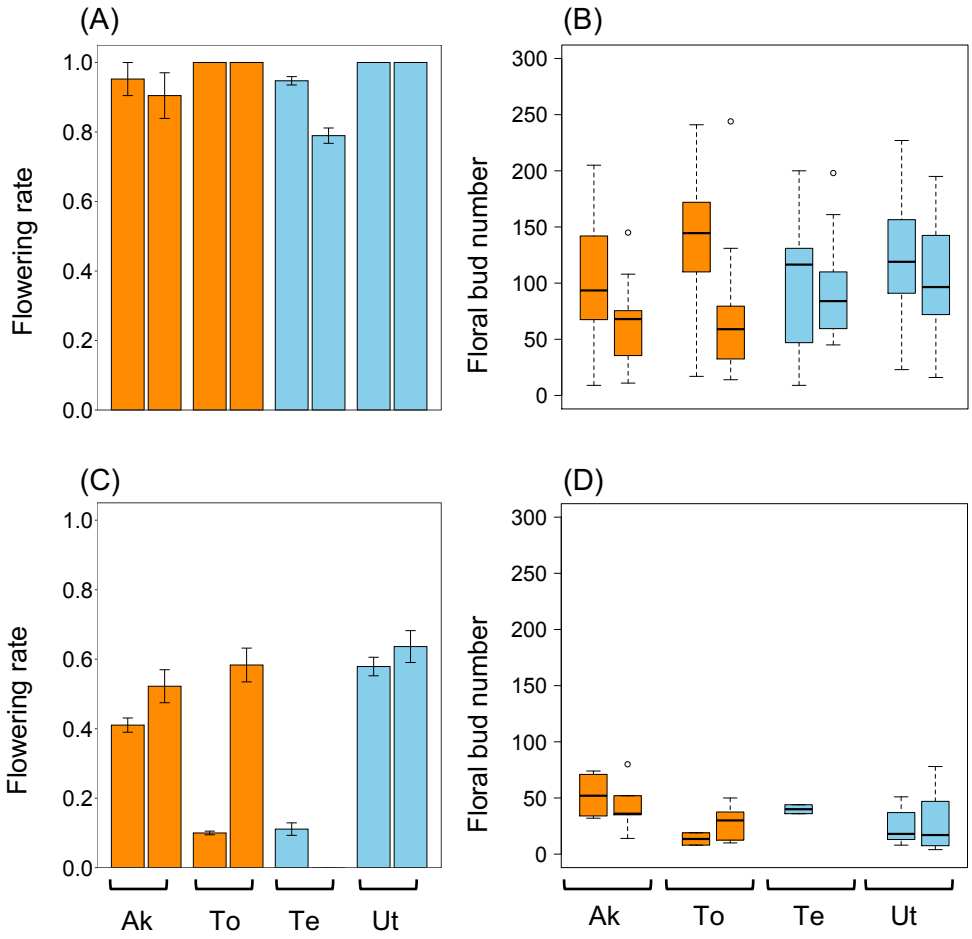

Figure 2-5. Comparisons of reproductive performance (flowering individual rate and floral bud number) among original populations in the reciprocal transplant experiment at NRO (A and B) and TOEF (C and D). Orange box: 2x-*kam*, blue box: 4x-*kam*. Ak: Akkeshi, To: Tomakomai, Te: Teshio, and Ut: Utoro. Left boxes and right boxes in each population mean 2022 and 2023, respectively.

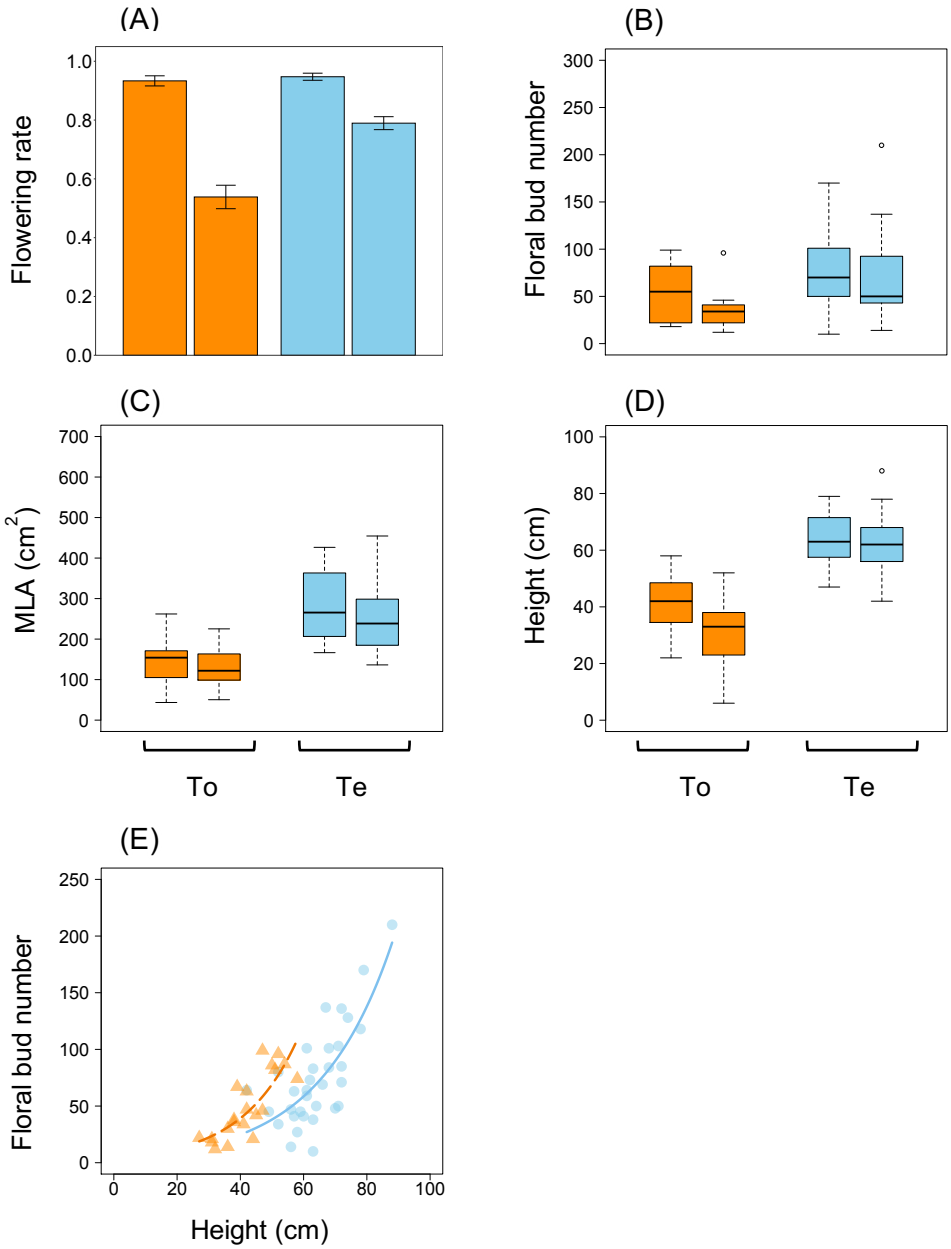

Figure 2-6. Comparisons of performance traits between diploid and tetraploid plants grown at GDRC common garden. (A) flowering individual rate, (B) floral bud number, (C) maximum leaf area, (D) plant height, and (E) relationship between plant height and floral bud number. Orange: 2x-*kam* originated Tomakomai population (To), blue: 4x-*kam* originated Teshio population (Te). Left boxes and right boxes of each population mean 2022 and 2023, respectively.

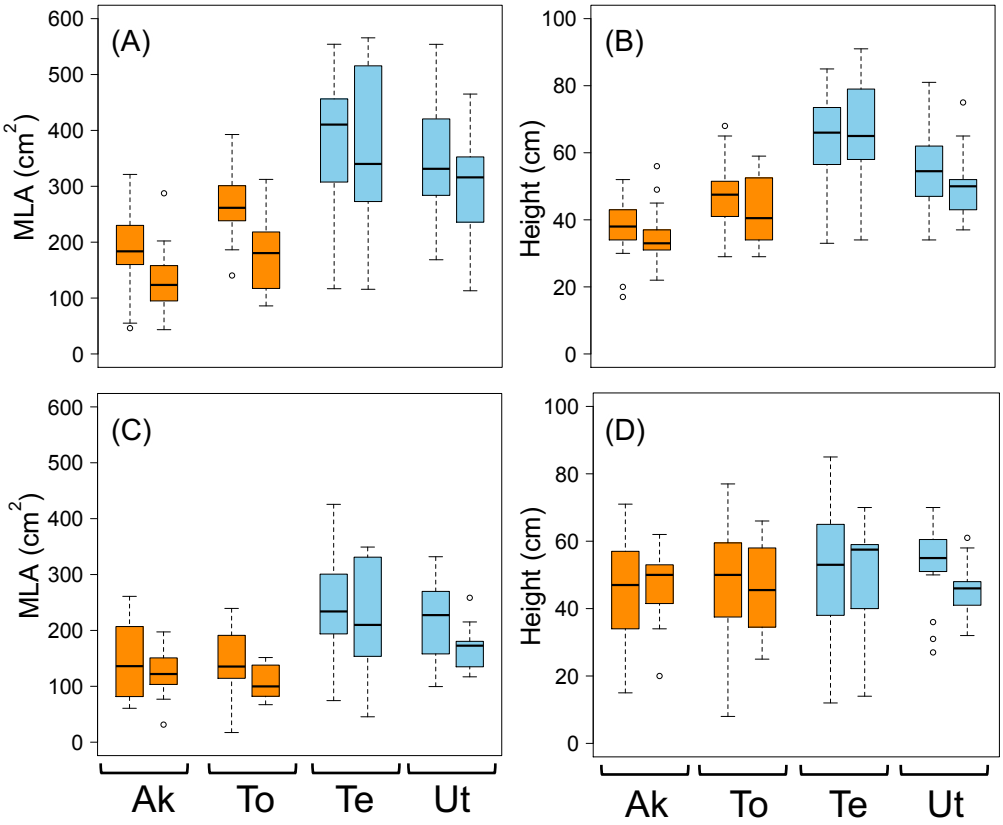

Figure 2-7. Comparisons of maximum leaf area (MLA) and plant height among original populations grown at NRO (A and B) and TOEF (C and D). Orange box: 2x-*kam* population, blue box: 4x-*kam* population. Ak: Akkeshi, To: Tomakomai, Te: Teshio, Ut: Utoro. Left boxes and right boxes of each population mean 2022 and 2023, respectively.

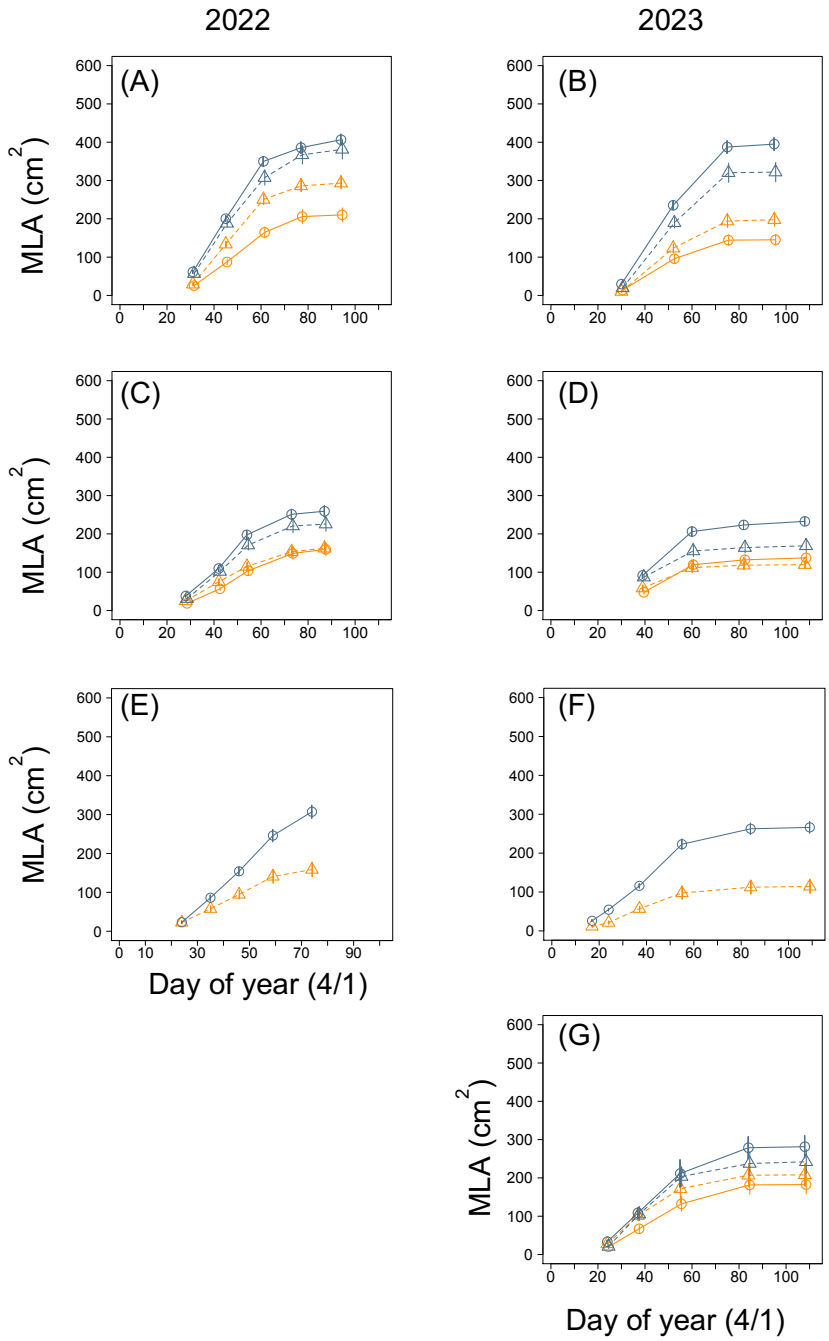

Figure 2-8. Comparisons of seasonal changes in maximum leaf area (MLA) among original populations grown at NRO (A and B), TOEF (C and D), GDRC (E and F), and re-transplanted from TOEF to GDRC (G). Orange circle: Akkeshi, orange triangle: Tomakomai, blue circle: Teshio, and blue triangle: Utoro.

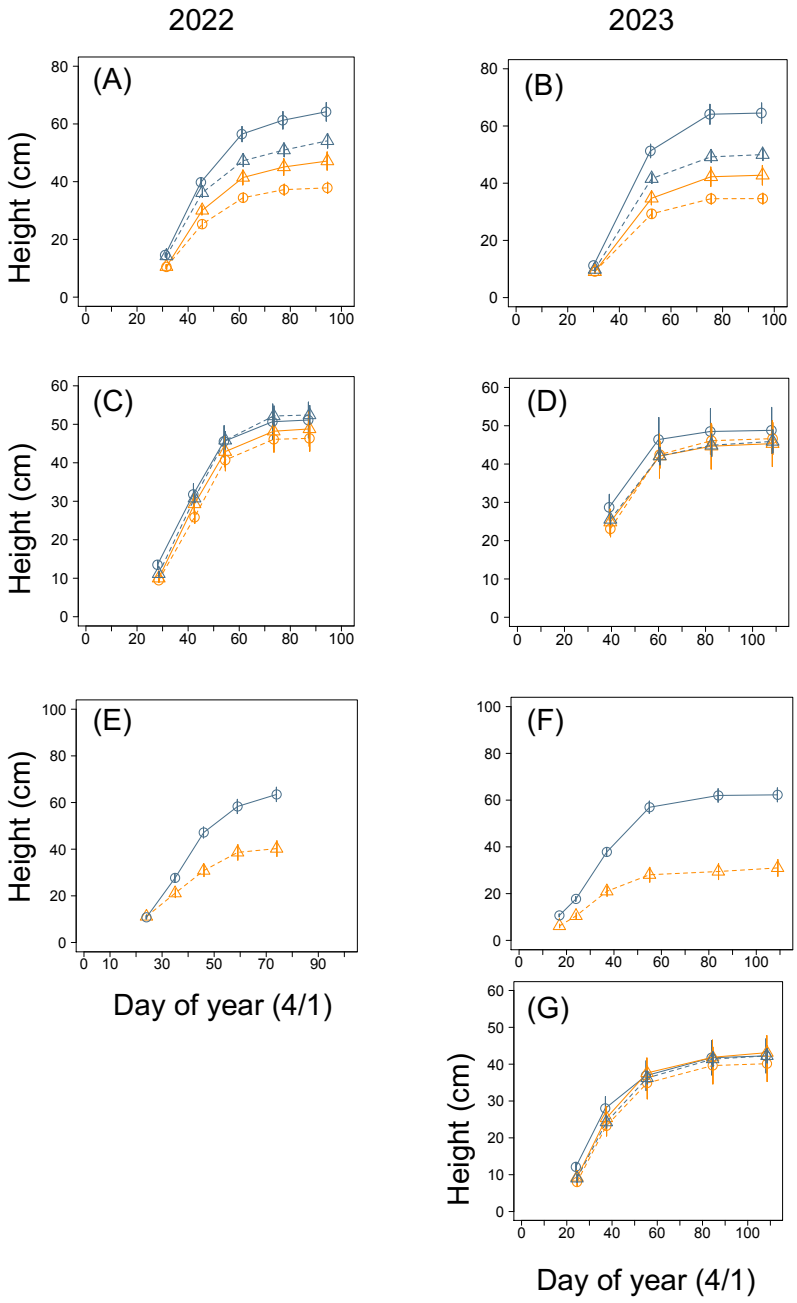

Figure 2-9. Comparisons of seasonal changes in plant height among original populations grown at NRO (A and B), TOEF (C and D), GDRC (E and F), and re-transplanted from TOEF to GDRC (G). Orange circle: Akkeshi, orange triangle: Tomakomai, blue circle: Teshio, and blue triangle: Utoro.

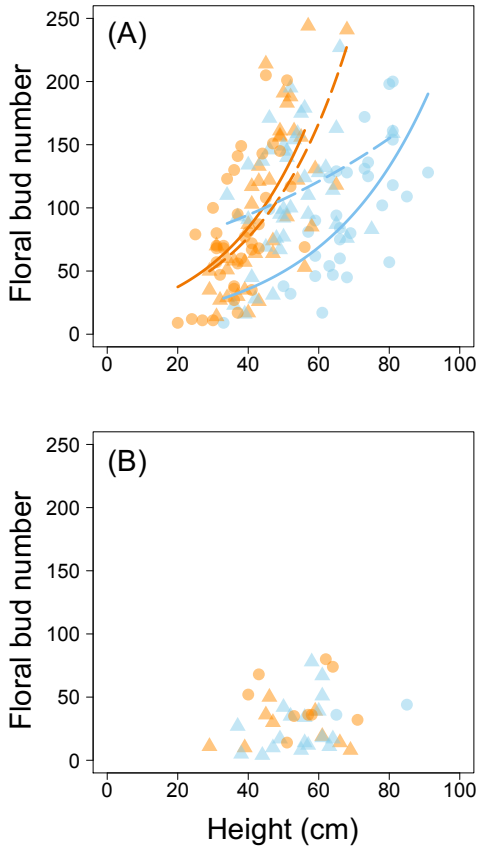

Figure 2-10. Relationship between plant height and floral bud number at NRO (A) and TOEF (B). Orange circle: Akkeshi origin, orange triangle: Tomakomai origin, blue circle: Teshio origin, and blue triangle: Utoro origin.

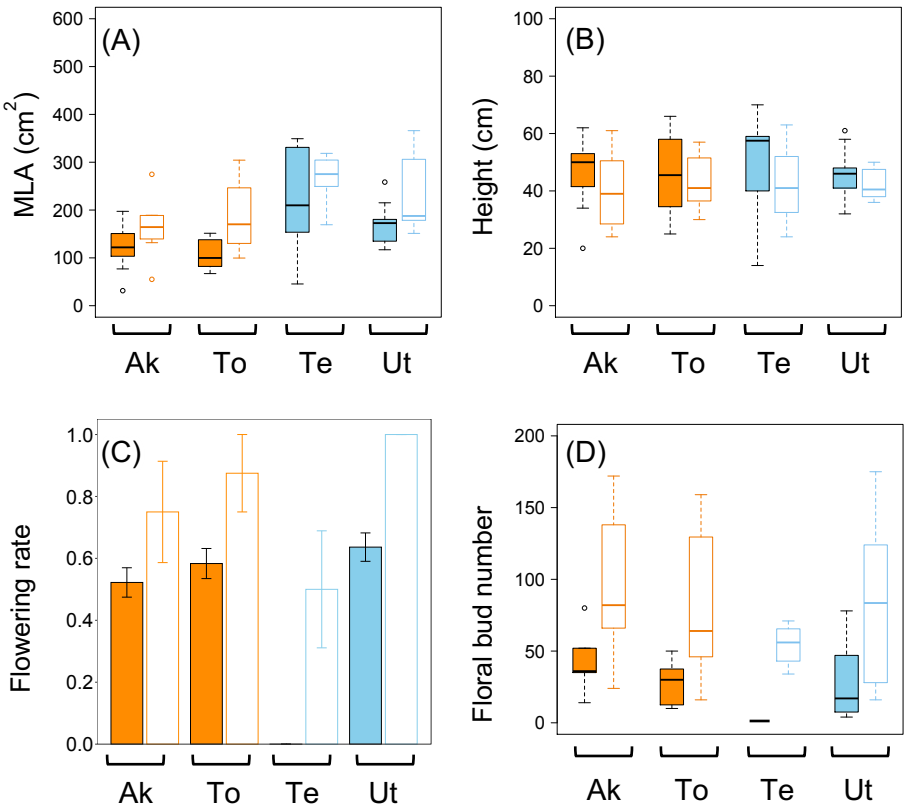

Figure 2-11. Comparisons of performance traits between plants left in TOEF (filled box) and re-transplanted from TOEF to GDRC in 2023 (blank box). (A) maximum leaf area, (B) plant height, (C) flowering individual rate, and (D) floral bud number. Orange: 2x-*kam*, and blue: 4x-*kam*. Ak: Akkeshi, To: Tomakomai, Te: Teshio, Ut: Utoro.

Table 2-1. GLM result of volumetric soil water contents among experimental sites (GDRC, TOEF, NRO). Coefficient, standard error, *t* value, and *P* value are shown.

Variable	Coefficient	SE	*t*	*P*	
Intercept (GDRC)	3.695	0.033	113.337	< 0.001	***
Date	-0.003	0.0003	-8.979	< 0.001	***
NRO	-0.003	0.033	-0.093	0.926	
TOEF	0.076	0.033	2.321	0.021	*

*** $P < 0.001$, * $P < 0.05$. Intercept = GDRC.

Table 2-2. GLMM results selected by AIC for leaf cell size of plants grown at TOEF and NRO. To: Tomakomai, Te: Teshio, Ak: Akkeshi, and Ut: Utoro for original population grown at TOEF and NRO.

(a) Epidermal cell

Variable	Coefficient	SE	*t*	*P*	
Intercept	4.759	0.050	94.81	< 0.001	***
NRO	0.190	0.071	2.68	0.007	**

*** $P < 0.001$, ** $P < 0.01$, Intercept = TOEF.

(b) Spongy tissue cell

Variable	Coefficient	SE	*t*	*P*	
Intercept	5.454	0.118	46.319	< 0.001	***
NRO	0.025	0.225	0.111	0.912	

*** $P < 0.001$, Intercept = TOEF.

(c) Guard cell

Variable	Coefficient	SE	*t*	*P*	
Intercept	6.246	0.044	140.927	< 0.001	***
To	0.106	0.063	1.687	0.092	+
Te	0.412	0.063	6.576	< 0.001	***
Ut	0.466	0.063	7.428	< 0.001	***

*** $P < 0.001$, ** $P < 0.01$, + $P < 0.1$, Intercept = Ak, TOEF.

Table 2-3. GLM results selected by AIC for the comparison of A_{max} among original populations grown at each of TOEF, NRO, and GDRC. To: Tomakomai, Te: Teshio, Ak: Akkeshi, and Ut: Utoro for original populations.

(a) TOEF

Variable	Coefficient	SE	*t*	*P*	
Intercept	2.113	0.085	24.996	< 0.001	***
Ak	0.235	0.120	1.967	0.057	+
Te	-0.155	0.120	-1.294	0.205	
Ut	0.16	0.120	1.356	0.184	
Season = July	-0.465	0.120	-3.888	< 0.001	***
Ak × July	-0.483	0.169	-2.859	0.007	**
Te × July	-0.343	0.169	-2.031	0.051	+
Ut × July	-0.390	0.169	-2.308	0.028	*

*** $P < 0.001$, ** $P < 0.01$, * $P < 0.05$, + $P < 0.1$, Intercept = To, May, To × May.

(b) NRO

Variable	Coefficient	SE	*t*	*P*	
Intercept	1.437	0.100	14.239	< 0.001	***
Ak	-0.082	0.143	-0.574	0.574	
To	0.178	0.143	1.248	0.230	
Ut	0.023	0.143	0.163	0.873	

*** $P < 0.001$, Intercept = Te.

(c) GDRC

Variable	Coefficient	SE	*t*	*P*	
Intercept	1.908	0.095	20.025	< 0.001	***
July	-0.780	0.135	-5.787	< 0.001	***

*** $P < 0.001$, Intercept = May.

Table 2-4. GLM results selected by AIC for the comparison of R_d among original populations grown at each of TOEF, NRO, and GDRC. To: Tomakomai, Te: Teshio, Ak: Akkeshi, and Ut: Utoro for original populations.

(a) TOEF

Variable	Coefficient	SE	*t*	*P*	
Intercept	0.364	0.126	2.890	< 0.001	***
Ak	-0.191	0.178	-1.073	0.291	
Te	-0.154	0.178	-0.864	0.394	
Ut	-0.115	0.178	-0.645	0.523	
Season = July	-1.566	0.178	-8.786	< 0.001	***
Ak × July	0.082	0.252	0.325	0.747	
Te × July	0.400	0.252	1.586	0.123	
Ut × July	-0.236	0.252	-0.940	0.354	

*** $P < 0.001$, Intercept = To, May, To × May.

(b) NRO

Variable	Coefficient	SE	*t*	*P*	
Intercept	-1.371	0.125	-10.998	< 0.001	***
Ak	0.045	0.176	0.254	0.803	
To	0.293	0.176	1.661	0.116	
Ut	0.164	0.176	0.928	0.367	

*** $P < 0.001$, Intercept = Te.

(c) GDRC

Variable	Coefficient	SE	*t*	*P*	
Intercept	-0.228	0.080	-2.838	0.017	*
July	-0.544	0.113	-4.796	< 0.001	***

*** $P < 0.001$, * $P < 0.05$, Intercept = May.

Table 2-5. GLM results selected by AIC for the comparisons of seed germination rate (a, b) and seedling survival rate (c, d) among original populations grown at TOEF and NRO. To: Tomakomai, Te: Teshio, Ak: Akkeshi, and Ut: Utoro for original populations.

(a) Germination rate at TOEF

Variable	Coefficient	SE	*z*	*P*	
Intercept	0.489	0.291	1.680	0.093	+
Ak	0.174	0.417	0.417	0.677	
Te	-0.812	0.409	-1.988	0.047	*
Ut	0.776	0.449	1.729	0.084	+

* $P < 0.05$, + $P < 0.1$, Intercept = To.

(b) Germination rate at NRO

Variable	Coefficient	SE	*z*	*P*	
Intercept	-0.847	0.1543	-5.491	< 0.001	***

*** $P < 0.001$.

(c) Seedling survival rate at TOEF

Variable	Coefficient	SE	*z*	*P*	
Intercept	-1.764	0.2551	-6.913	< 0.001	***

*** $P < 0.001$.

(d) Seedling survival rate at NRO

Variable	Coefficient	SE	*z*	*P*	
Intercept	0.475	0.2655	1.79	0.073	+

+ $P < 0.1$.

Table 2-6. GLM results selected by AIC for the comparisons of flowering rate among original populations grown at TOEF and NRO. To: Tomakomai, Te: Teshio, Ak: Akkeshi, and Ut: Utoro for original populations.

(a) TOEF

Variable	Coefficient	SE	*z*	*P*	
Intercept	-1.365	0.456	-2.993	0.003	**
Ak	0.069	0.573	0.120	0.905	
Te	-1.663	0.844	-1.970	0.049	*
Ut	1.430	0.561	2.550	0.011	*
Year (2023)	1.006	0.450	2.233	0.026	*

** $P < 0.01$, * $P < 0.05$, Intercept = To, Year (2022).

(b) NRO

Variable	Coefficient	SE	*z*	*P*	
Intercept	2.633	0.783	3.364	< 0.001	***
Ak	0.697	0.779	0.896	0.370	
To	18.677	2743.527	0.007	0.994	
Ut	18.677	2743.527	0.007	0.994	
Year (2023)	-1.222	0.854	-1.431	0.152	

*** $P < 0.001$, Intercept = Te, 2022.

(c) GDRC

Variable	Coefficient	SE	*z*	*P*	
Intercept	2.772	0.729	3.804	< 0.001	***
Year (2023)	-1.984	0.823	-2.412	0.016	*

*** $P < 0.001$, * $P < 0.05$, Intercept = 2022.

Table 2-7. GLM results selected by AIC for the comparisons of floral bud number among original populations grown at TOEF, NRO, and GDRC. To: Tomakomai, Te: Teshio, Ak: Akkeshi, and Ut: Utoro for original populations.

(a) TOEF

Variable	Coefficient	SE	*z*	*P*	
Intercept	2.603	0.193	13.524	< 0.001	***
Ak	1.358	0.204	6.643	< 0.001	***
Te	1.086	0.223	4.880	< 0.001	***
Ut	0.638	0.202	3.165	0.002	**
Year (2023)	0.698	0.206	3.396	< 0.001	***
Ak × (2023)	-0.888	0.227	-3.910	< 0.001	***
Te × (2023)	Na	Na	Na	Na	
Ut × (2023)	-0.547	0.225	-2.431	0.015	*

*** $P < 0.001$, ** $P < 0.01$, * $P < 0.05$, Intercept = To, 2022, To × 2022.

(b) NRO

Variable	Coefficient	SE	*z*	*P*	
Intercept	4.600	0.024	194.602	< 0.001	***
Ak	0.028	0.032	0.875	0.382	
To	0.316	0.030	10.376	< 0.001	***
Ut	0.200	0.031	6.417	< 0.001	***
Year (2023)	-0.067	0.036	-1.876	0.061	+
Ak × (2023)	-0.472	0.051	-9.173	< 0.001	***
To × (2023)	-0.621	0.049	-12.745	< 0.001	***
Ut × (2023)	-0.095	0.047	-2.046	0.041	*

*** $P < 0.001$, * $P < 0.05$, + $P < 0.1$, Intercept = Te, 2022, Te × 2022.

(c) GDRC

Variable	Coefficient	SE	*z*	*P*	
Intercept	4.003	0.036	110.874	< 0.001	***
Te	0.400	0.045	7.546	< 0.001	***
Year (2023)	-0.360	0.071	-5.050	< 0.001	***
Te × (2023)	0.314	0.082	3.846	< 0.001	***

*** $P < 0.001$, Intercept = To, 2021, To × 2022.

Table 2-8. GLM results selected by AIC for the comparisons of maximum leaf area among original populations grown at TOEF, NRO, and GDRC. To: Tomakomai, Te: Teshio, Ak: Akkeshi, and Ut: Utoro for original populations.

(a) TOEF

Variable	Coefficient	SE	*t*	*P*	
Intercept	4.950	0.072	68.382	< 0.001	***
Ak	0.040	0.096	0.413	0.680	
Te	0.599	0.099	6.090	< 0.001	***
Ut	0.412	0.097	4.262	< 0.001	***
Year (2023)	-0.207	0.072	-2.886	0.005	**

*** $P < 0.001$, ** $P < 0.01$, Intercept = To, Year (2022).

(b) NRO

Variable	Coefficient	SE	*t*	*P*	
Intercept	5.936	0.080	73.915	< 0.001	***
Ak	-0.696	0.111	-6.278	< 0.001	***
To	-0.359	0.112	-3.198	0.002	**
Ut	-0.064	0.112	-0.574	0.567	
Year (2023)	-0.035	0.114	-0.314	0.754	
Ak × (2023)	-0.330	0.157	-2.109	0.037	*
To × (2023)	-0.360	0.159	-2.271	0.025	*
Ut × (2023)	-0.123	0.159	-0.773	0.441	

*** $P < 0.001$, ** $P < 0.01$, * $P < 0.05$, Intercept = Te, 2022, Te × 2022.

(C) GDRC

Variable	Coefficient	SE	*t*	*P*	
Intercept	4.947	0.069	71.795	< 0.001	***
Te	0.655	0.091	7.217	< 0.001	***

*** $P < 0.001$, Intercept = To.

Table 2-9. GLM results selected by AIC for the comparisons of plant height among original populations grown at TOEF, NRO, and GDRC. To: Tomakomai, Te: Teshio, Ak: Akkeshi, and Ut: Utoro for original populations.

(a) TOEF

Variable	Coefficient	SE	*t*	*P*	
Intercept	3.883	0.027	141.9	< 0.001	***

*** $P < 0.001$.

(b) NRO

Variable	Coefficient	SE	*t*	*P*	
Intercept	4.198	0.039	105.736	< 0.001	***
Ak	-0.576	0.049	-11.694	< 0.001	***
To	-0.360	0.050	-7.227	< 0.001	***
Ut	-0.213	0.050	-4.280	< 0.001	***
Year (2023)	-0.066	0.035	-1.910	0.058	+

*** $P < 0.001$, + $P < 0.1$, Intercept = Te, Year (2022).

(c) GDRC

Variable	Coefficient	SE	*t*	*P*	
Intercept	3.723	0.064	57.745	< 0.001	***
Te	0.427	0.086	4.955	< 0.001	***
Year (2023)	-0.289	0.095	-3.057	0.003	**
Te × (2023)	0.270	0.125	2.168	0.034	*

*** $P < 0.001$, ** $P < 0.01$, * $P < 0.05$, Intercept = To, 2022, To × 2022.

Table 2-10. GLMM results selected by AIC for the comparisons of size-dependency of flower production among original populations grown at TOEF, NRO, and GDRC. To: Tomakomai, Te: Teshio, Ak: Akkeshi, and Ut: Utoro for original populations.

(a) TOEF

Variable	Coefficient	SE	*z*	*P*	
Intercept	3.103	0.311	9.970	< 0.001	***
Pant height (PH)	0.0002	0.006	0.032	0.974	
Ak	0.485	0.411	1.179	0.239	
Te	-0.054	0.916	-0.059	0.953	
Ut	-2.265	0.463	-4.893	< 0.001	***
PH × Ak	0.004	0.008	0.574	0.566	
PH × Te	0.010	0.013	0.784	0.433	
PH × Ut	0.045	0.009	5.299	< 0.001	***

*** $P < 0.001$, Intercept = To, PH × To.

(b) NRO

Variable	Coefficient	SE	*z*	*P*	
Intercept	2.265	0.160	14.196	< 0.001	***
Pant height (PH)	0.033	0.002	20.177	< 0.001	***
Ak	0.545	0.150	3.623	< 0.001	***
To	0.517	0.142	3.636	< 0.001	***
Ut	1.787	0.140	12.721	< 0.001	***
PH × Ak	0.008	0.003	2.789	0.005	**
PH × To	0.006	0.002	2.701	0.007	**
PH × Ut	-0.020	0.002	-9.531	< 0.001	***

*** $P < 0.001$, ** $P < 0.01$, Intercept = Te, PH × Te.

(c) GDRC

Variable	Coefficient	SE	*z*	*P*	
Intercept	1.406	0.184	7.656	< 0.001	***
Pant height (PH)	0.057	0.004	14.338	< 0.001	***
Te	0.091	0.233	0.388	0.69	
PH × Te	-0.014	0.004	-3.050	0.002	**

*** $P < 0.001$, ** $P < 0.01$, Intercept = To, PH × To.

Table 2-11. GLMM results selected by AIC for the comparisons of maximum leaf size, plant height, flowering rate, and floral bud number between plants re-transplanted to GDRC and left at TOEF in 2023. Estimated coefficient, standard error, *t* values, and *P* value are shown. To: Tomakomai, Te: Teshio, Ak: Akkeshi, and Ut: Utoro for original populations.

(a) Maximum leaf area

Variable	Coefficient	SE	*t*	*P*	
Intercept	4.771	0.084	56.840	< 0.001	***
Moved to GDRC	0.342	0.081	4.242	< 0.001	***
Ak	0.024	0.111	0.216	0.829	
Te	0.571	0.113	5.065	< 0.001	***
Ut	0.343	0.111	3.086	0.003	**

*** $P < 0.001$, ** $P < 0.01$, Intercept = To, left at TOEF

(b) Plant height

Variable	Coefficient	SE	*t*	*P*	
Intercept	3.841	0.039	97.698	< 0.001	***
Moved to GDRC	-0.105	0.061	-1.737	0.087	+

*** $P < 0.001$, + $P < 0.1$, Intercept = left at TOEF

(c) Flowering rate

Variable	Coefficient	SE	*z*	*P*	
Intercept	0.220	0.542	0.405	0.685	
Moved to GDRC	2.195	0.695	3.158	0.002	**
Ak	-0.696	0.750	-0.928	0.353	
Te	-2.780	0.908	-3.060	0.002	**
Ut	0.505	0.798	0.632	0.527	

** $P < 0.01$, Intercept = To, left at TOEF

(d) Floral bud number

Variable	Coefficient	SE	*z*	*P*	
Intercept	3.416	0.049	69.264	< 0.001	***
Moved to GDRC	0.978	0.047	20.947	< 0.001	***
Ak	0.202	0.051	3.990	< 0.001	***
Te	-0.400	0.078	-5.148	< 0.001	***
Ut	0.010	0.049	0.211	0.833	

*** $P < 0.001$, Intercept = To, left at TOEF

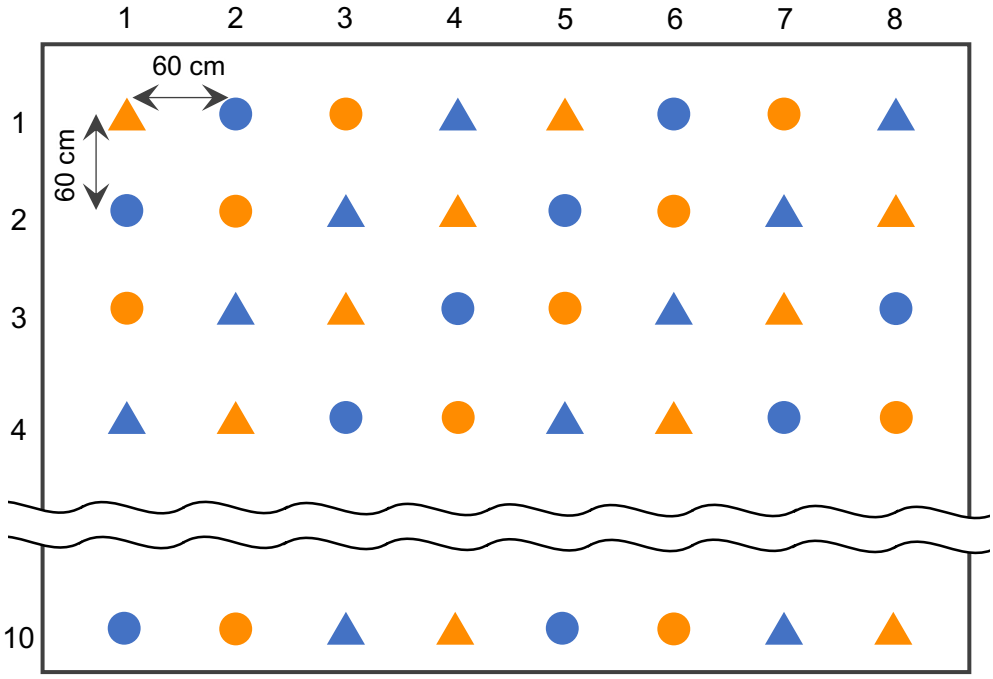

Figure S2-1. Plot design for the reciprocal transplant experiment at NRO and TOEF. Orange circle: Akkeshi, orange triangle: Tomakomai, blue circle: Teshio, and blue triangle: Utoro.

Table S2-1. Germination rate (a) and seedlings survival rate (b) of plants derived from different populations at each experimental site (TOEF and NRO). The number of sowed seeds in 2020 (a) and the number of germinated seeds in 2021 (b) are shown within parentheses.

(a) Germination rate (2021)

Population	TOEF	NRO
Tomakomai	62.0 % (50)	36.0 % (50)
Akkeshi	66.0 % (50)	20.0 % (50)
Teshio	42.0 % (50)	38.0 % (50)
Utoro	78.0 % (50)	26.0 % (50)

(b) Survival rate (2021-2022)

Population	TOEF	NRO
Tomakomai	12.9 % (31)	50.0 % (18)
Akkeshi	24.2 % (33)	60.0 % (10)
Teshio	4.8 % (21)	78.9 % (19)
Utoro	13.2 % (38)	53.8 % (13)

Table S2-2. Flowering rate and floral bud number of plants derived from different populations and grown at each experimental site (TOEF, NRO, GDRC) in 2022 and 2023. The number of measured individuals and the number of flowering individuals is shown within parentheses. Mean ± SD.

(a) Flowering rate (2022)

Population	TOEF	NRO	GDRC
Tomakomai	10.0 % (20)	100.0 % (20)	93.3 % (15)
Akkeshi	20.0 % (20)	95.2 % (21)	-
Teshio	11.1 % (18)	94.7 % (19)	94.7 % (19)
Utoro	57.9 % (19)	100.0 % (20)	-

(b) Flowering rate (2023)

Population	TOEF	NRO	GDRC
Tomakomai	58.3 % (12)	100.0 % (20)	53.8 % (13)
Akkeshi	45.5 % (11)	90.5 % (21)	-
Teshio	0.0 % (10)	78.9 % (19)	78.9 % (19)
Utoro	63. 6 % (11)	100.0 % (20)	-

(c) Floral bud number (2022)

Population	TOEF	NRO	GDRC
Tomakomai	13.50 ± 7.78 (2)	136.35 ± 56.62 (20)	54.78 ± 28.43 (14)
Akkeshi	52.50 ± 21.56 (4)	102.3 ± 53.90 (20)	-
Teshio	40.00 ± 5.66 (2)	99.44 ± 55.15 (18)	76.94 ± 39.73 (18)
Utoro	25.54 ± 14.92 (11)	121.45 ± 46.94 (20)	-

(d) Floral bud number (2023)

Population	TOEF	NRO	GDRC
Tomakomai	27.14 ± 15.69 (7)	68.55 ± 51.74 (20)	38.28 ± 28.17 (7)
Akkeshi	43.40 ± 24.51 (5)	59.68 ± 34.53 (19)	-
Teshio	na (0)	93.00 ± 43.45 (15)	73.60 ± 50.52 (15)
Utoro	29.71 ± 30.41 (7)	103.25 ± 50.51 (20)	-

Table S2-3. Maximum leaf area (cm^2) and plant height (cm) of plants derived from different populations and grown at each experimental site (TOEF, NRO, GDRC) in 2022 and 2023. The number of measured individuals is shown within parentheses. Mean ± SD.

(a) Maximum leaf area (2022)

Population	TOEF	NRO	GDRC
Tomakomai	146.20 ± 56.35 (20)	264.40 ± 56.20 (20)	147.52 ± 59.52 (15)
Akkeshi	143.91 ± 66.87 (20)	188.72 ± 75.32 (21)	-
Teshio	247.19 ± 101.17 (18)	378.46 ± 118.31 (19)	288.30 ± 91.29 (19)
Utoro	217.64 ± 72.56 (19)	354.86 ± 97.13 (20)	-

(b) Maximum leaf area (2023)

Population	TOEF	NRO	GDRC
Tomakomai	108.04 ± 30.69 (12)	177.97 ± 65.28 (20)	132.95 ± 53.05 (13)
Akkeshi	123.88 ± 45.89 (11)	130.84 ± 56.55 (21)	-
Teshio	223.45 ± 98.86 (10)	365.19 ± 150.42 (19)	253.84 ± 91.05 (19)
Utoro	166.95 ± 42.91 (11)	302.90 ± 99.55 (20)	-

(c) Plant height (2022)

Population	TOEF	NRO	GDRC
Tomakomai	48.80 ± 16.30 (20)	47.15 ± 9.25 (20)	41.4 ± 10.24 (15)
Akkeshi	46.30 ± 15.07 (20)	37.86 ± 8.75 (21)	-
Teshio	51.11 ± 19.69 (18)	64.21 ± 14.03 (19)	63.47 ± 8.92 (19)
Utoro	52.95 ± 11.04 (19)	54.15 ± 11.44 (20)	-

(d) Plant height (2023)

Population	TOEF	NRO	GDRC
Tomakomai	45.33 ± 13.45 (12)	42.80 ± 10.12 (20)	31.00 ± 12.96 (13)
Akkeshi	46.63 ± 11.80 (11)	34.62 ± 8.45 (21)	-
Teshio	48.80 ± 16.93 (10)	64.52 ± 15.28 (19)	62.26 ± 10.91 (19)
Utoro	45.91 ± 8.51 (11)	50.00 ± 9.31 (20)	-

Table S2-4. Maximum leaf area (cm^2), plant height (cm), flowering rate, and floral bud number of plants derived from different populations for plants left at TOEF (left plants) and re-transplanted from TOEF to GDRC (re-transplanted plants) in 2023. The number of measured individuals is shown within parentheses. Mean ± SD.

(a) Maximum leaf area (2023)

Population	left plants	re-transplanted plants
Tomakomai	108.04 ± 30.69 (12)	187.22 ± 73.01 (8)
Akkeshi	123.88 ± 45.89 (11)	164.39 ± 61.91 (8)
Teshio	223.45 ± 98.86 (10)	268.24 ± 49.24 (8)
Utoro	166.95 ± 42.91 (11)	232.70 ± 81.33 (8)

(b) Plant height (2023)

Population	left plants	re-transplanted plants
Tomakomai	45.33 ± 13.45 (12)	43.12 ± 9.38 (8)
Akkeshi	46.63 ± 11.80 (11)	40.12 ± 13.70 (8)
Teshio	48.80 ± 16.93 (10)	42.25 ± 13.09 (8)
Utoro	45.91 ± 8.51 (11)	42.25 ± 5.39 (8)

(c) Flowering rate (2023)

Population	left plants	re-transplanted plants
Tomakomai	58.3 % (12)	87.5 % (8)
Akkeshi	45.5 % (11)	75.0 % (8)
Teshio	0.0 % (10)	50.0 % (8)
Utoro	63. 6 % (11)	100.0 % (8)

(d) Floral bud number (2023)

Population	left plants	re-transplanted plants
Tomakomai	27.14 ± 15.69 (7)	84.29 ± 55.00 (7)
Akkeshi	43.40 ± 24.51 (5)	94.00 ± 53.28 (6)
Teshio	na (0)	54.25 ± 15.59 (4)
Utoro	29.71 ± 30.41 (7)	82.75 ± 57.42 (8)

Chapter III: The evolutionary process of vegetative reproduction by bulbil formation in *Parasenecio kamtschaticus* var. *bulbifer* and the consequence of polyploidization

Introduction

Polyploid populations tend to be distributed in harsh environments in comparison with conspecific or related diploid populations (Otto et al. 2007; Godfree et al. 2017). The higher tolerance to stressful environments in polyploids may be related to the ability of self-seed production (Barringer 2007) or vegetative reproduction (Otto and Whitton 2000) by which restriction of sexual seed reproduction can be compensated. Vegetative reproduction is often associated with polyploid events in plants (Stebbins 1950; Herben et al. 2017). The improvement of vegetative reproduction, such as rhizome blanching (Cheng et al. 2020), adventitious buds (Šingliarová et al. 2023), and bulbils (Becker et al. 2022), often occurs in polyploids. Despite many empirical studies, however, little is known about the mechanism by which polyploids can promote the ability of vegetative reproduction.

Frequent vegetative reproduction in polyploids has an advantage of overcoming the minority cytotype exclusion (MCE), that is, rare polyploids tend to receive pollen from dominant diploids, resulting in the production of inviable odd-ploidy offspring (Levin 1975; Husband and Schemske 1997). Vegetative reproduction can mitigate the effect of the MCE, as producing clonal ramets can increase the chance of within-cytotype mating (Baldwin and Husband 2013). Although some studies supported this possibility (Baldwin and Husband 2013; Herben et al. 2017), polyploidization may promote the ability of vegetative reproduction through the changes in gene expression, epigenetic interactions, and physiological traits without a process of adaptation (Van Drunen and Husband 2019). Furthermore, the effects of polyploidization on reproductive traits might be diverse and unpredictable (Siopa et al. 2020), and only part of polyploid species may be able to develop vegetative reproduction.

As another ecological significance of vegetative reproduction in polyploids, the process of local adaptation to harsh environments has been discussed (Schinkel et al. 2016). There are several studies reporting the advantages of vegetative reproduction at higher elevations and latitudes (Bauert 1993; Fischer et al. 2011). Seed production is generally limited under cold climate with short growing season, whereas propagules of vegetative reproduction (such as bulbils) can develop rapidly (Stöcklin et al. 2009). Thus, the ability of vegetative reproduction may be crucial for the establishment of populations under cold climate conditions, especially for herbaceous species with short life-span. The improvement of physiological ability for vegetative reproduction by polyploidization and increasing selective force for vegetative reproduction with environmental harshness may promote the evolution of vegetative reproduction in polyploid plants.

Parasenecio kamtschaticus is an ideal species for testing the evolutionary mechanism of vegetative reproduction in polyploids. A previous study based on allozyme analysis suggested that *P. kamtschaticus* var. *bulbifer* might be derived via two evolutionary steppes, polyploidization and subsequent bulbil production ability (Kudo and Hirao 2020). However, the origin of *P. kamtschaticus* var. *bulbifer* has not been clarified precisely due to a low resolution of genetic structure by the allozyme analysis. *Parasenecio kamtschaticus* var. *bulbifer* has high ability of vegetative reproduction by bulbil production on the leaf axils. Interestingly, bulbil formation is occasionally observed in some populations of *P. kamtschaticus* var. *kamtschaticus* at low frequency (Fig. 3-1).

To clarify whether the vegetative reproduction by bulbils is an adaptive trait at higher elevations and whether the ability of bulbil production is related to the polyploidization, I examined (1) the activities of sexual and vegetative reproduction of *P. kamtschaticus* var. *bulbifer* along elevation gradients, (2) the bulbil formation abilities of diploid *P. kamtschaticus* var. *kamtschaticus* (2x-*kam*), tetraploid *P. kamtschaticus* var. *kamtschaticus* (4x-*kam*), and

tetraploid *P. kamtschaticus* var. *bulbifer* (4x-*bulb*), and (3) the phylogenetic relationship among the populations of three taxonomic groups in *P. kamtschaticus* populations across the distribution range in northern Japan.

Methods

Activity of sexual and vegetative reproduction along the elevation gradient

To reveal the responses of sexual reproduction, vegetative reproduction, and growth activity along elevation gradient, I conducted field survey in three sites, where 4x-*bulb* is widely distributed; Mt. Shokanbetsu (1400 m elevation), Mt. Hira (1700 m elevation), and Numanohara in Taisetsu Mts. (1100 m elevation). In each site, I selected 4–5 populations to cover the elevational distribution range. In each population, 1–3 quadrats with a 1×1-m size were randomly set depending on the population size, and floral bud number, bulbil number, plant height, and leaf number were measured for flowering individuals.

First, reproductive activity along the elevation gradient was evaluated by GLMMs, postulating a Poisson error distribution (for flower and bulbil number) or a gamma error distribution (for bulbil ratio), in which the responsible variable was floral bud number, bulbil number or the ratio of bulbil number to total reproductive units (sum of flower and bulbil number), and the explanatory variable was elevation. Next, changes in the growth traits along the elevation gradient was evaluated by GLMMs, postulating a Poisson error distribution (for leaf number) or a gamma error distribution (for height), in which the response variable was plant height or leaf number, and the explanatory variable was elevation. Furthermore, size-dependency of flower and bulbil production was evaluated by GLMMs, postulating a Poisson error distribution, in which the response variable was floral bud number or bulbil number, and the explanatory variables were plant height, elevation, and their interaction. Finally, a trade-off relationship between sexual reproduction and vegetative reproduction was evaluated by a

GLMM, postulating a Poisson error distribution, in which the responsible variable was floral bud number, and the explanatory variable was bulbil number. All GLMM analyses were performed setting quadrat nested by site as a random factor, and the best-fit model was selected for each GLMM by the model selection using Akaike's information criterion using "MuMIn" package in R.

Comparison of bulbil formation among populations

In the field observation, I found that some 2x-*kam* and 4x-*kam* plants occasionally produced bulbils as well as 4x-*bulb* plants (Fig. 3-1). In spite of the presence of bulbils in some 2x-*kam* and 4x-*kam* populations, they are easily distinguishable from 4x-*bulb* populations based on the following things; 1) size and frequency of bulbils are apparently small in 2x-*kam* and 4x-*kam* populations, 2) bulbils are visible soon after the leaf emergence in 4x-*bulb* populations, while bulbils are detectable in the middle to late growth season in 2x-*kam* and 4x-*kam* populations, and 3) bulbils are frequently produced even on small-sized non-flowering plants in 4x-*bulb* populations. To clarify how polyploidization is related to the occurrence of vegetative reproduction, I compared the ability of bulbil formation among 2x-*kam*, 4x-*kam*, and 4x-*bulb* populations.

Field survey was conducted in seven 2x-*kam* populations, nine 4x-*kam* populations, and three 4x-*bulb* populations. In each population, plants having more than three leaves were randomly selected and the number of plants forming bulbils were recorded, and the bulbil diameter was measured if any. To compare the ability of bulbil formation between diploid and tetraploid populations, a GLM, postulating a binomial error distribution with logit-link function, was conducted. In the GLM, 4x-*bulb* populations were excluded because they showed almost 100 % of formation rate (see results). The response variable was the proportion of bulbil-formed individuals, and the explanatory variables were ploidy level (diploid or tetraploid), elevation,

latitude, and their interaction. To compare bulbil size between diploid (2x-*kam*) and tetraploid (4x-*kam* and 4x-*bulb*) populations, a GLMM, postulating a gamma error distribution with log-link function, was conducted. In the GLMM, the response variable was bulbil diameter, the explanatory variables were ploidy level, elevation, latitude, and their interaction, and sampling site was treated as a random factor. Furthermore, a GLMM was conducted for the analysis both including and excluding 4x-*bulb* populations. After that, the best-fit model was selected for each GLMM by "MuMIn" package.

Ploidy assessment, DNA extraction, and sequencing of cpDNA and nrDNA

To clarify the evolutionary process of vegetative reproduction (i.e., bulbil production) in the taxonomic groups of *P. kamtschaticus* using molecular techniques, leaf samples were collected from four individuals in each of 34 populations including 2x-*kam*, 4x-*kam*, and 4x-*bulb* in Hokkaido and northern Honshu. Sampling of leaves was conducted at 5-m intervals to avoid collection within the same genets. In most cases, I collected samples from the sites, whose ploidy level was known by previous studies (Nakagawa 2006; Kudo & Hirao 2020). Although Mt. Rakko population was treated as 4x-*kam* in a previous study (Kudo & Hirao 2020), I concluded that this population is 4x-*bulb* as well as Nakagawa (2006) based on the morphological characters. A detail information of sampling sites is shown in Table 3-1 and Fig. 3-2. Leaf samples were stored in silica gel at room temperature until analysis.

I conducted a flow cytometry analysis for samples from Bihoro, Omusaro, and Tsubetsu populations, whose ploidy level was unknown. Leaf fragments of three individuals in each population were sampled and stored in 200 µl of nuclei extraction buffer (CyStain UV precise P; Partec, Münster, Germany). Nuclear samples with the buffer were filtered using 30-µm nylon mesh and stained with 800 µl of 4,6-diamidino-2-phenylindole (DAPI) solution, including 10 mM Tris, 50 mM sodium citrate, 2 mM MgCl2, 1 % (w/v) PVP K-30, 0.1 % (v/v) Triton X-

100, and 2 mg L-1 DAPI (pH 7.5) for 3 minutes at room temperature (Mishiba et al. 2000). Finally, relative DNA contents were measured and ploidy level was assessed.

Genomic DNA was isolated from the dried leaf samples based on the CTAB method (Doyle and Doyle 1987). First, I sequenced chloroplast DNA (cpDNA). In order to test whether the cpDNA regions include intraspecific variations, five non-coding regions of cpDNA (*trnC-petN*, *rpl32-ndhF*, *ndhC-trnV*, *rps16-trnQ* and *trnT-trnL*) were preliminarily sequenced in two individuals from Teshio and Onneto populations, respectively. Because only two non-coding regions included intraspecific variations, *trnC-petN* and *trnT-trnL*, these regions were used for the analysis of genetic differentiation among populations. Two non-coding regions of cpDNA were amplified by PCR. The volume of total reaction mix was 20 µl, including 10 µl of Taq polymerase 2x master mix (Amplicon, Rødovre, Denmark), 8.4 µl of distilled water, 0.4 µl of each forward and reverse primers (10 pmol/µl) for *trnC-petN* or *trnT-trnL*, and 0.8 µl of diluted genomic DNA. I used "23F" and "25R" primers for *trnC-petN* (Ren et al. 2017) and "a" and "b" primers for *trnT-trnL* (Taberlet et al. 1991), respectively. The PCR cycle conditions were as below: initial 5 min at 95 °C, and 30 cycles of 95 °C for 60 seconds, 56 °C for 60 seconds, and 72 °C for 60 seconds. The sequencing of purified PCR product was performed using BigDye Terminator v.3.1 Cycle Sequencing Kit (Applied Biosystems, CA, USA) and DNA sequencing was performed on a 3730 Genetic Analyzer (Applied Biosystems).

Next, I sequenced nuclear ribosomal DNA (nrDNA). The internal transcribed spacer region (ITS) and the external transcribed spacer region (ETS) of nrDNA were amplified by PCR. First, two individuals from Teshio and Onneto populations were sequenced to test the intraspecific polymorphism. I used "ITS-leu" and "ITS4" primers (Baum et al. 1998; White et al. 1990) and "Ast-1" and "18S-ETS" primers (Baldwin and Markos 1998; Markos and Baldwin 2001) for the amplification of each ITS and ETS region, respectively. The reaction mix for PCR except for the primers and the PCR cycle conditions were the same as those of cpDNA amplification.

After the preliminary sequencing of nrDNA, both ITS and ETS showed intraspecific variations among the samples and heterozygosity at multiple loci within a sample. In this case, there are many possible alleles in a sample. For examples, if there are two heterozygous loci within a sample, A-G and T-C in ITS, possible allele combination should be (1) (A + T) and (G + C) or (2) (A + C) and (G + T). To determine the combination of allele in an individual, I used allele specific PCR method (Newton et al. 1989). I developed specific primers, where the 3' end of the nucleotide is complementary to one allele. The mismatch nucleotide was intentionally set at the third base from the 3' end of the developed primers to avoid non-specific amplification by decreasing binding efficiency between the primers and template DNA (Table S1, Hayashi et al. 2004). I conducted allele specific PCR for the samples showing multiple heterozygous loci by developed forward primers and universal reverse primers (ITS: ITS4, ETS: 18S-ETS, respectively) and sequencing those of PCR products.

All sequences were aligned by MEGA version X (Kumar et al. 2018). The cpDNA haplotypes were determined and a haplotype network analysis was conducted using TCS 1.23 (Clement et al. 2000) by statistical parsimony. All indels were regarded as point mutations. Ancestral haplotypes of cpDNA were speculated by phylogenetic analysis. Neighbor joining (NJ) trees were made in MEGA based on the sequences detected in this study and Ren et al. (2017) where closely related species with *P. kamtschaticus* were analyzed (Appendix. 3-1). Estimation of bootstrap support was conducted with 1000 replicates in MEGA. After determining ancestral haplotype of *P. kamtschaticus*, the sequences determined in this study and the sequence of *P. auriculatius* (DC.) J. R. Grant. (synonym of *P. kamtschaticus*) in China were used to create haplotype network. The nrDNA sequences showing multiple heterozygous loci were divided into two different haplotypes using the developed specific primers. I assumed all samples had two alleles in nrDNA regardless of ploidy level and heterozygosity.

Results

Sexual and vegetative reproduction along the elevation gradient

Flower production of the 4x-*bulb* populations was negatively correlated with elevation (z = -5.539, $P < 0.0001$; Fig. 3-3 A), whereas bulbil production did not change along the elevation gradient (z = 0.248, P = 0.804; Fig. 3-3 B). As a result, the ratio of bulbil production to total reproductive unit significantly increased with elevation (t = 4.013, $P < 0.0001$; Fig. 3-3 C). Regarding growth performance, both leaf number and plant height showed no significant change with elevation (z = 0.759, P = 0.448; t = -0.413, P = 0.680, respectively; Fig. 3-3 D, E). Flower production was positively correlated with plant height, although the interaction between elevation and plant height was negative (Table 3-2). The bulbil production was positively related to plant height, while the effect of elevation on bulbil production was removed in the best-fit model (Table 3-2). There was a positive correlation between floral bud number and bulbil number (z = 5.439, $P < 0.0001$; Fig. 3-3 F), indicating no trade-off relationship between sexual and vegetative reproduction. As expected from the morphological characteristics (bulbils are formed in the axil of leaves), bulbil number was strongly determined by leaf number (slope = 0.959, intercept = 0.673, $P < 0.0001$ in Linear Model; Fig. S3-1).

Comparison of bulbil formation among populations

I observed bulbil formation of 56–166 individuals with flowers per population depending on population size. The 4x-*bulb* populations formed bulbils at 100 % frequency (Table 3-3; Fig. 3-4). Bulbil formation was observed in several 4x-*kam* populations at low frequency, but Teshio population (35 %) and Tsubetsu population (20 %) showed relatively high bulbil formation rate. Bulbil formation in the 2x-*kam* populations was commonly low (0–8 %). The proportion of bulbil-formed plants in the 4x-*kam* populations was significantly higher than that in the 2x-*kam* populations (Table 3-4; Fig. 3-5). The proportion of bulbil-formed plants increased at higher

latitudes at a marginal significant level, but did not change significantly along the elevation gradient, and there were negative interactions between ploidy level and latitude or elevation gradient (Table 3-4).

Regarding bulbil size, the tetraploid (4x-*kam*) populations produced larger bulbils than the diploid (2x-*kam*) populations (Table 3-5 a, Fig. 3-6). Furthermore, bulbils size tended to increase with elevations and latitudes in both of the diploid (2x-*kam*) and tetraploid (4x-*kam* and 4x-*bulb*) populations (Table 3-5 b).

Ploidy levels of the samples in new localities

Flow cytometry analysis revealed that all samples from Bihoro, Omusaro, and Tsubetsu populations had twice as much DNA content as the sample from the diploid Tomakomai population (Fig. S3-2). This indicates these populations are tetraploid. Thus, updated distribution pattern of cytotypes in *Parasenecio kamtschaticus* is as shown in Figure 3-2 (see also Table 3-1).

Geographic pattern of genetic variation in *Parasenecio kamtschaticus*

In cpDNA, the length of aligned *trnC-petN* and *trnT-trnL* in *P. kamtschaticus* was 806 bp and 574 bp, respectively. In total of 129 individuals from 34 populations, only two haplotypes were found (haplotype C1 and C2). These haplotypes were separated by two substitutions. Although haplotype C1 was found only in 4x-*bulb* and northern 4x-*kam*, haplotype C2 was found widely across the research sites and taxonomic groups (Figs. 3-7 and 3-8). The phylogenetic tree and TCS network showed that haplotype C1 is the sequence reported in *P. auriculatus* growing in China and in other related species, such as *P. delphiniiphyllus, P. hastatus*, *P. kangxianensis,* and *P. komarovianus*. This indicates that haplotype C1 is an ancestral type in *P. kamtschaticus* and haplotype C2 is a derived type in Japan (Fig. 3-8, Fig. S3-3).

In nrDNA, the length of aligned ITS and ETS of *P. kamtschaticus* was 641 bp and 420 bp, respectively. In total of 135 individuals from 34 population, six haplotypes in ITS and four haplotypes in ETS were found. However, some haplotypes of ITS and ETS were only found in heterozygote within an individual, which might be attributed to non-random mating and the deviation from the Hardy-Weinberg equilibrium. Because ITS and ETS regions have multiple copies within a genome, these heterozygotes might be caused by the variation within a genome in an individual. Thus, I excluded ITS and ETS regions from my analysis because the variation within individual plants may make it difficult to clarify the phylogenetic relationships among populations.

Discussion

The advantage of vegetative reproduction in high elevation environments

The survey of sexual and vegetative reproduction in the 4x-*bulb* populations demonstrated that flower production decreased with elevation, but bulbil production, leaf production, and plant height did not change along the elevation gradient. Furthermore, the size-dependency of flower production tended to decrease with elevation, while size-dependency of bulbil production was not influenced by elevation. Generally, flower and seed production tend to decrease with elevation due to low temperature, low activity of pollinators, and short growing season (Huang and Hsieh 2014, Kudo and Suzuki 2002, Kudo and Hirao 2020). Thus, the decrease in flower production with keeping bulbil production in 4x-*bulb* may be a strategy to avoid the failure of sexual reproduction and save resources. Because bulbils of 4x-*bulb* start to develop soon after leaf expansion, development and dispersal of bulbils occur before fruiting season. In addition, large-sized and rapid growth seedlings derived from bulbils should be adaptive for the establishment at high elevations with harsh climate and short growing season (Stöcklin et al. 2009). In conclusion, vegetative reproduction by bulbils is crucial for maintaining populations

at high elevations (Kudo and Hirao 2020).

The evolution of vegetative reproduction by polyploidization

Bulbil formation was very rare and bulbil size was small in the 2x-*kam* populations in comparison with the 4x-*kam* populations, suggesting the linkage between bulbil production ability and polyploidization in this species. Unfortunately, physiological mechanism promoting bulbil formation is unclear in this study. There are several studies indicating the changes in meristem growth and gene expression for hormone control in polyploid plants (Hatano et al. 2012; Van Drunen and Husband 2018). In triploid *Lilium lancifolium* producing aerial bulbils, for example, change in axillary meristem structure, increment of starch and sucrose metabolism, and change in the synthetic efficiency of auxin and cytokinin in leaf axils are reported (Yang et al. 2017). Therefore, polyploidization is likely to enhance the potential for bulbil formation by any physiological control also in *Parasenecio kamtschaticus*.

When 2x-*kam* populations and 4x-*kam* populations were compared, there was no positive effects of elevation gradient on bulbil formation (Table 3-4) and size (Table 3-5 a). This may indicate that polyploidization improved the potential for vegetative reproduction, and natural selection to produce more bulbils might act in some specific tetraploid populations growing at higher elevations, promoted the evolution of a phenotype having high ability of vegetative reproduction, i.e., 4x-*bulb*.

Evolutionary process of 4x-*bulb* in Japan

Phylogenetic trees and haplotype network showed that the sequence of haplotype C1 is reported in *Parasenecio kamtschaticus* growing in China and other related species, while the sequence of haplotype C2 is only found in Japan. This indicates that haplotype C1 is the ancestral type. Interestingly, haplotype C1 was only found in some tetraploid populations (4x-*kam* in northern Hokkaido and 4x-*bulb*), whereas haplotype C2 is found widely in both diploid (2x-*kam*) and

tetraploid (4x-*kam* and 4x-*bulb*) populations. Because the shift from tetraploids to diploids is not likely to occur, haplotype C2 had been derived from haplotype C1 before the diploids of haplotype C1 completely disappeared. After that, the tetraploids of haplotype C2 (not 4x-*bulb*) would be derived from the diploids of haplotype C2. Assuming these processes, I discuss the two possible scenarios of the evolution of 4x-*bulb*: single origin and multiple origins scenarios.

Two possible processes are considerable for the single origin scenario. First process is that haplotype C1 disappeared in all diploid populations, and 4x-*bulb* was derived from northern 4x-*kam*. In this case, the existence of haplotype C2 in 4x-*bulb* populations might occur by a secondly gene flow after the establishment of 4x-*bulb* populations from any 4x-*kam* population having haplotype C2 (the candidate population is unknown). Another possibility of the single origin scenario is that 4x-*bulb* evolved from tetraploids of haplotype C2. In this case, existence of haplotype C1 in 4x-*bulb* populations might occur by a secondly gene flow from northern 4x-*kam* populations.

The multiple origins scenario is as follows: 4x-*bulb* of haplotype C1 was evolved from northern 4x-*kam*, and that of haplotype C2 was evolved from tetraploids of haplotype C2. In this study, it is difficult to select the most probable scenario of 4x-*bulb* evolution due to the small variations of cpDNA. In future studies, population genetics based on genome-wide SNP markers, such as Mig-seq method (Suyama and Matsuki 2015) should be conducted.

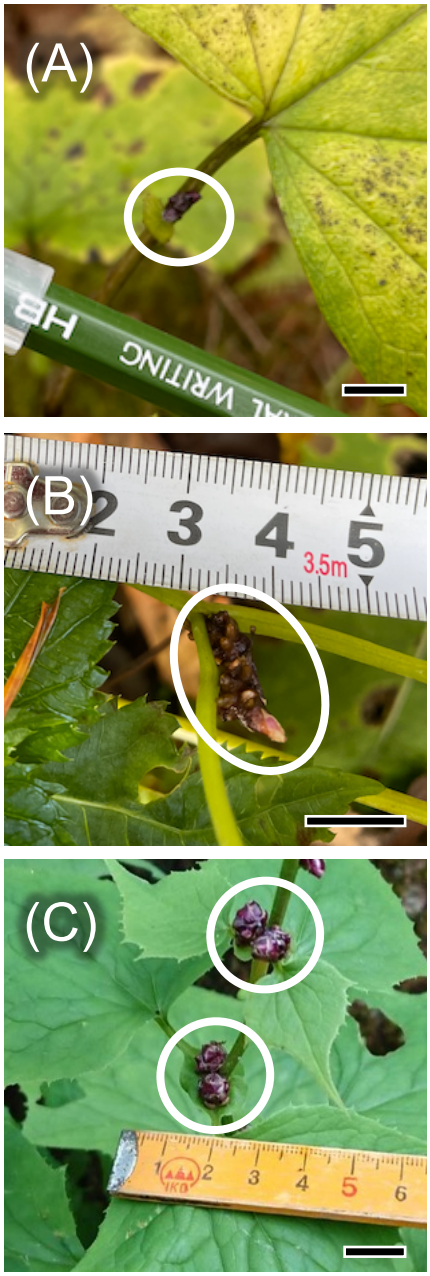

Figure 3-1. Morphological characteristics of axil bulbil in the three taxonomic groups of *Parasenecio kamtschaticus*. (A) 2x-*kam* in Mt. Soranuma, (B) 4x-*kam* in Nakagawa, and (C) 4x-*bulb* in Numanohara. Scale bars show 1 cm. Refer Table 3-1 for the description of sampling sites.

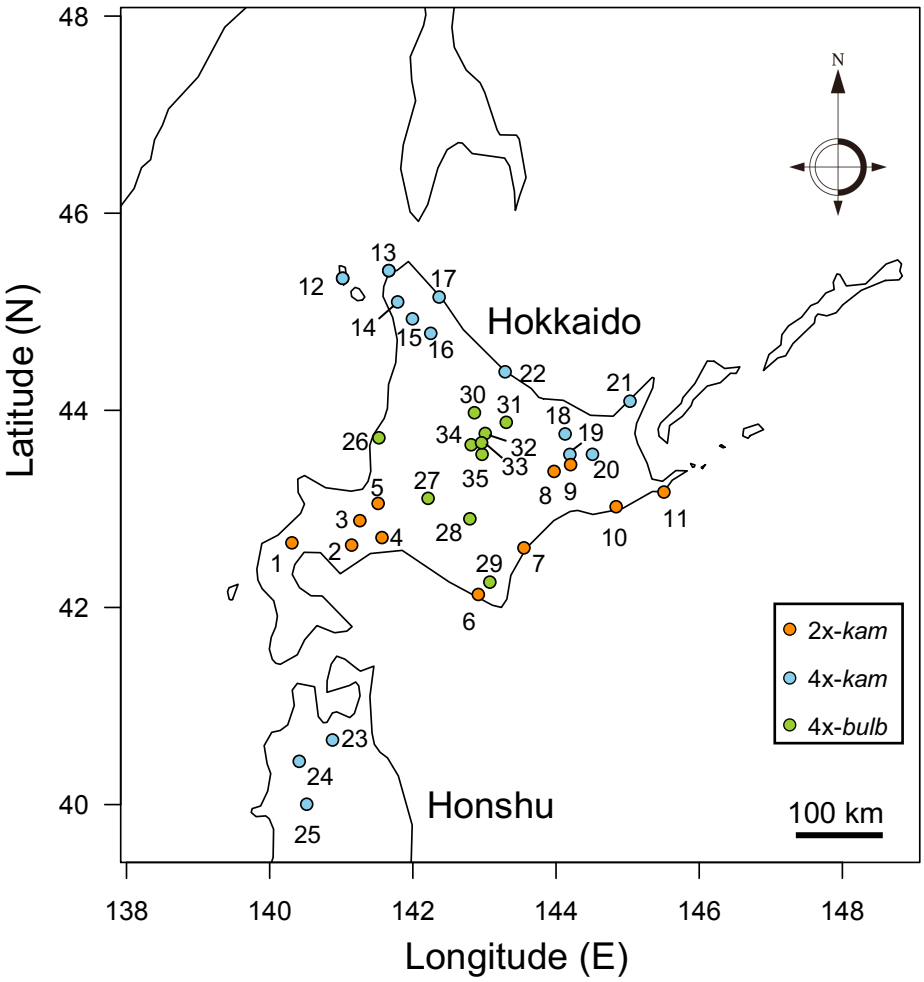

Figure 3-2. Geographical locations of sampling and study sites in Hokkaido and northern Honshu. Refer Table 3-1 for detail information of each site.

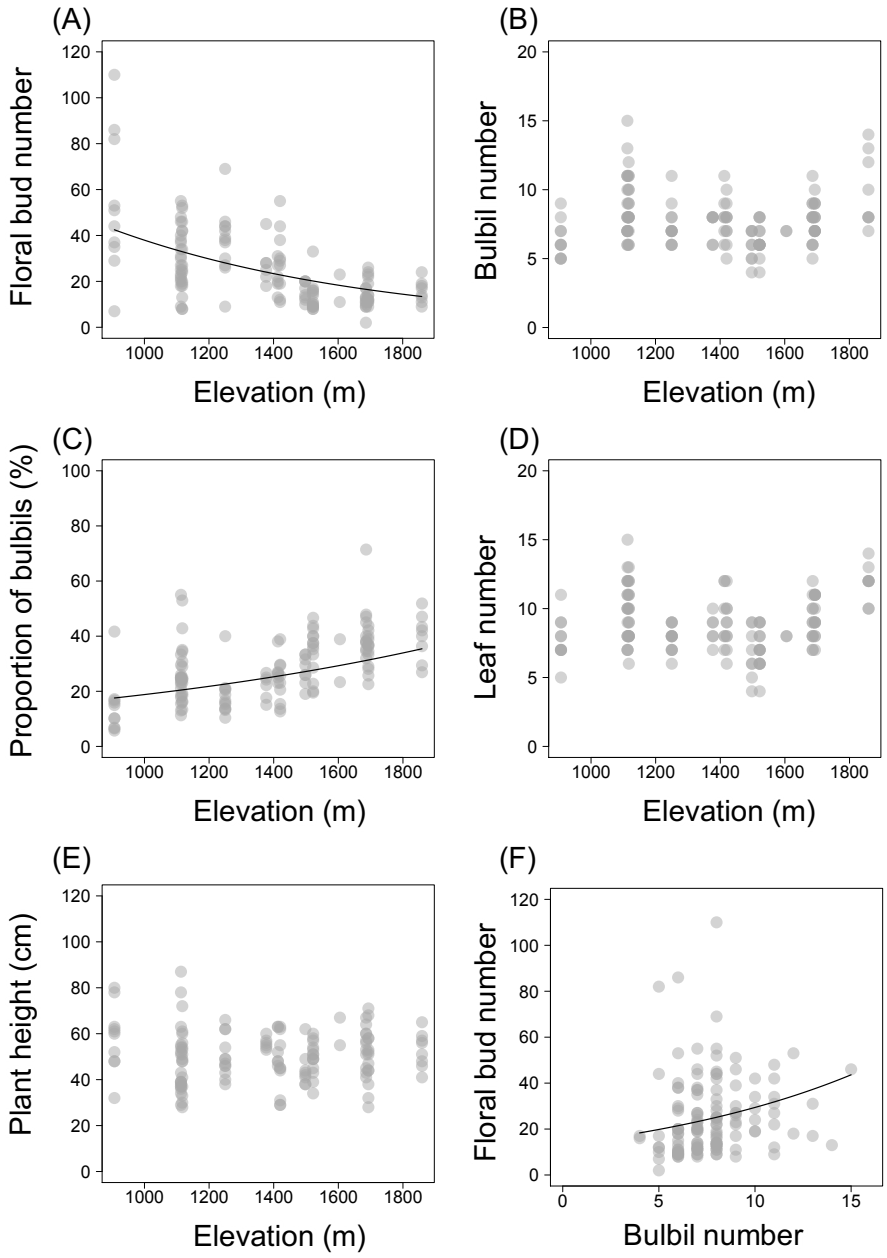

Figure 3-3. Changes in the reproductive and morphological traits along the elevation gradient in *Parasenecio kamtschaticus* var. *bulbifer*. (A) Floral bud number, (B) bulbil number, (C) the proportion of bulbil number to total reproductive unit (sum of floral buds and bulbils), (D) leaf number, (E) plant height, and (F) the relationship between flower production and bulbil production. Each dot indicates one flowering individual.

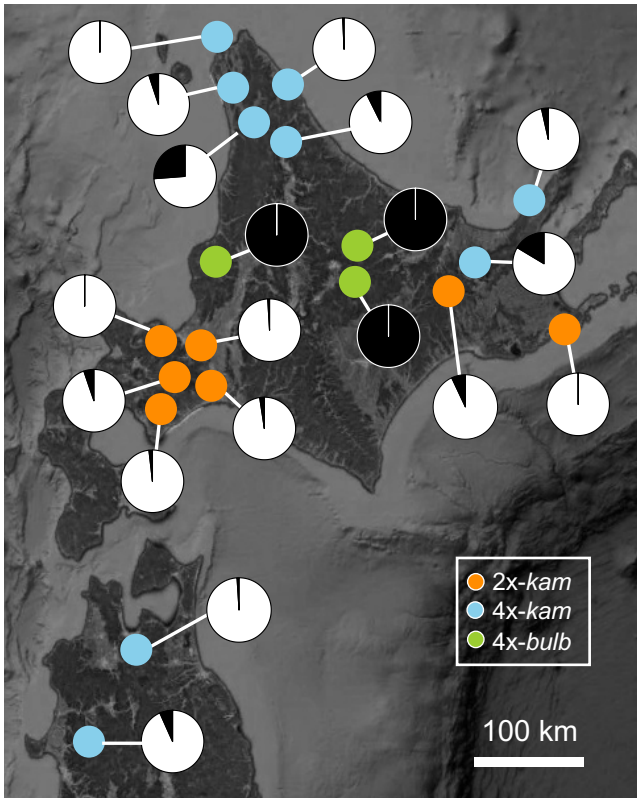

Figure 3-4. Comparisons of bulbil formation rates among three taxonomic groups (2x-*kam*, 4x-*kam*, 4x-*bulb*) of *Parasenecio kamtschaticus* in Hokkaido and northern Honshu. White: plants with no bulbil, black: plants produced bulbils.

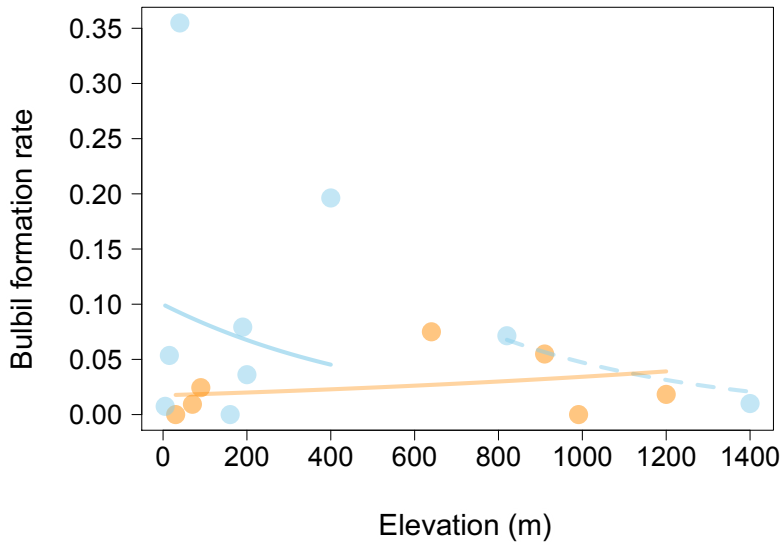

Figure 3-5. Bulbil formation patterns along the elevation gradient in 2x-*kam* populations and 4x-*kam* populations. Orange: 2x-*kam* populations, blue: 4x-*kam* populations. For 4x-*kam* populations, solid line indicates Hokkaido populations, and broken line indicates Honshu populations.

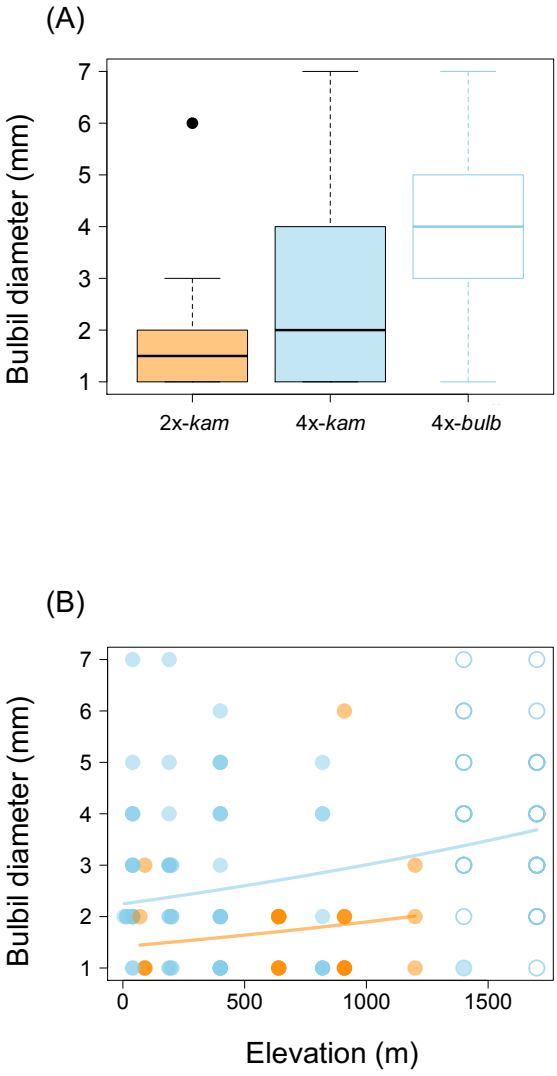

Figure 3-6. (A) Comparison of bulbil diameter among 2x-*kam* (orange), 4x-*kam* (filled blue box), and 4x-*bulb* (blank blue box). (B) Changes in bulbil size along the elevation gradient in 2x-*kam* (closed orange circle), 4x-*kam* (closed blue circle) and 4x-*bulb* (open blue circle).

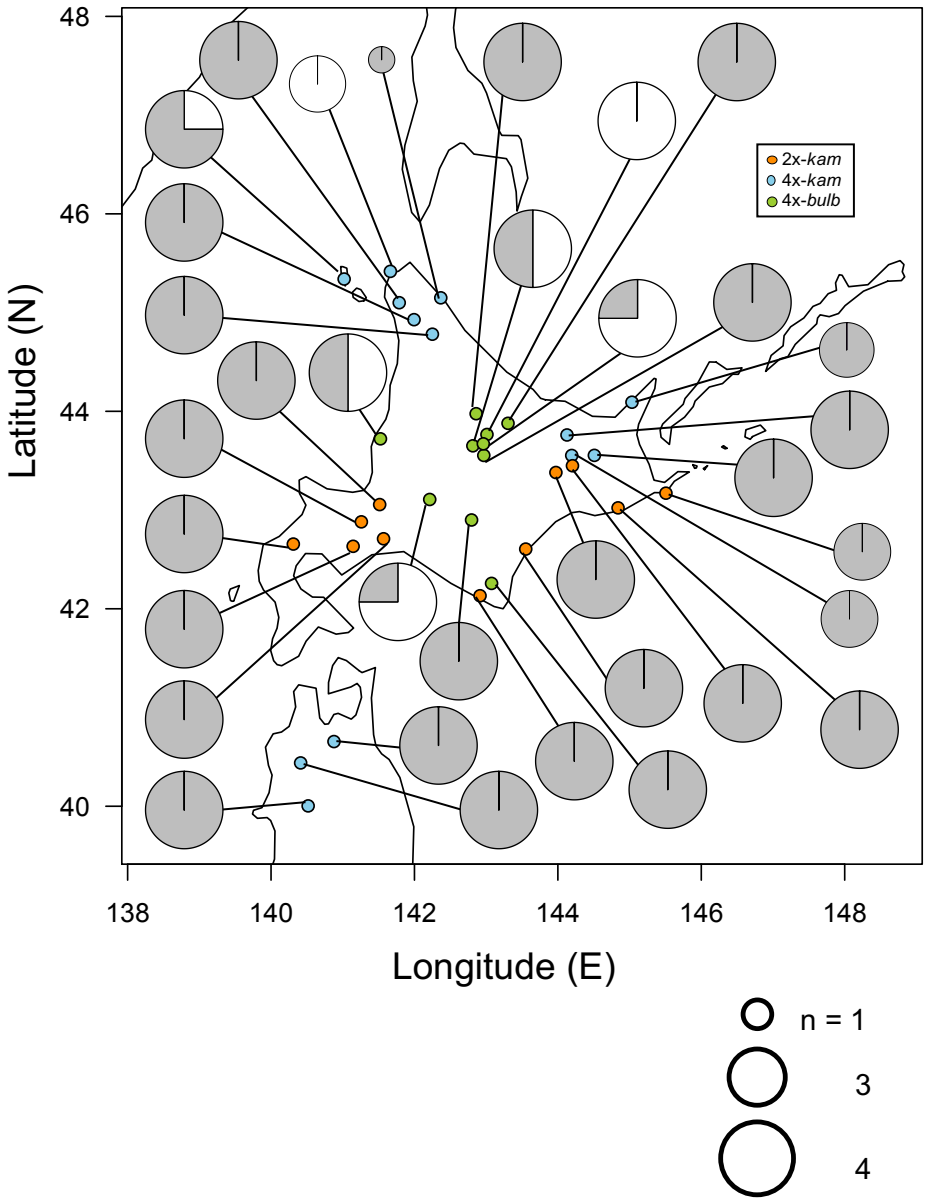

Figure 3-7. The distribution of chloroplast DNA (cpDNA) haplotypes in *Parasenecio kamtschaticus* populations. White: C1 haplotype, gray: C2 haplotype. The sample number are expressed by circle size.

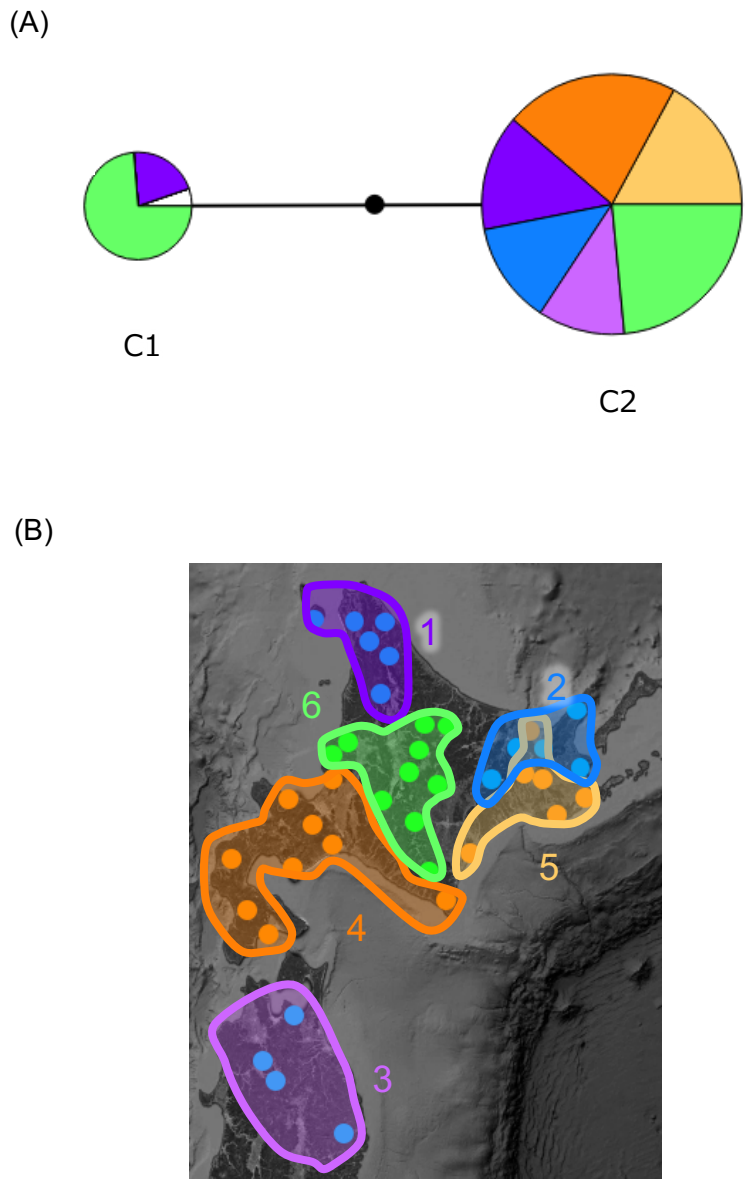

Figure 3-8. TCS haplotype network of *Parasenecio kamtschaticus* (A) and the distribution of each haplotype of *P. kamtschaticus* (B). In the TCS network, black node means one substitution, white part in haplotype C1 indicates the sequence of *P. auriculatus* in China, and other colors in the circle graphs indicate the haplotypes shown in the map (B). 1: northern 4x-*kam* populations, 2: eastern 4x-*kam* populations, 3: Honshu 4x-*kam* populations, 4: western 2x-*kam* populations, 5: eastern 2x-*kam* populations, and 6: 4x-*bulb* populations.

Table 3-1. Geographic locations of sampling sites. Ploidy: ploidy level (2x: diploid, 4x: tetraploid), Taxon (*kam*: *Parasenecio kamtschaticus* var. *kamtschaticus*, *bulb*: *P. kamtschaticus* var. *bulbifer*). See Fig. 3-1 for the locations in a map.

No.	Population	ID	Region	Latitude, N	Longitude, E	Elevation (m)	Ploidy	Taxon
1	Kuromatsunai	Kro	Western	42.65552	140.31059	70	2x	*kam*
2	Mt. Horohoro*	Mho	Western	42.63268	141.14476	1200	2x	*kam*
3	Mt. Soranuma*	Mso	Western	42.88040	141.25958	910	2x	*kam*
4	Tomakomai*	Tom	Western	42.70904	141.56889	90	2x	*kam*
5	Nopporo*	Nop	Western	43.05533	141.51495	70	2x	*kam*
6	Mt. Kannon	Mka	Western	42.13190	142.91456	90	2x	*kam*
7	Lake Yudo	Lyu	Eastern	42.60462	143.55179	5	2x	*kam*
8	Onneto	Onn	Eastern	43.38026	143.97252	640	2x	*kam*
9	Sokodai	Sok	Eastern	43.44874	144.20349	685	2x	*kam*
10	Akkeshi*	Akk	Eastern	43.02205	144.83947	30	2x	*kam*
11	Ochiishi*	Och	Eastern	43.17082	145.50724	45	2x	*kam*
12	Rebun	Reb	Northern	45.33971	141.01934	135	4x	*kam*
13	Wakkanai*	Wak	Northern	45.41740	141.66428	160	4x	*kam*
14	Toyotomi*	Toy	Northern	45.09989	141.78758	15	4x	*kam*
15	Teshio*	Tes	Northern	44.92815	141.99420	40	4x	*kam*
16	Nakagawa*	Nak	Northern	44.78098	142.25015	190	4x	*kam*
17	Hamatonbetsu*	Ham	Northern	45.14938	142.36714	5	4x	*kam*
18	Bihoro	Bih	Eastern	43.76030	144.12722	90	4x	*kam*
19	Tsubetsu*	Tsu	Eastern	43.55266	144.19332	400	4x	*kam*
20	Lake Mashu	Lma	Eastern	43.55380	144.50881	520	4x	*kam*
21	Utoro*	Uto	Eastern	44.09221	145.03321	200	4x	*kam*
22	Omusaro +	Omu	Eastern	44.39089	143.28873	5	4x	*kam*
23	Mt. Hakkoda*	Mha	Honshu	40.65505	140.87753	1400	4x	*kam*
24	Mt. Tashiro	Mta	Honshu	40.43868	140.41288	890	4x	*kam*
25	Mt. Moriyoshi*	Mmo	Honshu	40.00346	140.51744	820	4x	*kam*
26	Mt. Shokanbetsu*	Msh	Central	43.72123	141.52573	1400	4x	*bulb*

27	Mt. Yubari	Myu	Central	43.10701	142.21288	1000	4x	*bulb*
28	Mt. Memuro	Mme	Central	42.89930	142.79645	620	4x	*bulb*
29	Mt. Rakko	Mra	Central	42.25700	143.07542	350	4x	*bulb*
30	Mt. Teshio	Mte	Central	43.97560	142.86013	1200	4x	*bulb*
31	Maruseppu	Mar	Central	43.87846	143.30482	400	4x	*bulb*
32	Mt. Hira*	Mhi	Central	43.76526	143.01110	1700	4x	*bulb*
33	Mt. Aka	Mak	Central	43.67063	142.96027	1500	4x	*bulb*
34	Mt. Asahi	Mas	Central	43.65047	142.81459	1250	4x	*bulb*
35	Numanohara*	Num	Central	43.55346	142.96681	1100	4x	*bulb*

* These sites were used for the observations of bulbil formation. + This site was only used for the flow-cytometry analysis.

Table 3-2. GLM results of the size-dependency of flower production (a) and bulbil production (b) along the elevation gradient in 4x-*bulb* populations. The best-fit models are shown.

(a) Size-dependency of flower production

Variable	Coefficient	SE	*z*	*P*	
Intercept	2.816	0.630	4.473	< 0.001	***
Elevation	-0.0005	0.0005	-1.02	0.307	
Plant height	0.042	0.010	4.183	< 0.001	***
Elevation × plant height	-0.00002	0.00001	-2.049	0.041	*

(b) Size-dependency of bulbil production

Variable	Coefficient	SE	*z*	*P*	
Intercept	1.586	0.152	10.458	< 0.001	***
Plant height	0.009	0.003	3.197	0.002	**

*** $P < 0.001$, ** $P < 0.01$, * $P < 0.05$.

Table 3-3. Bulbil formation rates of 19 populations.

Population	Ploidy level	Taxon	Obs. date	Bulbil-formed	Sample size	Frequency (%)
Nopporo	2x	*kam*	Oct. 9, 2021	1	107	0.93
Soranuma	2x	*kam*	Sep. 28, 2021	9	164	5.49
Mt. Teine	2x	*kam*	Jul. 27, 2021	0	150	0
Mt. Horohoro	2x	*kam*	Sep. 10, 2021	3	164	1.83
Tomakomai	2x	*kam*	Sep. 1, 2021	4	164	2.44
Onneto	2x	*kam*	Sep. 24, 2023	9	120	7.50
Akkeshi	2x	*kam*	Sep. 5, 2020	0	150	0
Wakkanai	4x	*kam*	Sep. 17, 2021	0	71	0
Hamatonbetsu	4x	*kam*	Sep. 17, 2021	1	134	0.74
Toyotomi	4x	*kam*	Sep. 17, 2021	3	56	5.36
Teshio	4x	*kam*	Sep. 16, 2021	22	62	35.48
Nakagawa	4x	*kam*	Sep. 16, 2021	13	164	7.93
Utoro	4x	*kam*	Oct. 5, 2021	6	166	3.61
Tsubetsu	4x	*kam*	Oct. 6, 2021	21	107	19.63
Mt. Hakkoda	4x	*kam*	Aug. 17, 2023	1	100	1.00
Mt. Moriyoshi	4x	*kam*	Aug. 18, 2023	8	112	7.14
Mt. Hira	4x	*bulb*	Aug. 23, 2021	100	100	100
Mt. Shokanbetsu	4x	*bulb*	Sep. 5, 2021	105	105	100
Numanohara	4x	*bulb*	Aug. 4, 2021	100	100	100

Table 3-4. GLM result for bulbil formation rate between diploid (2x-*kam*) and tetraploid (4x-*kam*) populations. The best-fit model is shown.

Variable	Coefficient	SE	*z*	*P*	
Intercept	-65.65	35.91	-1.828	0.067	+
Ploidy (4x)	78.30	36.77	2.130	0.033	*
Latitude	1.433	0.832	1.719	0.086	+
Elevation	0.001	0.001	1.406	0.160	
Ploidy × latitude	-1.763	0.851	-2.071	0.038	*
Ploidy × elevation	-0.003	0.001	-2.651	0.008	**

** $P < 0.01$, * $P < 0.05$, + $P < 0.1$. Intercept = 2x-*kam*.

Table 3-5. GLMM results for the comparison of bulbil size between taxonomic groups. The best-fit models are shown.

(a) Comparison between 2x-*kam* and 4x-*kam*

Variable	Coefficient	SE	*t*	*P*	
Intercept	0.549	0.108	5.098	< 0.001	***
Ploidy (4x)	0.410	0.126	3.250	0.001	**

(b) Comparison between diploid (2x-*kam*) and tetraploid (4x-*kam* and 4x-*bulb*)

Variable	Coefficient	SE	*t*	*P*	
Intercept	-3.362	1.842	-1.825	0.068	+
Ploidy (4x)	0.461	0.120	3.853	< 0.001	***
Latitude	0.084	0.042	2.034	0.042	*
Elevation	0.0003	0.0001	4.040	< 0.001	***

*** $P < 0.001$, ** $P < 0.01$, * $P < 0.05$, + $P < 0.1$. Intercept = 2x-*kam*.

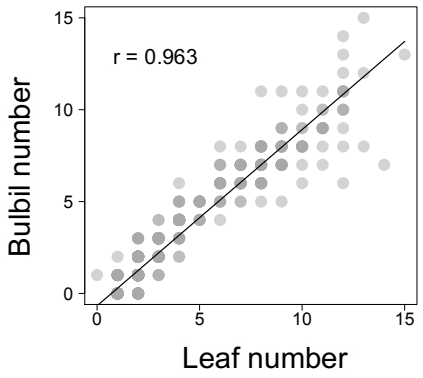

Figure S3-1. The relationship between leaf number and bulbil number in *Parasenecio kamtschaticus* var. *bulbifer*.

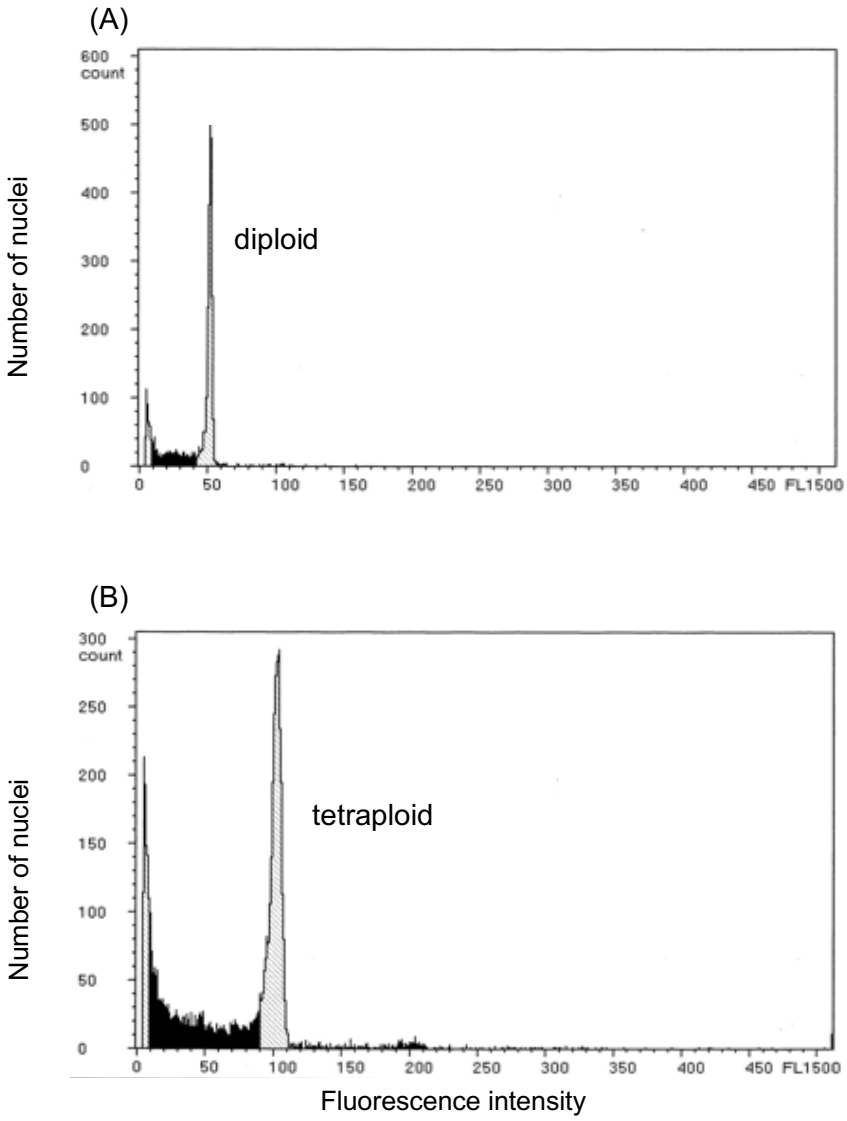

Figure S3-2. The results of flow cytometry analysis from (A) diploid population (Tomakomai) and (B) tetraploid population (Omusaro).

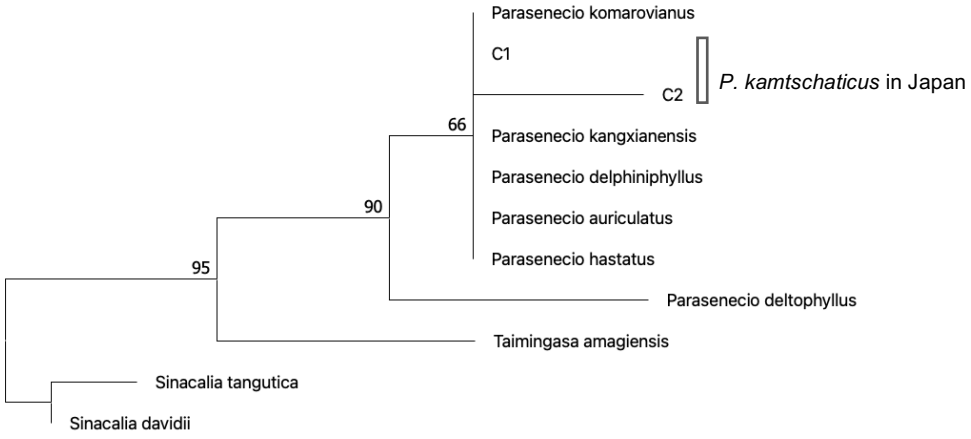

Figure S3-3. The neighbor-joining (NJ) trees based on cpDNA sequences detected in this study (C1 and C2) and other related *Parasenecio* species examined by Ren et al. (2017). The numbers with the branches indicate bootstrap values of more than 50 %.

Table S3-1. Primers sequences of allele specific primers for ITS and ETS. Bold letters show the bases complementary to allele specific variable sites. Small letters show the intentional mismatch bases.

Primer name (F: forward)	Sequence (5' to 3')
Specific Primers for ITS-F	CATGCTTCTCCGTTTGC<u>c</u>G**A**
Specific Primers for ETS-F	TGTTGGTTTTCTGTATT<u>c</u>A**T**

Table S3-2. Variable sites of cpDNA including *trnC-petN* and *trnT-trnL* between two haplotypes.

Haplotype	Variable site	
	trnC-petN	*trnT-trnL*
	627	309
C1	C	G
C2	T	T

Appendix 3-1. The information of used sequence data described in Ren et al. (2017). Summary of taxa, sampling site, accession numbers of *trnC-petN* and *trnT-trnL* are shown.

1. Parasenecio auriculatus (DC.) J. R. Grant, Fusong, Jilin, China, KY970625, KY970833.

2. P. deltophyllus (Maxim.) Y. L. Chen, Lintan, Gansu, China, KY970613, KY970821.

3. P. delphiniiphyllus (H. Lév.) Y. L. Chen, Qiaojia, Yunnan, China, KY970614, KY970822.

4. P. hastatus (L.) H. Koyama, Fusong, Jilin, China, KY970624, KY970832.

5. P. kangxianensis (Z.Ying Zhang & Y. H. Guo) Y. L. Chen, Kangxian, Gansu, China, KY970666, KY970874.

6. P. komarovianus (Pojark.) Y. L. Chen, Fusong, Jilin, China, KY970657, KY970865.

7. Sinacalia davidii (Franch.) H. Koyama, Baoxing, Sichuan, China, KY970674, KY970882.

8. S. tangutica (Maxim.) B. Nord., Shennongjia, Hubei, China, KY970602, KY970810.

9. Taimingasa amagiensis (Kitam.) H. Koyama, Shizuoka, Japan, KY970716, KY970924.

General discussion

Ecological diversification mechanisms by polyploidization

Polyploidization has been regarded as the drivers of intraspecific diversification in plants. Many studies reported the changes in morphological and ecological traits and the distribution patterns in polyploid populations compared to the diploid populations of the same or related species. Recent empirical studies focused on the direct effects of polyploidization by the comparison of synthesized autopolyploids with the original diploids, and revealed that a shift to self-compatibility (Siopa et al. 2020), enhancement of photosynthetic ability (Domínguez-Delgado et al. 2021), and larger resource investment in vegetative reproduction (van Drunen and Husband 2018) occurred immediately after polyploidization. The extent of these modifications varied largely among synthesized plants, indicating that the polyploidization expands the amplitude of intraspecific variations and increases the potential of adaptation to various environments (Soltis et al. 2014). In the present study, I clarified that the polyploidization in *P. kamtschaticus* increases the potential abilities of larger morphology and vegetative reproduction. Specifically, the increment of plant size and bulbil production enable the tetraploids to expand the distribution range from cool-temperate forests to boreal forests, and to high elevation regions, respectively. Although the relationship between the distribution pattern of polyploid populations and the preferential habitat type has been studied well, little is known about the possibility that multiple morphological changes promote the polyploid establishment in various environments within single species. The present study sheds light on this issue.

Mechanisms of the mitigation of the MCE and the establishment of polyploid populations

For the establishment of new polyploids, it is necessary to develop the mechanisms to avoid the minority cytotype exclusion (MCE). Previous studies suggested that niche differentiation may play a role in mitigating the MCE by reducing inter-cytotype crossing. The present study clarified that the increment of plant size by polyploidization leads to the advantage at vegetative growth stage, resulting in the change of niche preference between 2x-*kam* and 4x-*kam*; 2x-*kam* is advantageous in deciduous cool-temperate forests, whereas 4x-*kam* is advantageous in evergreen boreal forests. Because there is no phenological shift and induction of self-compatibility in 4x-*kam*, niche differentiation may be the most important mechanism to mitigate the MCE and establish new populations for 4x-*kam*. Previous studies clarified that various morphological and physiological changes by polyploidization are related to niche differentiation, e.g., higher tolerance to cold stress by apomixis (Karunarathne et al. 2018), drought stress by thicker leaves with dense pubescence (Li et al. 2009). This study indicated that the size increment could play a role in both mitigating the MCE and expansion to boreal forests in 4x-*kam* via niche shift. The size increment is a common trend in polyploids, thus the present study can provide insight into the process of polyploid establishments in perennial plants.

Regarding the establishment process of 4x-*bulb* populations, negative effects of the MCE might be small because the distributions of 4x-*bulb* are most isolated from the distribution range of 2x-*kam* populations. As predicted in this study, 4x-*bulb* populations might be derived from 4x-*kam* populations under the selective forces promoting the vegetative reproduction ability toward higher elevations.

Reproductive strategy of 4x-*bulb* populations at higher elevations

At high elevation sites, seed production of plants is often restricted due to harsh climate conditions and short growing season, and relative importance of vegetative reproduction tends to increase. Thus, tetraploids could expand to higher elevation habitat by the enhancement of the vegetative reproduction ability. Although floral bud number decreased with elevation, the 4x-*bulb* populations maintained flower production at a certain level even at higher elevations. In addition, the 4x-*bulb* populations showed low self-compatibility and maintained the ability of seed reproduction by outcrossing. The dominance of vegetative reproduction often decreases the genetic diversity of populations (Jusaitis and Adams 2005), and it may increase the risk of local extinction. Thus, occasional sexual reproduction in the 4x-*bulb* populations may be important to maintain the genetic diversity. In fact, previous study reported high genetic diversity in the 4x-*bulb* populations as well as that in the 2x-*kam* and 4x-*kam* populations (Kudo and Hirao 2020), indicating the effectiveness of sexual reproduction in the 4x-*bulb* populations.

Several studies demonstrated that many alpine plants that mainly reproduce asexually continue to produce flowers for sexual reproduction (Fan and Yang 2008; Stöcklin et al. 2009). This suggests the importance of sexual reproduction even under severe environmental conditions. The bulbil production in 4x-*bulb* plants may contribute to extend the life-span of genets (Kudo 2022) and it helps to conduct sexual reproduction in a good weather summer (with long growing period and less frost damage). In conclusion, the 4x-*bulb* populations at high elevations may be maintained by two reproductive strategies, i.e., genet persistence by vegetative reproduction and maintenance of genetic diversity by sexual reproduction.

Conclusion

Throughout the comparative studies of diploid and tetraploid populations in *Parasenecio kamtschaticus*, I demonstrated that polyploidization increased the potential ability of size increment and vegetative reproduction by axil bulbils. The large morphological stature enabled tetraploids to expand the distribution range to boreal forests in northeastern Hokkaido owing to the competitive advantages under light-limited conditions. In addition, the niche differentiation of tetraploids might be effective for the mitigation of the MCE by ancestral diploids without the shift of reproductive mode to self-compatibility. Furthermore, the potential ability of bulbil formation in tetraploids was accelerated by the natural selection at higher elevation habitat, where stable seed production is restricted, resulting in the evolution of bulbiferous phenotype, *P. kamtschaticus* var *bulbifer*. In conclusion, polyploidization may be an important mechanism driving the diversification of morphological traits, life-history traits, and distribution patterns within a single species and accelerating speciation. In future, direct effects of polyploidization on various ecological traits and the niche differentiation mechanism among cytotypes will be clarified by experimental approaches, such as the reciprocal transplant experiments using diploids and newly synthesized polyploids.

Acknowledgements

I am deeply grateful to my supervisor Assoc. Prof. Gaku Kudo for his helpful discussion, valuable suggestions, and patient encouragements throughout this study. I also thank to Prof. Shin-ichiro Aiba, Prof. Shiro Tsuyuzaki, and Assoc. Prof. Koh Nakamura for their kind advice and comments for this study.

I am grateful to Assoc. Prof. Makoto Kobayashi of Field Science Center for Northern Biosphere (FSC), Hokkaido University for his kind support for reciprocal transplant experiments. I would like to thank to Prof. Yoichiro Hoshino of FSC for providing me chances to use flow cytometers many times. I appreciate the staffs of Tomakomai Experimental Forest, Teshio Experimental Forest, Nakagawa Experimental Forest, Akkeshi Marine Station, Nayoro Research Office, and Genome Dynamics Research Center, Hokkaido University for permission to conduct field survey and transplant experiments and for their kind assistance in field work. I also appreciate the staffs of Shiretoko Nature Foundation, Bihoro Museum, and Sarobetsu Wetland Center for permission to conduct field survey and to collect plants and for providing me information of my study species.

This work was partly supported by the Hokkaido University DX Doctoral Fellowship and funding from Shirataki Geopark Promotion Council, Engaru-town, Hokkaido.

I thank Akari Shibata, Akimi Wakui, Nozomi Oshima, Akira Matsuura, Jun Shigeeda, Yohei Ito, Taietsu Nagase, Hiroaki Tomita, Keigo Takahashi, Xiao Shuqi, HaiXiang Liew, Akane Suzuki, Eri Abo, Megumi Shimada, Takayuki Ogawa, and Yasuhiko Otsuki for their kind assistance in field work and very helpful discussions, comments, and encouragements.

References

Anneberg, T. J., and K. A. Segraves. 2023. Neopolyploidy causes increased nutrient requirements and a shift in plant growth strategy in *Heuchera cylindrica*. Ecology 104:1–13.

Aversano, R., M. R. Ercolano, I. Caruso, C. Fasano, D. Rosellini, and D. Carputo. 2012. Molecular tools for exploring polyploid genomes in plants. Int. J. Mol. Sci. 13:10316–10335.

Baack, E. J., and M. L. Stanton. 2005. Ecological factors influencing tetraploid speciation in snowbuttercups (*Ranunculus adoneus*): niche differentiation and tetraploid establishment. Evolution 59:1936–1944.

Balao, F., J. Herrera, and S. Talavera. 2011. Phenotypic consequences of polyploidy and genome size at the microevolutionary scale: A multivariate morphological approach. New Phytol. 192:256–265.

Baldwin, B. G., and S. Markos. 1998. Phylogenetic utility of the external transcribed spacer (ETS) of 18S-26S rDNA: Congruence of ETS and ITS trees of *Calycadenia* (Compositae). Mol. Phylogenet. Evol. 10:449–463.

Baldwin, S. J., and B. C. Husband. 2013. The association between polyploidy and clonal reproduction in diploid and tetraploid *Chamerion angustifolium*. Mol. Ecol. 22:1806–1819.

Barker, M. S., N. Arrigo, A. E. Baniaga, Z. Li, and D. A. Levin. 2016. On the relative abundance of autopolyploids and allopolyploids. New Phytol. 210:391–398.

Barringer, B. C. 2007. Polyploidy and self-fertilization in flowering plants. Am. J. Bot. 94:1527–1533.

Bates, D. 2011. Mixed models in R using the lme4 package. Part 5: Generalized linear

mixed models. University of Wisconsin, Madison, Wisconsin, USA. Website: http://lme4.r-forge.r-project.org/.

Bauert, M. R. 1993. Vivipary in *Polygonum viviparum*: an adaptation to cold climate? Nord. J. Bot. 13:473–480.

Baum, D. A., R. L. Small, and J. F. Wendel. 1998. Biogeography and floral evolution of baobabs (Adansonia, Bombacaceae) as inferred from multiple data sets. Syst. Biol. 47:181–207.

Becker, F. W., K. C. Oberlander, P. Trávníček, and L. L. Dreyer. 2022. Inconsistent expression of the gigas effect in polyploid *Oxalis*. Am. J. Bot. 109:1607–1621.

Blanquart, F., O. Kaltz, S. L. Nuismer, and S. Gandon. 2013. A practical guide to measuring local adaptation. Ecol. Lett. 16:1195–1205.

Brochmann, C., A. K. Brysting, I. G. Alsos, L. Borgen, H. H. Grundt, A. C. Scheen, and R. Elven. 2004. Polyploidy in arctic plants. Biol. J. Linn. Soc. 82:521–536.

Casazza, G., F. C. Boucher, L. Minuto, C. F. Randin, and E. Conti. 2017. Do floral and niche shifts favour the establishment and persistence of newly arisen polyploids? A case study in an alpine primrose. Ann. Bot. 119:81–93.

Chen, T., Y. Sheng, Z. Hao, X. Long, F. Fu, Y. Liu, Z. Tang, A. Ali, Y. Peng, Y. Liu, L. Lu, X. Hu, J. Shi, and J. Chen. 2021. Transcriptome and proteome analysis suggest enhanced photosynthesis in tetraploid *Liriodendron sino-americanum*. Tree Physiol. 41:1953–1971.

Cheng, J., X. Yang, L. Xue, B. Yao, H. Lu, Z. Tian, J. Li, X. Zhou, Y. Zhang, Z. U. H. Mohammad, S. Wu, X. Song, S. Hu, and S. Qiang. 2020. Polyploidization contributes to evolution of competitive ability: a long term common garden study on the invasive *Solidago canadensis* in China. Oikos 129:713–723.

Clement, M., D. Posada, and K. A. Crandall. 2000. TCS: a computer program to estimate gene genealogies. Mol. Ecol. 9:1657–1660.

Comai, L. 2005. The advantages and disadvantages of being polyploid. Nat. Rev. Genet. 6:836–846.

Corneillie, S., N. De Storme, R. Van Acker, J. U. Fangel, M. De Bruyne, R. De Rycke, D. Geelen, W. G. T. Willats, B. Vanholme, and W. Boerjan. 2019. Polyploidy affects plant growth and alters cell wall composition. Plant Physiol. 179:74–87.

Dai, F., Z. Wang, G. Luo, and C. Tang. 2015. Phenotypic and transcriptomic analyses of autotetraploid and diploid mulberry (*Morus alba* L.). Int. J. Mol. Sci. 16:22938–22956.

Decanter, L., G. Colling, N. Elvinger, S. Heiðmarsson, and D. Matthies. 2020. Ecological niche differences between two polyploid cytotypes of *Saxifraga rosacea*. Am. J. Bot. 107:423–435.

Diallo, A. M., E. D. Kjær, A. Ræbild, and L. R. Nielsen. 2023. Coexistence of diploid and polyploid *Acacia senegal* (L. Willd.) and its implications for interploidy pollination. New For. 54:67–82.

Dominguez-Delgado, J. J., J. Lopez-Jurado, E. Mateos-Naranjo, and F. Balao. 2021. Phenotypic diploidization in plant functional traits uncovered by synthetic neopolyploids in *Dianthus broteri*. J. Exp. Bot. 72:5522–5533.

Doyle, J. J., and J. L. Doyle. 1987. A rapid DNA isolation procedure for small quantities of fresh leaf tissue. Phytochem. Bull. 19:11–15.

Fan, D. M., and Y. P. Yang. 2009. Altitudinal variations in flower and bulbil production of an alpine perennial, *Polygonum viviparum* L. (Polygonaceae). Plant Biol. 11:493–497.

Fischer, M., A. Weyand, K. Rudmann-Maurer, and J. Stöcklin. 2011. Adaptation of *Poa alpina* to altitude and land use in the Swiss Alps. Alp. Bot. 121:91–105.

Flegrová, M., and F. Krahulec. 1999. *Anthoxanthum odoratum* and *A. alpinum*: Life history parameters at two different altitudes. Folia Geobot. 34:19–31.

Fowler, N. L., and D. A. Levin. 2016. Critical factors in the establishment of allopolyploids. Am. J. Bot. 103:1236–1251.

Gao, S., Q. Yan, L. Chen, Y. Song, J. Li, C. Fu, and M. Dong. 2017. Effects of ploidy level and haplotype on variation of photosynthetic traits: Novel evidence from two *Fragaria* species. PLoS One 12:1–13.

Godfree, R. C., D. J. Marshall, A. G. Young, C. H. Miller, and S. Mathews. 2017. Empirical evidence of fixed and homeostatic patterns of polyploid advantage in a keystone grass exposed to drought and heat stress. R. Soc. Open Sci. 4.

Godsoe, W., M. A. Larson, K. L. Glennon, and K. A. Segraves. 2013. Polyploidization in *Heuchera cylindrica* (Saxifragaceae) did not result in a shift in climatic requirements. Am. J. Bot. 100:496–508.

Grime, J. P. 1977. Evidence for the existence of three primary strategies in plants and its relevance to ecological and evolutionary theory. Am. Nat. 111:1169–1194.

Han, T. S., Q. J. Zheng, R. E. Onstein, B. M. Rojas-Andres, F. Hauenschild, A. N. Muellner-Riehl, and Y. W. Xing. 2020. Polyploidy promotes species diversification of *Allium* through ecological shifts. New Phytol. 225:571–583.

Hatano, H., N. Mizuno, R. Matsuda, N. Shitsukawa, P. Park, and S. Takumi. 2012. Dysfunction of mitotic cell division at shoot apices triggered severe growth abortion in interspecific hybrids between tetraploid wheat and *Aegilops tauschii*. New Phytol. 194:1143–1154.

Hayashi, K., N. Hashimoto, M. Daigen, and I. Ashikawa. 2004. Development of PCR-based SNP markers for rice blast resistance genes at the *Piz* locus. Theor. Appl. Genet. 108:1212–1220.

Herben, T., J. Suda, and J. Klimešová. 2017. Polyploid species rely on vegetative reproduction more than diploids: A re-examination of the old hypothesis. Ann. Bot. 120:341–349.

Huang, C. T., and C. F. Hsieh. 2014. Asexual bulbil development and diversification of reproductive strategy between *Remusatia vivipara* and *Remusatia pumila* (Araceae). Taiwania 59:220–230.

Husband, B. C., and D. W. Schemske. 1997. The effect of inbreeding in diploid and tetraploid populations of *Epilobium angustifolium* (Onagraceae): Implications for the genetic basis of inbreeding depression. Evolution 51:737–746.

Hülber, K., M. Sonnleitner, J. Haider, M. Schwentenwein, M. Winkler, G. M. Schneeweiss, and P. Schönswetter. 2018. Reciprocal transplantations reveal strong niche differentiation among ploidy-differentiated species of the *Senecio carniolicus* aggregate (Asteraceae) in the easternmost Alps. Alp. Bot. 128:107–119.

Ida, T. Y., and G. Kudo. 2010. Seasonal patterns of carbon assimilation and allocation of a summer-green forest herb, *Parasenecio auriculata* (Senecioneae; Asteraceae). Plant Ecol. 210:181–193.

Jusaitis, M., and M. Adams. 2005. Conservation implications of clonality and limited sexual reproduction in the endangered shrub *Acanthocladium dockeri* (Asteraceae). Aust. J. Bot. 53:535–544.

Kadota, Y., H. Setoguchi, A. Soejima, T. Toma, M. Nakata, T. Morita, and K.

Yonekura. 2017. Asteraceae. In: Ohashi, H., Y. Kadota, J. Murata, K. Yonekura, and H. Kihara (eds.), Wild flowers of Japan II revised new edition. 5:198–372 (in Japanese). Heibonsha, Tokyo, Japan.

Karunarathne, P., M. Schedler, E. J. Martínez, A. I. Honfi, A. Novichkova, and D. Hojsgaard. 2018. Intraspecific ecological niche divergence and reproductive shifts foster cytotype displacement and provide ecological opportunity to polyploids. Ann. Bot. 121:1183–1196.

Kawecki, T. J., and D. Ebert. 2004. Conceptual issues in local adaptation. Ecol. Lett. 7:1225–1241.

Knotek, F., and F. Kolář. 2018. Different low-competition island habitats in Central Europe harbour similar levels of genetic diversity in relict populations of *Galium pusillum* agg. (Rubiaceae). Biol. J. Linn. Soc. Lond. 125:491–507.

Körner, C. 1999. Alpine Plant Life: Functional plant ecology of high mountain ecosystems. Springer-Verlag, Berlin, German.

Kudo, G. 2021. Habitat-specific effects of flowering advance on fruit-set success of alpine plants: a long-term record of flowering phenology and fruit-set success of *Rhododendron aureum*. Alp. Bot. 131:53–62.

Kudo, G. 2022. Outcrossing syndrome in alpine plants: Implications for flowering phenology and pollination success. Ecol. Res. 37:288–300.

Kudo, G., and A. S. Hirao. 2020. Geographical distribution, genetic diversity, and reproductive traits of mixed polyploid populations in *Parasenecio kamtschaticus* (Senecioneae; Asteraceae). Plant Syst. Evol. 306:1–11.

Kudo, G., and S. Suzuki. 2002. Relationships between flowering phenology and fruit-set of dwarf shrubs in alpine fellfields in Northern Japan: a comparison with a

subarctic heathland in northern Sweden. Arct. Antarct. Alp. Res. 34:185–190.

Kudo, G., T. Y. Ida, and T. Tani. 2008. Linkages between phenology, pollination, photosynthesis, and reproduction in deciduous forest understory plants. Ecology 89:321–331.

Kumar, S., G. Stecher, M. Li, C. Knyaz, and K. Tamura. 2018. MEGA X: molecular evolutionary genetics analysis across computingplatforms. Mol. Biol. Evol. 35:1547–1549.

Laport, R. G., R. L. Minckley, and J. Ramsey. 2016. Ecological distributions, phenological isolation, and genetic structure in sympatric and parapatric populations of the *Larrea tridentata* polyploid complex. Am. J. Bot. 103:1358–1374.

Levin, D. A. 1975. Minority cytotype exclusion in local plant populations. Taxon 24:35–43.

Levin, D. A. 1983. Polyploidy and novelty in flowering plants. Am. Nat. 122:1–25.

Li, W., D. K. Biswas, H. Xu, C. Xu, X. Wang, J. Liu, and G. Jiang. 2009. Photosynthetic responses to chromosome doubling in relation to leaf anatomy in *Lonicera japonica* subjected to water stress. Funct. Plant Biol. 36:783–792.

López-Jurado, J., E. Mateos-Naranjo, and F. Balao. 2019. Niche divergence and limits to expansion in the high polyploid *Dianthus broteri* complex. New Phytol. 222:1076–1087.

Mable, B. K. 2004. Polyploidy and self-compatibility: Is there an association? New Phytol. 162:803–811.

Manzaneda, A. J., P. J. Rey, J. M. Bastida, C. Weiss-Lehman, E. Raskin, and T. Mitchell-Olds. 2012. Environmental aridity is associated with cytotype segregation

and polyploidy occurrence in *Brachypodium distachyon* (Poaceae). New Phytol. 193:797–805.

Markos, S., and B. G. Baldwin. 2001. Higher-level relationships and major lineages of *Lessingia* (Compositae, Astereae) based on nuclear rDNA internal and external transcribed spacer (ITS and ETS) sequences. Syst. Bot. 26:168–183.

Martin, S. L., and B. C. Husband. 2013. Adaptation of diploid and tetraploid *Chamerion angustifolium* to elevation but not local environment. Evolution 67:1780–1791.

McIntyre, P. J., and S. Strauss. 2017. An experimental test of local adaptation among cytotypes within a polyploid complex. Evolution 71:1960–1969.

Mishiba, K. I., T. Ando, M. Mii, H. Watanabe, H. Kokubun, G. Hashimoto, and E. Marchesi. 2000. Nuclear DNA content as an index character discriminating taxa in the genus *Petunia sensu* Jussieu (Solanaceae). Ann. Bot. 85:665–673.

Miyashita, A., D. Sugiura, K. Sawakami, R. Ichihashi, T. Tani, and M. Tateno. 2012. Long-term, short-interval measurements of the frequency distributions of the photosynthetically active photon flux density and net assimilation rate of leaves in a cool-temperate forest. Agric. For. Meteorol. 152:1–10.

Nakagawa, M. 2006. Ploidy, geographical distribution and morphological differentiation of *Parasenecio auriculata* (Senecioneae; Asteraceae) in Japan. J. Plant Res. 119:51–61.

Newton, C. R., A. Graham, L. E. Heptinstal, S. J. Powell, C. Summers, N. Kalsheker, J. C. Smith, and A. F. Markham. 1989. Analysis of any point mutation in DNA. The amplification refractory mutation system (ARMS). Nucleic Acids Res. 17:2503–2516.

Otto, C. R. V. 2007. The evolutionary consequences of polyploidy. Cell 131:452–462.

Otto, C. R. V., J. W. Snodgrass, D. C. Forester, J. C. Mitchell, and R. W. Miller. 2007. Climatic variation and the distribution of an amphibian polyploid complex. J. Anim. Ecol. 76:1053–1061.

Otto, S. P., and J. Whitton. 2000. Polyploid incidence and evolution. Annu. Rev. Genet. 34:401–437.

Pegoraro, L., J. M. De Vos, S. Cozzolino, and G. Scopece. 2019. Shift in flowering time allows diploid and autotetraploid *Anacamptis pyramidalis* (Orchidaceae) to coexist by reducing competition for pollinators. Bot. J. Linn. Soc. 191:274–284.

Petit, C., P. Lesbros, X. Ge, and J. D. Thompson. 1997. Variation in flowering phenology and selfing rate across a contact zone between diploid and tetraploid *Arrhenatherum elatius* (Poaceae). Heredity 79:31–40.

Petit, C., F. Bretagnolle, and F. Felber. 1999. Evolutionary consequences of diploid-polyploid hybrid zones in wild species. Trends Ecol. Evol. 14:306–311.

Pluess, A. R., and J. Stöcklin. 2005. The importance of population origin and environment on clonal and sexual reproduction in the alpine plant *Geum reptans*. Funct. Ecol. 19:228–237.

Ramsey, J., and T. S. Ramsey. 2014. Ecological studies of polyploidy in the 100 years following its discovery. Philos. Trans. R. Soc. B Biol. Sci. 369:15–19.

Ramsey, J., and D. W. Schemske. 1998. Pathways, mechanisms, and rates of polyploid formation in flowering plants. Annu. Rev. Ecol. Syst. 29:467–501.

R Core Team. 2019. R: a language and environment for statistical computing. Vienna: R Foundation for Statistical Computing. Website: https://www.R-project.org/.

Ren, C., Y. Hong, L. Wang, and Q. E. Yang. 2017. Generic recircumscription of *Parasenecio* (Asteraceae: Senecioneae) based on nuclear ribosomal and plastid

DNA sequences, with descriptions of two new genera. Bot. J. Linn. Soc. 184:418–443.

Rice, A., P. Šmarda, M. Novosolov, M. Drori, L. Glick, N. Sabath, S. Meiri, J. Belmaker, and I. Mayrose. 2019. The global biogeography of polyploid plants. Nat. Ecol. Evol. 3:265–273.

Sakuma, T. 1987. Characterization of soils in the Tomakomai experiment forest: especially on the characteristics of organic horizons and their alteration following the partial cutting. Research Bulletin of the Hokkaido University Forests 44:749–759 (in Japanese).

Schinkel, C. C. F., B. Kirchheimer, A. S. Dellinger, S. Klatt, M. Winkler, S. Dullinger, and E. Hörandl. 2016. Correlations of polyploidy and apomixis with elevation and associated environmental gradients in an alpine plant. AoB PLANTS 8:plw064.

Schneider, C. A., W. S. Rasband, and K. W. Eliceiri. 2012. NIH Image to ImageJ: 25 years of image analysis. Nat. Methods 9:671–675.

Segraves, K. A. 2017. The effects of genome duplications in a community context. New Phytol. 215:57–69.

Shimono, Y., M. Watanabe, A. S. Hirao, N. Wada, and G. Kudo. 2009. Morphological and genetic variations of *Potentilla matsumurae* (rosaceae) between fellfield and snowbed populations. Am. J. Bot. 96:728–737.

Šingliarová, B., D. Hojsgaard, H. Müller-Schärer, and P. Mráz. 2023. The novel expression of clonality following whole-genome multiplication compensates for reduced fertility in natural autopolyploids. Proc. R. Soc. B Biol. Sci. 290:20230389.

Siopa, C., M. C. Dias, M. Castro, J. Loureiro, and S. Castro. 2020. Is selfing a

reproductive assurance promoting polyploid establishment? Reduced fitness, leaky self-incompatibility and lower inbreeding depression in neotetraploids. Am. J. Bot. 107:526–538.

Soltis, P. S., and D. E. Soltis. 1999. Polyploidy: recurrent formation and genome evolution. Trends in Ecol. Evol. 14:348–352.

Soltis, P. S., and D. E. Soltis. 2000. The role of genetic and genomic attributes in the success of polyploids. Proc. Natl. Acad . Sci. 97:7051–7057.

Soltis, D. E., C. J. Visger, and P. S. Soltis. 2014. The polyploidy revolution then...and now: Stebbins revisited. Am. J. Bot. 101:1057–1078.

Stebbins, G. L. 1950. Variation and evolution in plants. Geoffrey Cumberlege, London, UK.

Stebbins, G. L. 1971. Chromosomal evolution in higher plants. Edward Arnold, London, UK.

Stöcklin, J., P. Kuss, and A. R. Pluess. 2009. Genetic diversity, phenotypic variation and local adaptation in the alpine landscape: case studies with alpine plant species. Bot. Helv. 119:125–133.

Stuessy, T. F., H. Weiss-Schneeweiss, and D. J. Keil. 2004. Diploid and polyploid cytotype distribution in *Melampodium cinereum* and *M. leucanthum* (Asteraceae, Heliantheae). Am. J. Bot. 91:889–898.

Sugiyama, S. I. 2005. Polyploidy and cellular mechanisms changing leaf size: Comparison of diploid and autotetraploid populations in two species of *Lolium*. Ann. Bot. 96:931–938.

Suyama, Y., and Y. Matsuki. 2015. MIG-seq: an effective PCR-based method for genome-wide single-nucleotide polymorphism genotyping using the next-

generation sequencing platform. Sci. Rep. 5:16963.

Taberlet, P., L. Gielly, G. Pautou, and J. Bouvet. 1991. Universal primers for amplification of three non-coding regions of chloroplast DNA. Plant Mol. Biol. 17:1105–1109.

Thébault, A., F. Gillet, H. Müller-Schärer, and A. Buttler. 2011. Polyploidy and invasion success: Trait trade-offs in native and introduced cytotypes of two Asteraceae species. Plant Ecol. 212:315–325.

Theodoridis, S., C. Randin, O. Broennimann, T. Patsiou, and E. Conti. 2013. Divergent and narrower climatic niches characterize polyploid species of European primroses in *Primula* sect. *aleuritia*. J. Biogeogr. 40:1278–1289.

Treier, U. A., O. Broennimann, S. Normand, A. Guisan, U. Schaffner, T. Steinger, and H. MüLler-SchäRer. 2009. Shift in cytotype frequency and niche space in the invasive plant *Centaurea maculosa*. Ecology 90:1366–1377.

Ulum, F. B., F. Hadacek, and E. Hörandl. 2021. Polyploidy improves photosynthesis regulation within the *Ranunculus auricomus* complex (Ranunculaceae). Biology 10:811.

Van Drunen, W. E., and B. C. Husband. 2018. Immediate vs. Evolutionary consequences of polyploidy on clonal reproduction in an autopolyploid plant. Ann. Bot. 122:195–205.

Van Drunen, W. E., and B. C. Husband. 2019. Evolutionary associations between polyploidy, clonal reproduction, and perenniality in the angiosperms. New Phytol. 224:1266–1277.

Vleugels, T., B. Ceuppens, G. Cnops, P. Lootens, F. R. van Parijs, G. Smagghe, and I. Roldán-Ruiz. 2016. Models with only two predictor variables can accurately

predict seed yield in diploid and tetraploid red clover. Euphytica 209:507–523.

Wakui, A., and G. Kudo. 2021. Ecotypic differentiation of a circumpolar Arctic-alpine species at mid-latitudes: Variations in the ploidy level and reproductive system of *Vaccinium vitis-idaea*. AoB PLANTS 13:1–13.

Wang, Z., C. Zhong, D. Li, C. Yan, X. Yao, and Z. Li. 2021. Cytotype distribution and chloroplast phylogeography of the *Actinidia chinensis* complex. BMC Plant Biol. 21:325.

Wei, N., R. Cronn, A. Liston, and T. L. Ashman. 2019. Functional trait divergence and trait plasticity confer polyploid advantage in heterogeneous environments. New Phytol. 221:2286–2297.

White, T. J., T. Bruns, S. Lee and J. Taylor. 1990. Amplification and direct sequencing of fungal ribosomal RNA genes for phylogenetics. In: Innis, M.A., D. H. Gelfand, J. J. Sninsky, and T. J. White (eds.), PCR Protocols: A Guide to Methods and Applications. 18:315–322. Academic Press, New York, US.

Wood, T. E., N. Takebayashi, N. S. Barker, I. Mayrose, P. B. Greenspoon, and L. H. Rieseberg. 2009. The frequency of polyploid speciation in vascular plants. Proc. Natl. Acad. Sci. U. S. A. 106:13875–13879.

Yang, P. P., L. F. Xu, H. Xu, Y. C. Tang, G. R. He, Y. W. Cao, and J. Ming. 2017. Histological and transcriptomic analysis during bulbil formation in *Lilium lancifolium*. Front. Plant Sci. 8:1508.

Yang, X., J. Cheng, B. Yao, H. Lu, Y. Zhang, J. Xu, X. Song, K. Sowndhararajan, and S. Qiang. 2021. Polyploidy-promoted phenolic metabolism confers the increased competitive ability of *Solidago canadensis*. Oikos 130:1014–1025.

Zhang, Y., B. Wang, S. Qi, M. Dong, Z. Wang, Y. Li, S. Chen, B. Li, and J. Zhang.

2019. Ploidy and hybridity effects on leaf size, cell size and related genes expression in triploids, diploids and their parents in *Populus*. Planta 249:635–646.

Zozomová-Lihová, J., I. Malánová-Krásná, P. Vit, T. Urfus, D. Senko, M. Svitok, M. Kempa, and K. Marhold. 2015. Cytotype distribution patterns, ecological differentiation, and genetic structure in a diploid-tetraploid contact zone of *Cardamine amara*. Ame. J. Bot. 102:1380–1395.